TUDelft

Delft University of Technology

Energy Performance of Ships

An Operational Data-Driven Analysis, Modelling, and Optimisation Approach for Ship Energy Systems

Vasilikis, Nikolaos

DOI
10.4233/uuid:b1557091-334c-4a14-bc5f-eb7601ea2107

Publication date
2025

Document Version
Final published version

Important note
To cite this publication, please use the final published version (if applicable).
Please check the document version above.

ENERGY PERFORMANCE OF SHIPS

An operational data-driven analysis, modelling, and optimisation approach for ship energy systems

NIKOLAOS VASILIKIS

ENERGY PERFORMANCE OF SHIPS

PROEFSCHRIFT

TER VERKRIJGING VAN DE GRAAD VAN DOCTOR AAN DE
TECHNISCHE UNIVERSITEIT DELFT,
OP GEZAG VAN DE RECTOR MAGNIFICUS
PROF.DR.IR. T.H.J.J. VAN DER HAGEN,
VOORZITTER VAN HET COLLEGE VOOR PROMOTIES,
IN HET OPENBAAR TE VERDEDIGEN OP
VRIJDAG, 31 JANUARI 2025 OM 10:00 UUR

DOOR

Nikolaos VASILIKIS

DIPLOMA IN NAVAL ARCHITECTURE AND MARINE ENGINEERING
NATIONAL TECHNICAL UNIVERSITY OF ATHENS
GEBOREN TE ATHENE, GRIEKELAND

Dit proefschrift is goedgekeurd door de promotoren.

Samenstelling promotiecommissie bestaat uit:

voorzitter: Rector Magnificus
promotor: dr.   A. Coraddu
copromotor: dr. ir.   R. D. Geertsma

onafhankelijke leden:

    prof. dr.   Kari Tammi   Aalto University
      dr. ir.   Theo Hofman   Eindhoven University of Technology
    prof. dr. ir.   Tiedo Tinga   University of Twente
    prof. dr.   Mark Sumner   University of Nottingham
    prof. dr. ir.   Leo Veldhuis   Delft University of Technology

ENERGY PERFORMANCE OF SHIPS

NIKOLAOS VASILIKIS

I love the peace and melancholy of the night. No obligations, just the promise of a coming new day in which you can change everything.

SUMMARY

This dissertation addresses the increasing global demand for reducing greenhouse gas emissions in the maritime industry. It provides methods and results on ship energy performance assessment and enhancement using high-frequency operational data. These methods can be used to inform operator decisions to increase operational performance, to assess modifications to power and propulsion systems and its control strategies and to evaluate hybrid propulsion and power generation systems for future ship design for ships with similar operating profiles and conditions. The developed methodologies can be implemented on a wide range of ship types and missions, particularly on vessels with highly uncertain mission profiles and operating conditions. The case in this work is the *Holland* class Ocean-going Patrol Vessels (OPV) of the Royal Netherlands Navy, which are multi-function ships, equipped with hybrid propulsion, that operate a very diverse operating profile worldwide.

First, this study examines the energy performance assessment of ships, discussing the limitations of existing energy efficiency measures such as the EEDI, EEXI, SEEMP, and CII, which do not fully account for operational and environmental uncertainties. It suggests a methodology to enrich datasets of operational data in case certain parameters are not logged, and it provides a number of qualitative and quantitative tools in the assessment of operational and environmental uncertainty, and energy performance, at a ship and component level. In this way, this methodology provides conclusions on design and operational decisions, such as the decision to equip vessels with hybrid propulsion.

Secondly, this research introduces a digital twin modelling approach for energy performance prediction using high-frequency operational data. This steady state approach combines statistical and well established first-principle techniques to model system components and compensate for the accuracy of sensors and uncertainties linked to information provided by the manufacturers and shipbuilder. Results demonstrate the effectiveness of the adopted approach to predict carbon intensity over more than seventy different and diverse actual sailing intervals with high accuracy. The model shows not only a mean absolute percentage error of less than 5% on predicting instant fuel consumption on both mechanical and electrical modes, but also a carbon intensity prediction accuracy within 2.5% with a 95% confidence interval, which justifies a significant improvement over traditional models.

Finally, this study examines the design optimisation of ship energy systems. Building on the conclusions of the previous chapters, it examines the topology selection and sizing problem for the case study class of vessels. This chapter proposes a robust multi-objective optimisation framework using actual sailing profiles. It

proves its robustness using actual sailing profiles of different vessels of the same class, and it examines new designs with environmental, financial and technical objectives. Results highlight the importance of accounting for realistic operational and environmental conditions in the design of ship energy systems, but also the environmental and financial benefits of design by optimisation methods.

As a final note and recommendation, this dissertation encourages the collection and use of operational data in design and operational decisions, and it offers tools and directions in which carbon emissions of ship operations can be reduced in a financially and technically viable manner.

SAMENVATTING

Dit proefschrift richt zich op de toenemende wereldwijde vraag naar vermindering van broeikasgasemissies in de maritieme industrie. Het biedt methoden en resultaten voor de beoordeling en verbetering van scheepsenergieprestaties met behulp van hoogfrequente operationele data. Deze methodes kunnen toegepast worden om scheepspersoneel te adviseren over hun bedieningskeuzes voor een efficientere operatie, om aanpassingen aan de voortstuwing en energieopwekking en diens regelstrategiën te vealueren en om ontwerpkeuzes voor hybride voortstuwing en energieopwekking van nieuwe schepen met soortgelijke operatieprofielen en operatiegebieden te evalueren. De ontwikkelde methodes kunnen toegepast worden op een grote diversiteit aan scheepstypes en missies, en is vooral van toepassing op dienstverlende schepen met een onzeker operatieprofiel en operatoegebied. De methodes zijn toegepast op het praktijkvoorbeeld van een *Holland* klasse Ocean-going Patrol Vessels (OPV) van de Koninklijke Marine, multifunctionele dienstverlenende partrouilleschepen met diverse take die uitgesust zijn met hybride voortstuwing die wereldwijd opereren met een divers operatieprofiel.

Allereerst, onderzoekt deze studie de energieprestatie-beoordeling van schepen en bespreekt de beperkingen van bestaande energie-efficiëntiemaatregelen zoals de EEDI, EEXI, SEEMP en CII, die niet volledig rekening houden met operationele onzekerheden weersomstandigheden. Dit hoofdstuk stelt een methodologie voor om datasets met operationele gegevens te verrijken wanneer bepaalde parameters niet worden geregistreerd, en reikt een aantal kwalitatieve en kwantitatieve instrumenten aan voor de beoordeling van operationele onzekerheden, weerscondities, en energieprestaties, op het niveau van schepen en componenten. Op deze manier levert deze methodologie conclusies op voor ontwerpkeuzes en operationele beslissingen, zoals de beslissing om schepen uit te rusten met hybride aandrijving.

Ten tweede introduceert dit onderzoek een digitale tweelingmodel-benadering voor het voorspellen van energieprestaties met behulp van hoogfrequente operationele gegevens. Deze statische benadering combineert statistische en gevestigde natuurkundige modelleertechnieken om systeemcomponenten te modelleren en te compenseren voor de onnauwkeurigheid van sensoren en onnauwkeurigheid van informatie die door fabrikanten en scheepsbouwers wordt verstrekt. De resultaten tonen de effectiviteit van de gekozen aanpak om de koolstofintensiteit over meer dan zeventig werkelijke vaarintervallen met hoge nauwkeurigheid te voorspellen. Het model toont niet alleen een gemiddelde absolute procentuele fout van minder dan 5% bij het voorspellen van het onmiddelijle brandstofverbruik in zowel mechanische als elektrische modi, maar ook een nauwkeurigheid bij het voorspellen van de koolstofintensiteit binnen 2,5% met een betrouwbaarheidsinterval van 95% over

een operatieprofiel, wat een aanzienlijke verbetering is ten opzichte van traditionele modellen.

Tot slot onderzoekt deze studie de optimalisatie van het ontwerp van scheepsenergiesystemen. Voortbouwend op de conclusies van de eerste hoofdstukken, wordt het probleem van topologieselectie en dimensionering van schepen met hybride voortstuwing en energieopwekking onderzocht. Dit hoofdstuk stelt een robuuste multicriteria optimalisatie aanpak voor die nieuwe ontwerpen kan evalueren vanuit milieubelastende, financiële en technische perspectieven op basis van echte en onzekere operatieprofielen. De robuustheid wordt aangetoond aan de hand van werkelijke vaarprofielen van verschillende schepen van dezelfde klasse en er worden nieuwe ontwerpen met milieubelastende, financiële en technische doelstellingen onderzocht. De resultaten laten zien hoe belangrijk het is om rekening te houden met realistische operationele omstandigheden en weerscondities bij het ontwerpen van scheepsenergiesystemen, maar ook wat de milieubelastingende en financiële voordelen zijn van ontwerpen met optimalisatiemethoden.

Als laatste opmerking en aanbeveling moedigt dit proefschrift het verzamelen en gebruiken van operationele gegevens in ontwerp- en operationele beslissingen aan, en biedt het hulpmiddelen en richtingen waarin milieubelastende uitstoot van scheepsoperaties op een financieel en technisch haalbare manier kunnen worden verminderd.

CONTENTS

Latin

b_e	Specific fuel consumption of main diesel engines
b_{gen}	Specific fuel consumption of diesel generators
c_e	Purchase cost coefficient of main diesel engines
c_g	Purchase cost coefficient of diesel generators
c_m	Purchase cost coefficient of electrical motors
c_μ	Maintenance cost coefficients
C_{capex}	Capital expenditure
C_{opex}	Net present value of operational expenditure
$C_{opex,y}$	Annual operational expenditure
C_{maint}	Maintenance cost
D	Propeller diameter
f_{CO_2}	Carbon factor
h^L	Lower calorific value of fuel
i_f	Inflation rate
i_m	Market interest
$\mathbf{i}$	Input optimisation scanario
J	Advance coefficient
K_T	Thrust coefficient
K_Q	Torque coefficient
$K_{Q,ow}$	Open water torque coefficient
$\dot{m}_{f,e}$	Main diesel engines fuel consumption
$\dot{m}_{f,gen}$	Diesel generators fuel consumption
$\dot{m}_{f,tot}$	Total fuel consumption
M_f	Amount of fuel consumed
M_{CO_2}	Amount of carbon dioxide emissions
M_{psh}	Propeller shaft torque
n	Propeller shaft speed
n_e	Main diesel engine speed
n_m	Electrical motor speed
n_{psh}	Propeller shaft speed
n_{virt}	Virtual shaft speed
N_a	Number of type a diesel generators
N_b	Number of type b diesel generators

N_y	Years under consideration
p	Propeller pitch
$p(v,T)$	Frequency of occurrence for the corresponding tuple (v,T)
$\mathbf{p}$	Vector of fixed parameters describing the examined system
p_0	Zero-thrust propeller pitch
p_{nom}	Nominal propeller pitch
P_a	Rated power of type a diesel generators
P_b	Rated power of type b diesel generators
P_{psh}	Propeller shaft power
P_{loss}	Power losses
P_m	Power provided by the electrical motors (rated in Chapter 4)
$P_{m,el}$	Electrical power provided to the motors
P_e	Main diesel engine power (rated in Chapter 4)
P_g	Rated power of diesel generators
P_{gen}	Generated electrical power
P_{hotel}	Hotel electrical power
P_Q	Power delivered to the propellers
P_T	Propeller thrust power
P_{TE}	Effective propeller thrust power
Q_f	Heat flow from burning fuel
r_e	Reduction ratio of main diesel engine
r_m	Reduction ratio of electrical motor
R	Vessel resistance
R_{tow}	Vessel towing resistance
t	Thrust deduction factor
T	Total propeller thrust
T_{air}	Ambient air temperature
v	Vessel speed
v_{log}	Vessel speed (logged)
v_a	Speed in the ship's wake
$\bar{v}$	Average speed of a voyage interval
w	Taylor's wake factor
W_e	Total weight of the main diesel engines
W_g	Total weight of the diesel generators
W_m	Total weight of the electrical motors
W_{red}	Total weight of the redundant diesel generators
W_{tot}	Total weight of the system
$\mathbf{x}$	Vector of independent decision variables

GREEK

δt	Time step
Δt	Duration of a voyage interval
Δs	Distance of a voyage interval

ζ_{cpd}	Carbon energy effectiveness
ζ_{fpd}	Fuel energy effectiveness
η_{e}	Energy efficiency of main diesel engines
η_{gb}	Energy efficiency of gearboxes
η_{gen}	Energy efficiency of diesel generators
η_{prop}	Energy efficiency of propellers
$\eta_{\mathrm{propulsion}}$	Propulsion energy efficiency
η_{psh}	Energy efficiency of propeller shafts
η_{RQ}	Relative rotative efficiency
$\hat{\eta}_{\mathrm{RQ}}$	Propeller uncertainty correction factor
η_{supply}	Power supply energy efficiency
η_{tot}	Total energy efficiency
λ	Weight expressing the importance of different objectives
μ	Mean value
ρ	Sea water density
σ	Standard deviation

ACRONYMS

APE   Absolute percentage error
CAPEX   Capital expenditure
CCD   Climb, cruise & descend cycle
CI   Carbon intensity of a voyage interval
CII   Carbon intensity indicator
CPP   Controllable pitch propeller
DGEN   Diesel generator
EEDI   Energy efficiency design index
EEXI   Energy efficiency existing ship index
EEOI   Energy efficiency operational indicator
EE   Error estimation
EM   Electrical mode
GA   Genetic algorithm
GB   Gearbox
GHG   Greenhouse gas
IMO   International Maritime Organisation
IPCC   Intergovernmental Panel on Climate Change
IPMS   Integrated platform monitoring system
ISO   International organization for standardization
KRLS   Kernel regularised least square
LTO   Landing, take-off cycle
M   Electrical motor
MAE   Mean average error
MAPE   Mean absolute percentage error
MDE   Main diesel engine
MLP   Multilayer perceptron network
MM   Mechanical mode
MOCO   Multi-objective combinatorial optimisation
MS   Model selection
NO_x Nitrogen oxides
NPV   Net present value
OPEX   Operational expenditure
PM   Particulate matter
PSH   Propeller shaft
PTI   Power take-in

PWC	Present worth cost
REP	Relative error percentage
RF	Random forest
RLS	Regularised least square
RMSE	Root mean squared error
RNLN	Royal Netherlands navy
SEEMP	Ship energy efficiency management plan
SO_x	Sulphur oxides
SVR	Support vector regression
WHR	Waste heat recovery
WLTC	World harmonized light-vehicle test cycle

INTRODUCTION

1.1 CLIMATE CHANGE AND MARITIME INDUSTRY

Industrial revolution started in the 18th century and affected the lives of millions of people. Primarily in Europe and the United States of America, it resulted in significant economic and population growth, but also in crucial societal changes. However, this improvement came at a cost. Characterised by the introduction of machines and extensive fossil fuels consumption, it also resulted in substantial atmospheric pollution with the abundance of long-lived gases like carbon dioxide (CO_2), methane (CH_4), nitrous oxide (N_2O), and chlorofluorocarbons (CFCs), collectively called greenhouse gases (GHGs) [4]. The report presented by the Intergovernmental Panel on Climate Change (IPCC) in 2023 [1] clarifies that the increase of GHGs concentration in the atmosphere is accelerating as demonstrated in Figure 1.1, with almost half of emissions after 1850, emitted in the last three decades.

This increase in GHGs proportionally affects the heat being trapped near the earth's surface, resulting in the so-called greenhouse phenomenon [5]. IPCC concludes that GHGs together with other anthropogenic factors are unequivocally the main cause of this phenomenon [1], [6], [7]. Climate change takes place at an unprecedented speed, and its impact on mankind's living environment is severe. Observed changes include an increase in the mean sea level between 1901 and 2018 of 20 cm, an increase of the combined land and ocean surface temperature in 2011-2020 compared to 1850-1900 of 1.1°C, and the acidification of the oceans. Just a look at the projection of global surface temperature by 2100 reveals that a catastrophic increase of 4°C is possible as seen in Figure 1.2. Reports by IPCC also indicate how vulnerable human and natural systems are to those changes, irrespective of their cause, and relate numerous extreme events such as extreme hot or cold temperatures, increased sea levels, and heavy precipitation to them. Finally, they point to the injustice of climate change as vulnerable communities who have historically contributed the least to it are disproportionately affected.

Attempts to tackle this phenomenon commenced with the establishment of the United Nations Climate Change Secretariat and the adoption of the United Nations
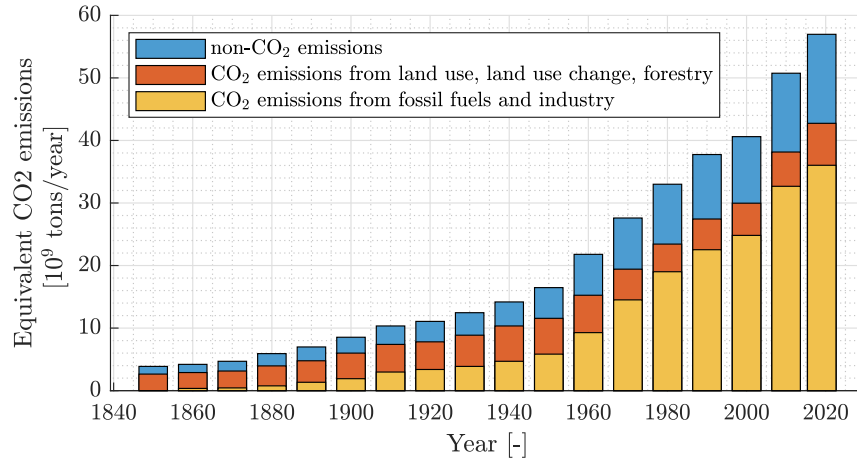
Figure 1.1: Yearly equivalent carbon dioxide emissions from year 1850 to 2019 [1].

Framework Convention on Climate Change (UNFCCC) in 1992 by participating members. This convention set the basis for developed countries to accept responsibility of high GHGs, take measures to mitigate anthropogenic effects on the environment, but also assist financially and technologically developing countries in this direction. It was followed by the Kyoto Protocol (1997) and Paris Agreement (2015) which came into force in February 2005 and November 2016, respectively. The Kyoto Protocol established emission targets distributed into two commitment periods, 2005 to 2012 and 2013 to 2020. The Paris Agreement established National Determined Contributions (NDCs), meaning that each ratifying member country has to set goals at a national level, keep track of all emission sources and regularly report their progress.

This status quo can perform successfully for most industrial activities except for two sectors. According to Bows-Larkin [8], international aviation and shipping release their emissions in international airspace and waters which are not covered by such policies. Those two sectors operate under the regulations of the International Civil Aviation Organization (ICAO) and the International Maritime Organization (IMO). The maritime industry still delivers more than 80% of global trade, overcoming fluctuations caused by the COVID-19 pandemic [9]. In 2007, international shipping CO2 emissions stood for 2.7% of the total global emissions. Future economic growth and transport demand indicate that maritime carbon dioxide emissions will increase between 50% to 250% by 2050 compared to the 2012 level [10]. To reduce the impact of shipping on the environment, IMO adopted mandatory energy efficiency measures already back in 2011 [11]. However, adopting these measures did not prevent a further 9.6% increase in GHG emissions from shipping between 2012 and 2018 [12]. Nevertheless and despite the large scale of operations, IMO decided in its updated GHG reduction strategy not only to target cutting those emissions in half by 2050 [13] but to aim for net-zero emissions around the same period [14].
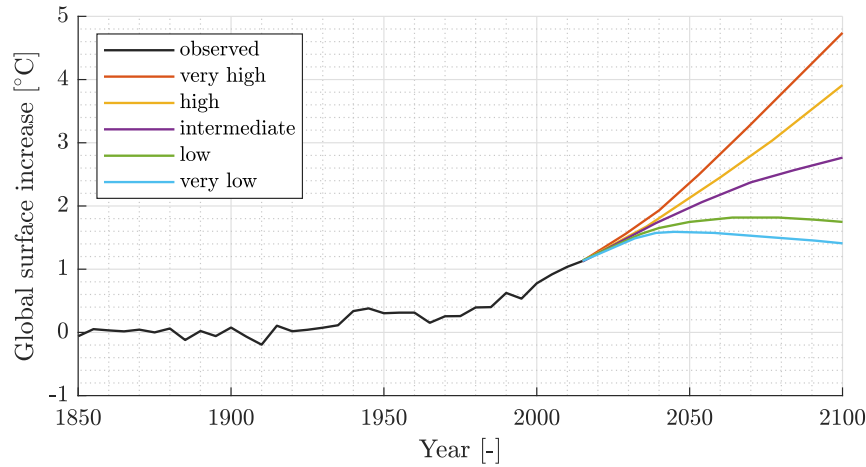
Figure 1.2: Global surface temperature increase scenarios and observed values from year 1850 to 2100 [1].

1.2 LEGISLATION

The first step in regulating maritime industry GHG emissions was the amendment of the 1973 International Convention for the Prevention of Pollution from Ships (MARPOL) with Annex VI by the Marine Environment Protection Committee (MEPC), IMO's senior technical body on marine pollution matters, in 1997. This Annex included, for the first time, requirements on air pollution and emissions from ships. Furthermore, following an initiative by IMO, four studies assess the current status and future trends of maritime emissions, conducted in 2000 [15], in 2009 [16], in 2014 [10] and 2020 [12]. The most prominent regulations by IMO require ships to follow and keep a Ship Energy Efficiency Management Plan (SEEMP) and comply with reference limits of indices and indicators that, in principle, indicate the amount of carbon dioxide (CO_2) emissions per transport work, also called carbon intensity. Their calculation is done either on a single sailing point as in the case of the Energy Efficiency Design Index (EEDI) [17] and Energy Efficiency Existing ship Index (EEXI) [18] or by averaging the carbon footprint over a year of operations as in the case of Carbon Intensity Indicator (CII) [19].

The energy efficiency of new ship designs for the majority of ship types is regulated with EEDI. In a one-time calculation, all existing ships were also examined using the EEXI. Although the name implies the assessment of the energy efficiency of vessels, EEDI examines carbon intensity [20], [21] on a single sailing point determined by the rated power of main propulsors and vessel resistance in calm water conditions, favoring ships with smaller main engines and sailing at slower speeds. Underpowered ships, though, do not comply with the initial goal of designing ships with improved hulls, engines, and propellers [22]. They impose a safety concern too, as the propulsion and manoeuvring in adverse sea conditions can be poor [23]. Moreover, one sailing point does not consider the operational and environmental uncertainty at sea [24] and part-load efficiency as in the case of power take-off generators that bring significant energy savings in off-design operating conditions. Thus, EEDI is incomplete because it does not account for the entire life of a vessel and it is flawed because it does not promote green operation [25]. Ultimately, using

EEDI instead of actual operating profiles underestimates the lifetime energy savings of different solutions and their use should be limited to early design phase approximations [26]. Other transportation fields like the automotive and aviation have already taken steps forward, as carbon emissions and fuel economy are evaluated based on driving cycles and flight profiles accordingly [27], [28].

Operational phase decisions contribute equally to the carbon footprint of maritime operations. That was the driving force behind the introduction of SEEMP, which provides a framework for establishing and tracking the implementation of energy related measures. Before 2023, the Energy Efficiency Operational Indicator (EEOI) was voluntarily used to test the effectiveness of operational emission reduction measures. This indicator expressed the average carbon intensity over a certain number of voyages [29]. Decided in 2021 and coming into force for the first time in 2023, operational energy efficiency is assessed using CII [30]. This indicator provides an A to E energy labelling for most vessels based on their annual average carbon intensity. Contrary to the volunteering philosophy of EEOI, the CII score will impact vessel operations. Ships labelled as C will be offered a three-year period to improve their efficiency, and ships labelled as E will be requested to urgently upgrade their energy label the following year. While useful for evaluating the operation of cargo vessels, the method is considered less valuable for ships with a diverse operating profile, as the uncertainty of the operating speeds, in combination with the uncertainty of the operating conditions, hinders fair comparison between different missions. Moreover, balancing out the effect of this uncertainty over the course of one year does not provide substantial feedback on the operational and design decisions, especially in the case of multi-function vessels that do not perform the same type of operations over time, as demonstrated in this dissertation.

However, IMO is not the only policy body (regulator) that has acted to reduce maritime GHG emissions. Despite a lack of authority in international waters, different countries can impose requirements on all ships calling their ports or territory. The European Parliament, keeping track of a 2030 framework to cut domestic GHG emissions by at least 40% compared to 1990 levels, has already introduced regulations in that direction. Regulation (EU) 2015/757 came into force in January 2018 and requires ships to accurately monitor, report and verify carbon dioxide emissions, and nitrous oxide and methane emissions as of January 2024, and other relevant information (MRV Maritime regulation) [31]. Furthermore, the European Parliament and Council decided to include maritime in the Emissions Trading System [32]. Finally, the Commission decided to approach emissions reduction from an additional angle, other than solely improving energy efficiency on board. This approach, expressed through the GHG intensity index, evaluates the equivalent carbon dioxide emissions both from tank to wake (TtoW), but also from well to tank (WtoT), per unit energy used [33], [34]. In this way, it promotes greater use of renewable and low-carbon fuels and new technologies.

1.3 MITIGATION STRATEGIES

Mitigation of maritime contribution to climate change requires measures that can be described as technological, operational, and market-based [35]. Focusing on the first two categories and accounting for numerous studies in literature, Vergara,

McKesson and Walczak [36] and Bouman, Lindstad, Rialland *et al.* [37] concluded that a combination of technological and operational measures can potentially bring a 75% reduction in maritime GHG emissions by 2050, but current technologies alone cannot lead maritime industry decarbonisation.

The most high-impact technological measure is the use of alternative fuels like carbon neutral synthetic fuels, biofuels, hydrogen, and ammonia. Their adoption requires the development of cost effective power supply systems, and design solutions to storage space and weight issues [38]. According to Horvath, Fasihi and Breyer [39], hydrogen fuel cells are likely to be economically competitive against fossil internal combustion engines for certain ship types and sizes by 2040, if they follow their current projected development. The main drawback of such systems, though, is the lower energy density compared to systems running on fossil fuels. Hence, energy efficiency improvement is necessary to maintain financial competitiveness without implementing a carbon dioxide cost.

Technological solutions also consider the selection of different system architectures and control strategies [40]. Electrification of ships plays an important role in this, though an electric propulsion system suffers from a number of disadvantages. Hybrid propulsion systems are considered a promising alternative, though the right sizing and selection of components is not a simple design problem and depends very much on the actual operational profile of the vessel. Moreover, improved hull design, reduced resistance, and propulsion augments are expected to provide further savings.Therefore, in the design phase hull design, system architecture and control should be evaluated over the actual operations of the vessel.

Supplementary to technological measures, a plethora of operational measures such as optimal fleet capacity utilization, optimal ports operation and better advised crew decisions, can provide similar or even higher savings. According to Bouman, Lindstad, Rialland *et al.* [37], in particular weather-based route planning and execution can reduce carbon dioxide emissions up to 48%, optimal draught and trim selection up to 10%, and vessel speed optimisation up to 60%. Of course, in order to achieve these savings, these operational measures should be assessed with accurate energy performance prediction models that take operational and environmental uncertainties into account.

1.4 CHALLENGE

Previous paragraphs stressed the importance of reduced carbon footprint and enhanced energy performance of ship design and operations. The implementation of different technical and operational solutions results in ships that are more complex than in the past [40]. Both ship design and operation regularly involve solving a number of complex optimisation problems [41]. In particular, ship energy systems consist of a large number of interacting components that show non-linear behaviour [42], resulting in optimisation problems of non-linear environmental, social, economic, and technical objective functions, and numerous constraints [43]. Moreover, these objectives depend on many uncertain parameters as fuel, maintenance, and unit capital costs.

Their evaluation requires simulation models which consider different system limits and fidelity level [44], [45]. The trade-off between prediction accuracy and

computational cost determines the model type, application scope, and fidelity level and it has been discussed in the work of many authors [42], [46], [47]. The usual practice in modelling components of ship energy systems is a combination of first principle and semi-empirical models. These models are calibrated on information provided by the component manufacturers or a number of special scale tests in towing tanks [46]–[49], though accumulating modelling discrepancies result in large prediction errors. Validation of those models can also become challenging. At a component level, there is a number of calibration and validation examples [50]–[52]. However, such methodologies at a whole system level are lacking due to limited sensor availability of monitoring platforms and diversity in systems architecture.

Ultimately, the successful integration of different technological and operational solutions requires their assessment on scenarios that are realistic as to the actual conditions at sea [53]. The usual consideration in literature is a limited number, if not only one condition to describe the complex effect of operational and environmental uncertainty at the different design and operational phases [54]–[57]. Therefore, novel methodologies that consider the influence of diverse operational and environmental conditions on energy efficiency are needed [58], [59].

1.5   OPPORTUNITY

The increasing availability of high frequency operational data in contrast to bias-sensitive noon reports has the potential to assist maritime industry with the evaluation of mandatory design and operational measures [60]–[62]. These datasets and advancements in research on data-driven techniques can help the maritime industry evaluate energy performance of ship operations, build computationally efficient and accurate prediction models, and quantify uncertainty. Hybrid models leveraging first-principle and data-driven modelling techniques show improved accuracy and low running times compared to advanced physics-based models [51], [52]. Large datasets of operational data are also used in the calibration and validation of those models [47]. Finally, the use of actual operating profiles or multiple operating conditions improves the accuracy of lifetime energy saving evaluation in optimisation problems [26], [58], [63]–[67]. In this work, we thus provide novel methodologies to account for realistic operating conditions either in the case of assessing operational procedures, developing digital twins that leverage traditional and data-driven methods, and evaluating new energy system designs.

1.6   PROBLEM STATEMENT AND RESEARCH QUESTIONS

Ship designers do not receive feedback on the actual operation of their designs apart from sea acceptance trials. Hence ship design continues even to this day to rely on sets of semi-empirical rules and formulas. Crews operating the vessels do not receive a clear picture of the energy performance and environmental footprint of different options offered to them either. Moreover, people managing a vessel do not have tools that assist them in the comparison of different ship operations from an environmental point of view. The availability of high-frequency operational data provides an opportunity to assist maritime industry in taking a step further,

both in the design and operation of ships. Thus, the following problem statement is answered in this dissertation:

How can the collection, process and use of operational data, hence the feedback shown in Figure 1.3, improve the operation and design of ships from an environmental, financial and technical point of view?

This problem statement leads to a number of research questions. First, on the energy performance assessment of ship operations:

- How can we quantify and depict operational and environmental uncertainty using operational data analysis?

- What energy performance indicators can sufficiently describe ship operations and provide feedback to both designers and operators of the vessels?

- Which parameters influence the attained energy performance?

then on the modelling of ship energy systems:

- Should we use first-principle, statistical, or hybrid models with large operational datasets?

- How can we achieve the best trade-off between prediction accuracy and computational cost?

- What is a suitable prediction model formulation in terms of input, output and utilised parameters?

- What is the selected time-dependency of a model calibrated and validated over large datasets and used in optimisation iterations?

- Are steady-state models used in automotive sufficient in maritime applications?

- What needs to be the modelling fidelity level of different components?

and finally on the optimal design of ship energy systems:

- What is a complete and holistic optimisation framework for topology selection and sizing of different system?

- What are the needed objectives?

- What are the sufficient simulation scenarios to capture actual operational and environmental conditions at sea?

- What are the constraints?

- What is the mathematical optimisation problem type and solving method?

- How can a computational efficient digital twin be used to extend design space exploration?
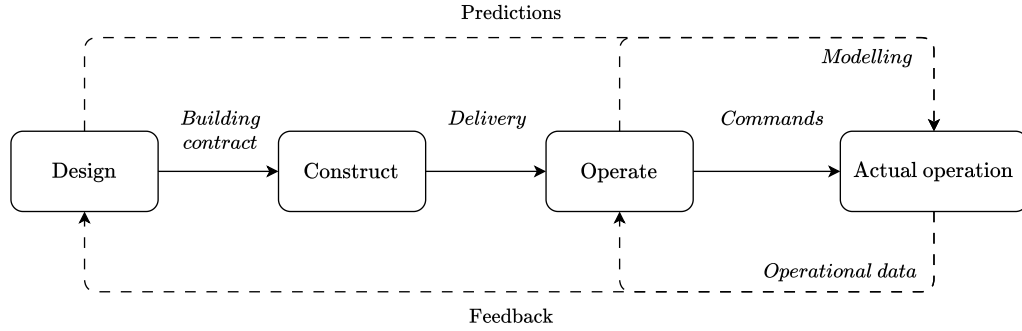
Figure 1.3: The missing feedback to designers and users in the maritime industry.

1.7   STRUCTURE OF THE DISSERTATION

This dissertation is structured around one introductory, three main body and one conclusive chapter. Chapter 2 provides a methodology to assess the energy performance of ship operations using high-frequency operational data, it provides feedback to ship designers and operators, and it describes realistic operational and environmental conditions to be utilised in the design of new ship energy systems. Chapter 3 provides a steady-state digital twin approach for the carbon intensity prediction of ships operation leveraging first-principle and data-driven techniques. It accounts for the aggregate effect of both operational and environmental conditions and balances computational cost and prediction accuracy. Chapter 4 provides a design by optimisation framework for ship energy systems. This framework utilises computationally efficient and accurate digital twin approaches as the one introduced in Chapter 3 and it seeks the trade-off from an environmental, technical, and financial perspective. Finally, Chapter 5 discusses the progress made towards the goal of this dissertation, its limitations, its conclusions and the recommendations for future research.

1.8   CONTRIBUTION

The main contribution of this dissertation with respect to energy performance assessment of ship operations is fivefold:

- It casts light on the actual operational conditions under which vessels, especially multi-function ones, operate.

- It presents a method for enriching an operational dataset in case key parameters are missing, using well-established models.

- It uses the resulting dataset to evaluate the energy performance of the vessel over the whole operational range, not only examining a limited number of operating points.

- It introduces suitable energy performance indicators and visual tools in order not only to assess the previous operation of the vessel, but also in order to assist in enhancing its future performance.

- It examines the impact of design and operational decisions on the resulting energy performance of vessels equipped with hybrid propulsion.

The main contribution with respect to digital twin modelling approaches is a methodology to build a digital twin of ship energy systems that can be used to evaluate operational decisions, design changes, and contribute to enhanced future designs. In particular:

- It accounts for realistic operational and environmental conditions.

- It demonstrates qualitative and quantitative tools for the systematic statistical validation of models of the whole energy system in the presence of large operational datasets.

- It proposes data-driven modelling techniques to compensate for uncertainty related to sensor measurements and the limited availability of information from shipbuilders and component manufacturers.

- It provides a case study that demonstrates the capability of steady-state models coupled with data-driven techniques in accurately predicting fuel consumption over actual dynamic and quasi-static sailing conditions.

- It provides a direct comparison between electrical and mechanical propulsion over actual sailing profiles.

Finally, the main contribution with respect to ship energy system design by optimisation is:

- It provides a complete and holistic optimisation framework for the hybrid propulsion topology selection and system sizing at the concept design stage.

- It uses the existing knowledge on actual operational and environmental conditions variation, result of monitoring vessels of existing classes that serve similar mission types, to find the necessary resolution of examined scenarios.

- This holistic framework takes into consideration environmental, financial and technical objectives, and focuses on the demonstration of competing mechanisms rather than on the case specific individual solutions.

- It demonstrates the stability of the suggested optimisation problem formulation and solving algorithms.

Chapter 1
Introduction

Operational data

Manufacturers &
shipbuilder data

Chapter 2

Ship operation

- physics-informed data
  analysis
- operational and envir/ntal
  uncertainty assessment
- energy performance
  assessment indicators

Chapter 3

Ship energy system
modelling

- machine learning models

- first-principle models

- validation methodology

Chapter 4

Design optimisation

- robust (actual sailing profiles)

- holistic (environmental,
  financial, technical objectives)

- design space exploration

- pareto front design selection

Chapter 5

Reflection

- conclusions   - limitations   - recommendations

Figure 1.4: Structure of this dissertation.

2

ENERGY PERFORMANCE ASSESSMENT OF SHIP OPERATIONS

This chapter is reproduced from [21]:

ABSTRACT

Ship designers hardly ever receive feedback from the actual operation of their designs apart from sea acceptance trials. Similarly, crews operating the vessels do not receive a clear picture on the energy performance and environmental footprint of different options. This chapter proposes an energy performance assessment methodology methodology based on operational data from continuous monitoring. Subsequently, it applies the methodology on an ocean patrol vessel of the Royal Netherlands Navy in order to identify the impact of diverse operational conditions on energy performance over the whole operating range, but also to examine the decision to equip the vessel with hybrid propulsion. Specifically, it introduces the mean energy effectiveness indicator and mean total energy efficiency over discretised vessel speed, as the main tool in quantifying the energy gains and losses to assist in taking better advised design and operational decisions. Moreover, it demonstrates a dataset enrichment procedure, using manufacturers information, in case not all needed sensors are available. Results suggest that electrical propulsion was 15% to 25% less efficient than the best mechanical propulsion mode, and on the overall energy performance of the vessel, increasing speed by 1 knot caused 7% and 14% increase over the minimum CO_2/mile emissions between 8 and 14, and above 14 knots respectively.

2.1 INTRODUCTION

The Intergovernmental Panel on Climate Change has concluded that greenhouse gases together with other anthropogenic factors are extremely likely to be the main cause of global warming and climate change [6]. Future economic growth and transport demand indicate that maritime carbon dioxide emissions will increase

between 50% to 250% by 2050 compared to the 2012 level [10]. At the same time, legislation on energy efficiency enhancement and emissions, such as the IMO Energy Efficiency Design Index (EEDI) and the Ship Energy Efficiency Management Plan (SEEMP) aim to reduce carbon dioxide concentration. However, a reduction in greenhouse gas emissions from shipping, within the same time interval, is only expected in the most conservative and strict scenario.

2.1.1   *Related work*

When evaluating energy performance, naval architects come across high uncertainty regarding the energy performance assessment of their implemented designs [55]–[57]. Required propeller thrust while sailing at a certain vessel speed is one of the main contributors to this uncertainty, which is transferred to the propulsion plant by the component interaction mechanism described in [68]. The main factors causing the uncertainty in propeller thrust are weather conditions, which show strong geographical and seasonal variation, loading conditions [69], fouling level [70], [71], acceleration phases [72] and manoeuvring activity [73]. Aiming to demonstrate the extent of this issue, some studies present their results for a number of resistance-thrust curves as in the case of Geertsma, Visser and Negeborn [46] and Geertsma, Negeborn, Visser *et al.* [49], where three curves corresponding to trial, design and off-design operational conditions were used, while other studies try to find thrust curve bounds as in the case of Haseltalab and Negenborn [74]. It is more common though for authors to assume resistance in calm water with no hull fouling, obtained either from towing tank model tests or from using systematic series and empirical formulas [75], [76], and evaluate added resistance according to ITTC [77] as in [78] and [47].

Another challenge in the design phase is the prediction of the vessel's speed profile. As mentioned by Georgescu, Godjevac and Visser [54], design objectives related to the power supply and propulsion system change at different design phases and the operational profile knowledge level changes as well. System architecture selection at the concept design phase relies significantly on the amount of time spent sailing at various speeds, but unfortunately this knowledge is limited at that stage and its estimation can prove to be difficult especially for naval vessels. This is also the case with decisions at a later phase of the design process such as component sizing, control strategy selection [2], [40], and subsystem working parameters optimisation [79], [80]. Focusing on the aforementioned importance of the operational profile, Yrjänäinen, Johnsen, Dæhlen *et al.* [81] proposed a profiling tool based on high fidelity model-based simulations taking into account historical weather data and task oriented split of the whole vessel's mission requirements. Ultimately, Jafarzadeh and Schjølberg [82] presented the effect of the operational profile at a fleet level, by analysing the profiles for the majority of vessel types sailing in Norwegian waters, while examining hybrid propulsion integration.

2.1.2 *Aim and contribution*

Both thrust requirement and vessel speed profile heavily influence the working points of the propulsion and power supply systems, hence the energy performance of vessels. On the contrary, energy performance assessment of new and existing designs, using EEDI and EEXI, respectively, does not account for the changes in energy performance over the range of actual operational conditions and speeds and thus leads to suboptimal designs [83]. Moreover, the suggested operational energy performance assessment methodologies for all ships using EEOI and CII, although offering a quantification tool for the different carbon dioxide emissions levels within a certain time window, fail to provide insight into how operational conditions influence attained energy performance as partly demonstrated in [84].

This chapter introduces an operational data-driven methodology for the energy performance assessment of ship operations. Its novelty is fivefold:

- It casts light on the actual operational conditions under which vessels, especially multi-function ones, operate.

- It presents a method for enriching an operational dataset in case key parameters are missing, using well-established models.

- It uses the resulting dataset to evaluate the energy performance of the vessel over the whole operational range, not only examining a limited number of operating points.

- It introduces suitable energy performance indicators and visual tools in order not only to assess the previous operation of the vessel, but also in order to assist in enhancing its future performance.

- It examines the impact of design and operational decisions on the resulting energy performance of vessels equipped with hybrid propulsion.

2.2 CASE STUDY SYSTEM DESCRIPTION

The proposed methodology is suitable to investigate the energy performance of ships with electrical propulsion, ships with mechanical propulsion and ships with hybrid propulsion, equipped either with fixed or controllable pitch propellers. It requires data from the ship's monitoring system platform at a regular sampling frequency, typically 1 to 3 seconds. The minimum required parameters are illustrated in Figure 2.1 as measured parameters. In this chapter, the methodology is demonstrated with data from a case study ocean patrol vessel, equipped with hybrid propulsion and controllable pitch propellers, as described in Appendix A.

2.2.1 *Case study dataset*

The Integrated Platform Monitoring System (IPMS) installed on the vessel provides continuous monitoring capabilities for a large number of operational parameters, significantly improving the accuracy of energy performance evaluation over other means, such as noon reports [60]. The dataset used in this analysis consisted of
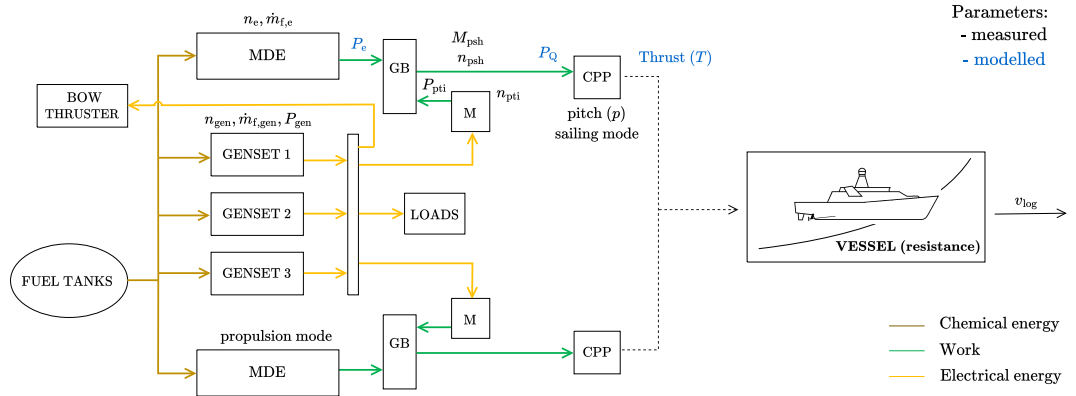
Figure 2.1: Depiction of the vessel's energy system with measured and modelled parameters.

Table 2.1: Logged IPMS parameters used.

Parameter	Symbol
Main diesel engine speed	n_e
Main diesel engine fuel consumption	$\dot{m}_{f,e}$
Diesel generators speed	n_{gen}
Diesel generators power	P_{gen}
Diesel generators fuel consumption	$\dot{m}_{f,gen}$
PTI motor speed	n_{pti}
PTI motor power	P_{pti}
Propeller shaft speed	n_{psh}
Propeller shaft torque	M_{psh}
Propeller pitch	p
Vessel speed through water	v_{log}
Propulsion mode	-
Sailing mode	-

13 276 800 measurements at a 3 seconds time step δt, corresponding to 15 months of operation. The 13 parameters included in this analysis are listed in Table 2.1. In order to clean the data, the dataset was split into a number of voyages rejecting data corresponding to periods that the vessel was out of operation. Some of the voyages were rejected too for containing periods of faulty sensor functioning. This resulted in processing a total number of 3 400 686 measurements per parameter or about 4 months of actual sailing operation.

2.2.2 *Dataset restrictions*

The available dataset does not include parameters for propeller thrust, main diesel engine power and power delivered to the propeller as seen in Figure 2.1. This means that the energy efficiency of the main diesel engines and propellers cannot be directly evaluated using only measured parameters, since knowledge of the input and output power level of each component is needed. All these three parameters were modelled using the available working point parameters and manufacturers'

data. Propeller thrust prediction model was the most complex of all because of the higher number of derived parameters used in corresponding diagrams.

The use of first principle models based on manufacturers data of the performance in factory acceptance conditions assumes the components maintain performance under healthy condition. Therefore, the resulting extended dataset cannot be used to evaluate component energy efficiency degradation. Moreover, the effect of system degradation in the used dataset is expected to be limited, as data was collected during the first 15 months of vessel life. In order to evaluate component, subsystem and system energy efficiency degradation, the following additional sensors should be installed:

- Thrust sensor on the propulsion shaft. This would enable to more accurately establish thrust and evaluate propeller degradation separate from hull fouling and the effect of weather conditions.

- Torque sensor or cylinder pressure measurement system to establish engine mechanical or indicated torque and evaluate engine efficiency degradation.

- Torque sensor close to the propeller. This could be replaced by the torque sensor on the output shaft of the gearbox, to evaluate degradation of gearbox and shaft-line efficiency as one joint efficiency.

2.3 METHODOLOGY

This chapter proposes a novel operational data-driven energy performance assessment methodology that uses logged measurements of a ship's monitoring system. First, the method enriches the data by using manufacturers' specifications and figures to evaluate parameters that were not directly measured. Subsequently, the instant value of a number of energy performance parameters is evaluated at a vessel, power supply and propulsion subsystems, and component level. Finally, mean values and standard deviations of those parameters over discretised vessel speed or main diesel engine speed are used to explore the contributing factors to a vessel's energy performance and CO_2 footprint.

2.3.1 *Dataset enrichment*

Measured IPMS parameters can be found in Figure 2.1. The work described in this dissertation involves the enrichment of the examined dataset with a number of parameters, most importantly total propeller thrust and main diesel engines brake torque, utilising information provided by the shipbuilder and component manufacturers. All relevant figures can be found in Appendix A.

First, propeller shaft power P_{psh} was evaluated in kW using corresponding torque M_{psh} in kNm and speed n_{psh} in rad/s as:

$$P_{\text{psh}} = M_{\text{psh}}\, n_{\text{psh}} \,. \tag{2.1}$$

Then, power delivered by the main diesel engines P_{e}, accounting for gearbox losses $P_{\text{loss,gb}}$, in kW is given from:

$$P_{\text{e}} = P_{\text{psh}} + P_{\text{loss,gb}} \,, \tag{2.2}$$

where gearbox losses $P_{\text{loss,gb}}$ are modelled using the linear torque losses model proposed in [85] and the data provided by the gearbox manufacturer:

$$P_{\text{loss,gb}} = c_2\, P_{\text{e}} + c_1\, n_{\text{e}}{}^2 + c_0\, n_{\text{e}}\ . \tag{2.3}$$

c_0 is equal to 0.0081, c_1 is equal to 9.002e-05 and c_2 is equal to 0.005. Power delivered to the propeller P_{Q} was evaluated afterwards, accounting for shaft losses $P_{\text{loss,psh}}$, in kW from:

$$P_{\text{Q}} = P_{\text{psh}} - P_{\text{loss,psh}}\ . \tag{2.4}$$

Torque propeller shaft losses $M_{\text{loss,psh}}$ were also evaluated using manufacturer's data as a linear function of shaft speed, thus:

$$P_{\text{loss,psh}} = \left(c_3\, n_{\text{psh}} + c_2\right) n_{\text{psh}} = c_3\, n_{\text{psh}}^2 + c_2\, n_{\text{psh}}\ . \tag{2.5}$$

Propeller thrust T in kN and thrust power P_{T} in kW were established using the following relations:

$$T = K_{\text{T}}\, \rho\, n_{\text{psh}}^2\, D^4\ , \tag{2.6}$$

$$P_{\text{T}} = T\, v_{\text{a}}\ , \tag{2.7}$$

where ρ is salt water density equal to $1\,025$ kg/m³, D is propeller diameter in m and v_{a} water speed in the ship's wake in m/s, obtained from vessel speed through water v_{log} in m/s and Taylor's wake factor w as:

$$v_{\text{a}} = v_{\text{log}}\left(1 - w\right)\ . \tag{2.8}$$

Thrust coefficient K_{T} was evaluated by reading the corresponding propeller open water diagram with advance coefficient J and pitch to diameter P/D values. Advance coefficient J was evaluated from:

$$J = \frac{v_{\text{a}}}{n_{\text{psh}}\, D}\ , \tag{2.9}$$

Another important parameter evaluated is effective thrust power P_{TE} in kW, as seen in Figure 2.2:

$$P_{\text{TE}} = T\, v_{\text{log}} = \frac{T\, v_a}{(1 - w)} = \frac{P_T}{(1 - w)}\ , \tag{2.10}$$

and finally, required propeller thrust T_{req} in constant speed sailing was evaluated as a reference for obtained results, using ship towing resistance R_{tow} and thrust deduction factor t from towing tank tests, as:

$$T_{\text{req}} = R = \frac{R_{\text{tow}}}{1 - t}\ . \tag{2.11}$$
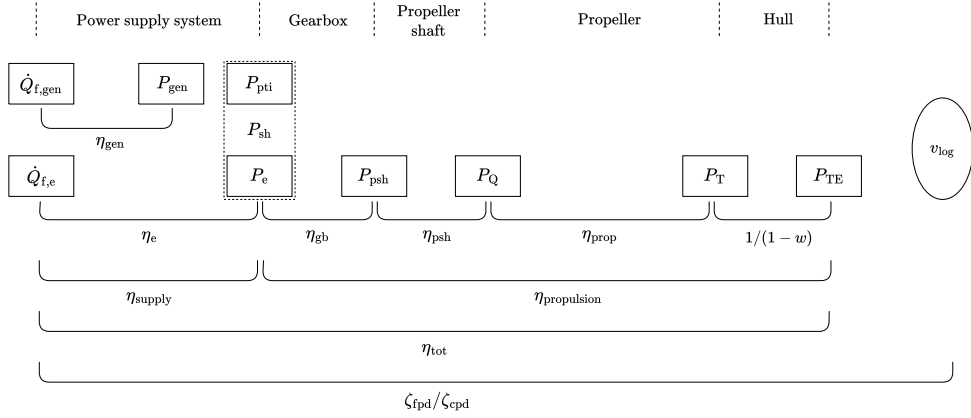
Figure 2.2: Energy performance indicators and parameters involved.

2.3.2 Energy efficiency

The majority of ships use fossil fuels in order to meet their power supply needs. The three main consumers on each ship in descending order are its main and auxiliary engines, and its boilers. Boilers' contribution is almost neglegible for all vessel types except for oil tankers [10]. In conventional maritime power systems, chemical energy saved in fuels is released as heat through combustion. Main engines, most often diesel engines, convert this heat into work and provide it to the propellers either directly or through reduction gearboxes. Then, propellers turn this work into propulsion thrust in order to counter vessel resistance and accelerate the vessel. Auxiliary diesel engines on the other hand convert heat to work, work to electrical power and provide it to the electrical grid of the ship. These power conversions and transmissions introduce a number of component, subsystem and whole system energy efficiencies which in this study are evaluated from measured and derived parameters as described in Section 2.3.1.

2.3.2.1 Component level

Main diesel engine efficiency η_e is defined as:

$$\eta_e = \frac{P_e}{Q_{f,e}} = \frac{P_e}{\dot{m}_{f,e}\, h^L} \,, \tag{2.12}$$

where $Q_{f,e}$ is heat flow released from fuel combustion in kW, $\dot{m}_{f,e}$ is fuel consumption in kg/s and h^L stands for fuel lower heating value assumed equal to 42,500 kW/kg. Diesel generator set efficiency η_{gen} is defined in a similar way:

$$\eta_{gen} = \frac{P_{gen}}{Q_{f,gen}} = \frac{P_{gen}}{\dot{m}_{f,gen}\, h^L} \,, \tag{2.13}$$

where P_{gen} is the electrical power provided in kW, $Q_{f,gen}$ corresponds to heat flow in kW and $\dot{m}_{f,gen}$ to fuel consumption in kg/s. Gearbox efficiency η_{gb} is defined as:

$$\eta_{gb} = \frac{P_{psh}}{P_{sh}} \,, \tag{2.14}$$

where P_{psh} is power delivered to the propeller shaft in kW and P_{sh} is the power provided by the main diesel engines or the electrical motors to the intermediate shaft in kW, as follows:

$$P_{sh} = \begin{cases} P_e & \text{Other modes} \\ P_{pti} & \text{PTI mode} \end{cases} . \tag{2.15}$$

Propeller shaft efficiency η_{psh} is evaluated using power delivered to the propeller shaft P_{psh} and to the propeller P_Q in kW, as:

$$\eta_{psh} = \frac{P_Q}{P_{psh}} . \tag{2.16}$$

Finally, propeller efficiency η_{prop} is provided by:

$$\eta_{prop} = \frac{P_T}{P_Q} = \frac{T \, v_a}{P_Q} , \tag{2.17}$$

and open water propeller efficiency $\eta_{prop,ow}$ using required propeller torque in open water testing conditions $M_{Q,ow}$ by:

$$
\begin{aligned}
\eta_{prop,ow} &= \frac{P_T}{P_{Q,ow}} = \frac{T \, v_a}{M_{Q,ow} \, n_{psh}} \\
&= \frac{K_T \, \rho \, n_{psh}^2 \, D^4}{K_{Q,ow} \, \rho \, n_{psh}^2 \, D^4} \frac{v_a}{D \, n_{psh}} = \frac{K_T}{K_{Q,ow}} J .
\end{aligned}
\tag{2.18}
$$

2.3.2.2 System and subsystem level

Power supply and propulsion subsystems energy efficiency was evaluated using total heat flow $Q_{f,tot}$, shaft power P_{sh} for both power supply options defined in Equation 2.15, and effective thrust power P_{TE} in kW as:

$$\eta_{supply} = \frac{P_{sh}}{Q_{f,tot}} = \frac{P_{sh}}{\left(\dot{m}_{f,e} + \dot{m}_{f,gen} \right) h^L} , \tag{2.19}$$

$$\eta_{propulsion} = \frac{P_{TE}}{P_{sh}} . \tag{2.20}$$

Ultimately, energy efficiency of the whole power system was provided by:

$$\eta_{tot} = \frac{P_{TE}}{Q_{f,tot}} = \frac{P_{sh}}{Q_{f,tot}} \frac{P_{TE}}{P_{sh}} = \eta_{supply} \, \eta_{propulsion} . \tag{2.21}$$

It must be noted that effective thrust power P_{TE} was selected as the end point of the energy chain defined in Equation 2.10, instead of effective towing power P_E seen in [86]. The main reason is that this analysis examines the dynamic energy performance of the system while sailing under real operational conditions, on the contrary to static considerations at the design phase, which are established through scale model tests. As a result a thrust based power parameter seems more suitable compared to ship's towing R_{tow} or actual resistance R. Moreover, despite the IPMS dataset restrictions described in Section 2.2.2, thrust parameter T can be directly

measured using a thrust sensor. On the contrary, evaluation of actual resistance R requires knowledge of the vessel's actual and hydrodynamic added mass and acceleration. In the case of using towing resistance R_{tow}, which is a theoretical parameter as the vessel is not towed, information concerning thrust deduction factor t is additionally needed.
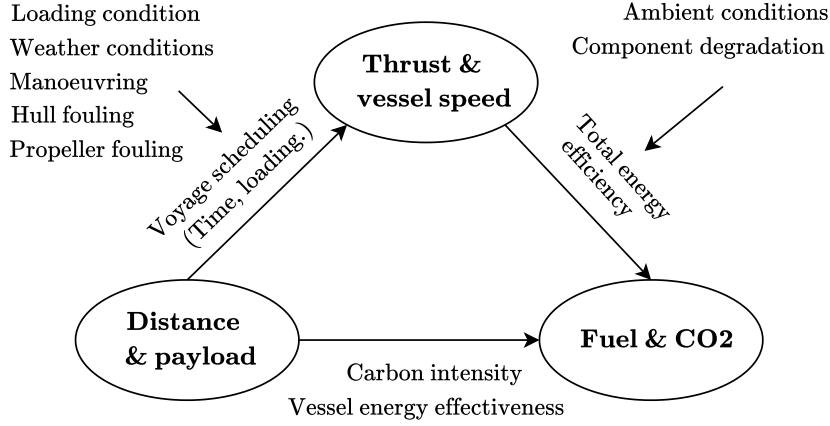
Figure 2.3: Illustration of the relation between vessel energy effectiveness, total energy efficiency and influencing factors.

2.3.3 *Vessel energy effectiveness*

Mission requirement of most vessels is the transportation of a certain payload over an indicated distance. This is achieved, as discussed in the previous subsection, by consuming fuel resources into their power systems. Energy efficiency η_{tot} of the whole system provides a good indication on the fraction of resources that turns into useful output, but it does not offer though any information on the amount of resources required by the vessel in the first place. A factor providing resources 'paid' in order to reach a certain transportation level seems more appropriate. Effectiveness, in contrast to efficiency, appears to conceptually describe this difference to an adequate degree, hence is the term selected in this analysis. Figure 2.3 provides a graphical representation of the used terminology and the influencing factors.

Literature on mechanical engineering applications, specifically on heat exchange applications, determines effectiveness as the ratio of actual heat transfer rate to the theoretical maximum [87], [88], but such a consideration in the case of energy conversion and transmission is already described by exergy or also called rational efficiency [89]. Finally, Sui, Stapersma, Visser *et al.* [47] also discuss the use of this term in the energy analysis of maritime systems, but proceed with a different set of definitions.

In this study, we use in the assessment of the vessel's energy performance, the energy effectiveness indicator defined as:

$$\zeta = \frac{M_{\text{f,tot}}}{W\,d} = \frac{\dot{m}_{\text{f,tot}}}{W\,v}\,, \tag{2.22}$$

where $M_{f,tot}$ is the total amount of fuel consumed, d is the covered distance, v is vessel speed, and W a typical transportation weight.

When deadweight and displacement do not show significant variation, as in the case of patrol vessels, we can ignore the weight term W and consider covered distance as the main operational benefit. By further not accounting for current effects, vessel speed through water v_{log} is used. Consequently, energy effectiveness indicator is provided by:

$$\zeta_{fpd} = \frac{\dot{m}_{f,tot}}{v_{log}} = \frac{\dot{m}_{f,e} + \dot{m}_{f,gen}}{v_{log}} \; . \tag{2.23}$$

Accounting for the environmental impact and aligned with the indices and indicators introduced by IMO, the cost of sailing can also be expressed by the production of carbon dioxide emissions $\dot{m}_{CO_2}$. The energy effectiveness indicator can also be written then as:

$$\zeta_{cpd} = \frac{\dot{m}_{CO_2}}{v_{log}} = \frac{\dot{m}_{f,tot} \, f_{CO_2}}{v_{log}} \; , \tag{2.24}$$

where f_{CO_2} is the mass ratio constant between carbon dioxide emissions and fuel. Fuel composition plays an important role on this constant. The first IMO greenhouse gas study [15] suggested a value of 3.170 for all fuel types, the second study [16] a value of 3.021 for heavy fuel oil and 3.082 for marine gas and diesel oils, while EEDI calculation methodology a value of 3.110.

2.3.3.1 *Mean energy effectiveness indicator and standard deviation*

Vessels sail in operational conditions that vary a lot, posing different energy requirements. Application of all previously mentioned energy efficiency and effectiveness indicators results in a population of instant values as seen for instance in the case of propeller thrust in Figure 2.4. Despite the fact that these populations provide the limits of actual vessel operation, they do not offer any information on the achieved energy performance of the vessels.

In order to overcome this issue, this methofdology introduces weighted mean energy effectiveness indicator ζ_{fpd} and corresponding standard deviation ζ_{fpd_σ} over discretised vessel speed v as the main energy performance assessment tool utilizing operational data, as follows:

$$\zeta_{fpd_\mu}(v) = \frac{\sum\limits_{i=1}^{n} \zeta_{fpd_i} N_i}{\sum\limits_{i=1}^{n} N_i} \; , \tag{2.25}$$

$$\zeta_{fpd_\sigma}(v) = \sqrt{\frac{\sum\limits_{i=1}^{n} \left(\zeta_{fpd_i} - \zeta_{fpd_\mu} \right)^2 N_i}{\sum\limits_{i=1}^{n} N_i - 1}} \; , \tag{2.26}$$

where ζ_{fpm_i} is one of the n different energy effectiveness indicator values found within the limits $[v - \delta v/2, v + \delta v/2)$, and N_i play the role of weights, being the number of measurements for each different value i. The same formulas were used for
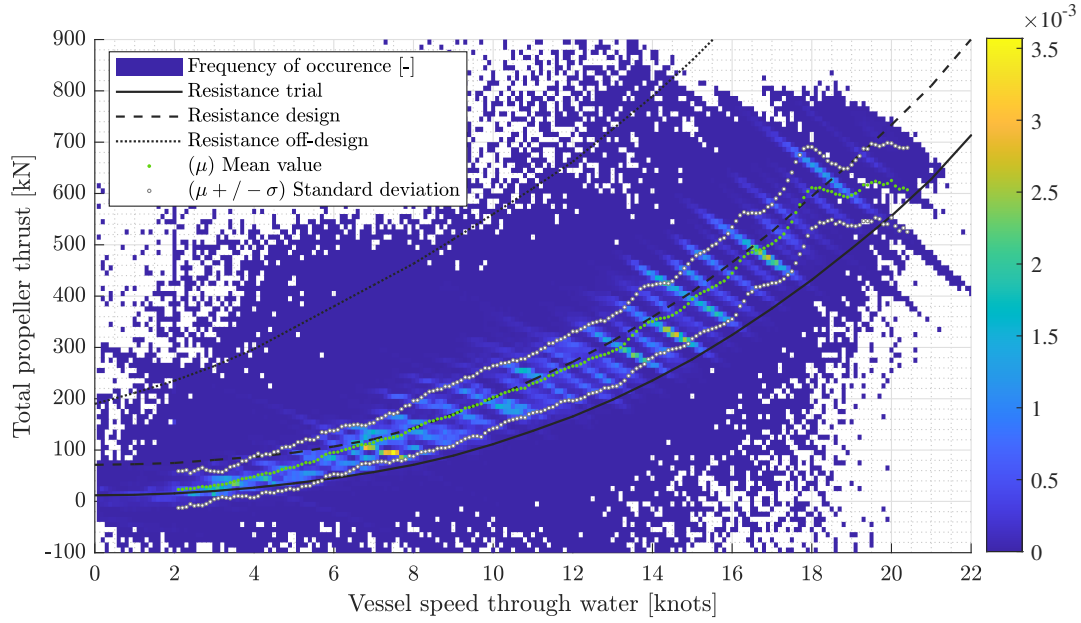
Figure 2.4: Two dimensional histogram, mean value, and standard deviation of evaluated total propeller thrust over discretised vessel speed.

Table 2.2: Reference weather and fouling conditions.

Condition	Sea state	Wind speed	Fouling
trial	0	max 5 knots	no
design	4	max 21 knots (Beaufort scale 5)	6 months out of dock
off-design	6	max 47 knots (Beaufort scale 9)	6 months out of dock

calculating discretised mean value and standard deviation of every other parameter or energy performance indicator.

Finally, the importance of mean energy effectiveness indicator can be seen from its relation to the actual amount of fuel consumed while sailing at a certain speed $M_f(v)$ and the carbon dioxide emissions $M_{CO_2}(v)$, which are provided by:

$$
\begin{aligned}
M_f(v) &= \sum_{i=1}^{n} \dot{m}_{f,tot_i} \, N_i \, \delta t \;=\; \dot{m}_{f,tot_\mu} \sum_{i=1}^{n} N_i \, \delta t \\
&= \frac{\dot{m}_{f,tot_\mu}}{v} \, v \, N_{tot} \, \delta t \;=\; \zeta_{fpd_\mu} \, v \, N_{tot} \, \delta t \,,
\end{aligned}
\tag{2.27}
$$

and

$$
M_{CO_2}(v) \;=\; \zeta_{cpd_\mu} \, v \, N_{tot} \, \delta t \,.
\tag{2.28}
$$

Equations 2.27 and 2.28 suggest that using an estimation of the mean energy effectiveness indicators $\zeta_{fpd_\mu}(v)$ and $\zeta_{cpd_\mu}(v)$ over the whole vessel speed range and of the operational profile $N_{tot}(v)$, we can estimate the total amount of required fuel and carbon dioxide emissions within a certain time horizon, necessary in life-cycle assessment analyses.

This section presents and discusses the results of the proposed methodology with the case study *Holland* class patrol vessel. First, it discusses the operational uncertainties under which the vessel sailed. Then, it demonstrates the use of mean energy effectiveness indicator in describing the energy performance of the vessel, both within an examined period and for future predictions, and it also stresses the importance of vessel speed profile in life cycle fuel cost assessments. Next, it demonstrates how total system, subsystem and component energy efficiency analysis can be used to improve the design and provide feedback to operators on the available operational modes, and finally, it discusses on the decision to adopt hybrid propulsion by the case study vessel.

2.4.1   *Operational uncertainties*

The impact of the various uncertainties that influence the operating profile and therefore energy performance of multifunction vessels is best demonstrated by the thrust distribution that the vessel encounters, presented in the dimensions vessel speed and thrust. Figure 2.4 shows the frequency of occurence, mean value and standard deviation of thrust, against three curves used at the design phase of the vessel. Those curves correspond to trial, design and off-design operational conditions, and they were produced by running model tank tests. Their description is given in Table 2.2. This figure clearly demonstrates that propeller thrust during normal operating conditions can actually vary as much as 25% of its nominal value, within the one standard deviation range, near full speed and 100% near half speed. This variation is caused by environmental factors like wind and waves, by operational factors like loading condition and rudder activity, by maintenance conditions such as propeller and hull fouling, and also by ship acceleration and deceleration. The evaluated mean propeller thrust is in good agreement with the
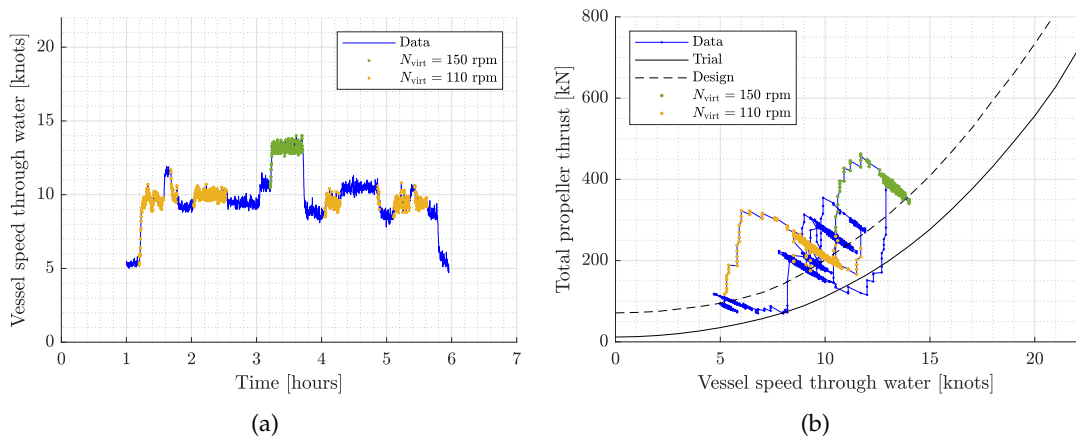
Figure 2.5: Propeller thrust (b) and vessel speed through water (a) with highlighted areas of bounded virtual shaft speed. Hypothetical acceleration and deceleration phases are also demonstrated.

design curve, being equal between 8 and 10 knots and within 5% between 7 and 18 knots. Below 7 knots, however, the design curve does not intersect zero thrust

at zero ship speed, as it assumes head wind. Therefore, the quadratic fit through the design resistance at an intermediate speed of 7 to 10 knots should be assumed for low ship speeds, up to 7 to 10 knots, to account for wind from all directions, if measured mean value of thrust is not available. Above 18 knots, mean thrust leans towards the trial conditions curve. The resulting mean value of evaluated thrust as a function of ship speed is a good measure for life cycle analysis, as it accounts for the average load over the various ship speeds. Furthermore, we observe that thrust is indeed bounded between the trial and off-design curves, but the vessel hardly ever sailed in such adverse weather conditions as described by the off-design curve. Thus, using this curve as a design driver might be over-conservative.

Figure 2.4 also shows that the thrust-vessel speed distribution is not uniformly distributed. Diagonal areas of increased frequency of occurrence exist. As demonstrated in Figure 2.5, these areas refer to constant virtual shaft speed setting, provided by:

$$n_{\text{virt}} = \frac{p - p_0}{p_{\text{nom}} - p_0} n_{\text{prop}} \, , \tag{2.29}$$

where p is propeller pitch, p_0 is zero thrust pitch, p_{nom} is nominal pitch and n_{prop} is propeller speed. According to Geertsma, Negeborn, Visser *et al.* [49], virtual shaft speed, being linearly related to vessel speed is the command provided by the crew to the propulsion system. This means that in order to either accelerate or decelerate to a different sailing speed, an increased or decreased virtual shaft speed is set. Due to vessel inertia, thrust moves to another diagonal under almost constant speed and then speed and thrust balance at the intersection point with the theoretical resistance curve shown in the same figure.
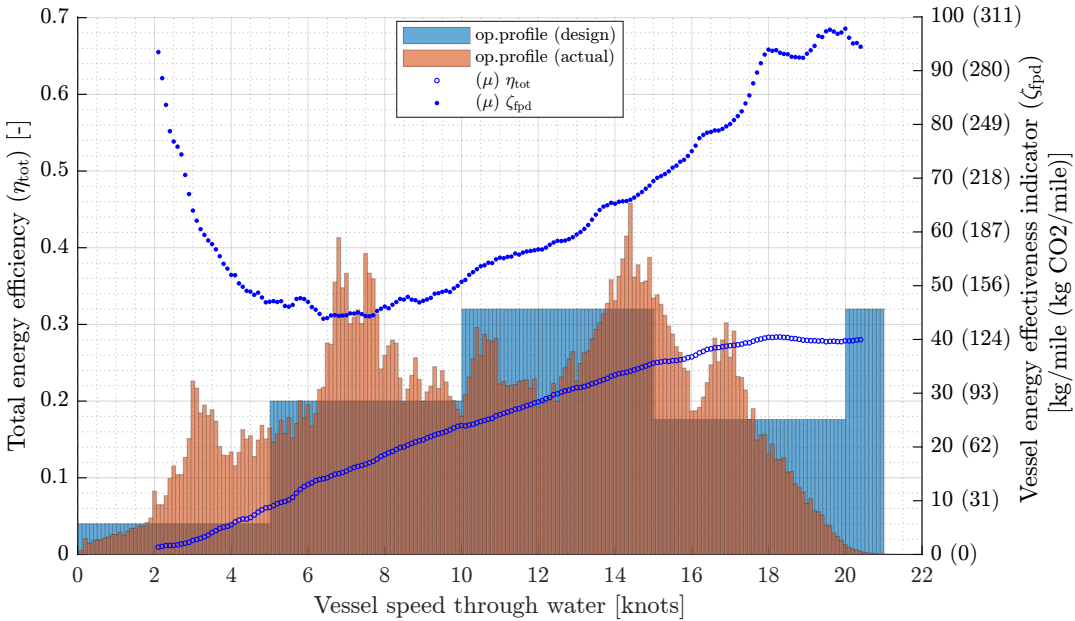
Figure 2.6: Mean energy effectiveness indicator and mean total energy efficiency over discretised vessel speed, with additional demonstration of the difference between the design and the actual vessel speed profile.

2.4.2   *Vessel's energy performance and CO$_2$ footprint*

This chapter introduced the use of mean energy effectiveness indicator, providing the fuel-carbon resource cost of sailing at a certain vessel speed under various operational conditions, as the main tool in quantifying the obtained energy performance and carbon dioxide footprint of ships within an examined period. It also distinguished between energy effectiveness, and total energy efficiency expressing the ability of the system to exploit a certain amount of fuel resources. Figure 2.6 visualises this information by presenting mean energy effectiveness indicator and mean total energy efficiency against discretised vessel speed through water.

The results suggest that although mean total energy efficiency gradually increases to its maximum value of 28% near full speed, mean energy effectiveness indicator shows a convex curve behaviour with a minimum value of 44 kg/mile or 137 kg CO_2/mile near 7 knots, and maximum values of 95 kg/mile or 296 kg CO_2/mile and 98 kg/mile or 305 kg CO_2/mile at 2 and 20 knots respectively. Specifically:

- Below 4 knots mean energy effectiveness indicator increases by 20 kg/mile or 62 kg CO_2/mile per 1 knot drop.

- Between 4 and 6 knots mean energy effectiveness indicator increases by 3.5-4 kg/mile or 11-12 kg CO_2/mile per 1 knot drop.

- Between 6 and 8 knots mean energy effectiveness indicator is almost constant, equal to 45-46 kg/mile or 140 kg CO_2/mile.

- Between 8 and 14 knots mean energy effectiveness indicator increases by 3 kg/mile or 9.3 kg CO_2/mile per 1 knot increase.

- Above 14 knots mean energy effectiveness indicator increases by 6 kg/mile or 18.6 kg CO_2/mile per 1 knot increase.

Mean energy effectiveness indicator can also be used in life cycle fuel cost and carbon emissions analyses, when specific operational conditions are not taken into account, coupled with the prediction of the vessel's speed profile, according to Equations 2.27 and 2.28.

Figure 2.6 also presents the difference between the actual vessel's speed profile, which is associated with the high frequency of occurence of certain virtual shaft speed settings shown in Figure 2.4, and the design profile reported in [90]. The crew sailed more frequently below 10 knots, less frequently between 10 and 14, and more frequently between 14 and 17 knots. It also sailed less above 17 knots, and hardly ever sailed above 20 knots while the design scenario considered 8% of total sailing time. The design scenario, which considered increased fuel consumption by 25%, suggests key sailing speeds of 14 to 15 and 19 to 21 knots, while our analysis indicates 14 to 16, and 17 knots.

2.4.3   *Energy performance on different operational modes*

The previous section discussed the use of mean energy effectiveness indicator, instead of EEOI or CII, in the energy performance assessment of ships. Important
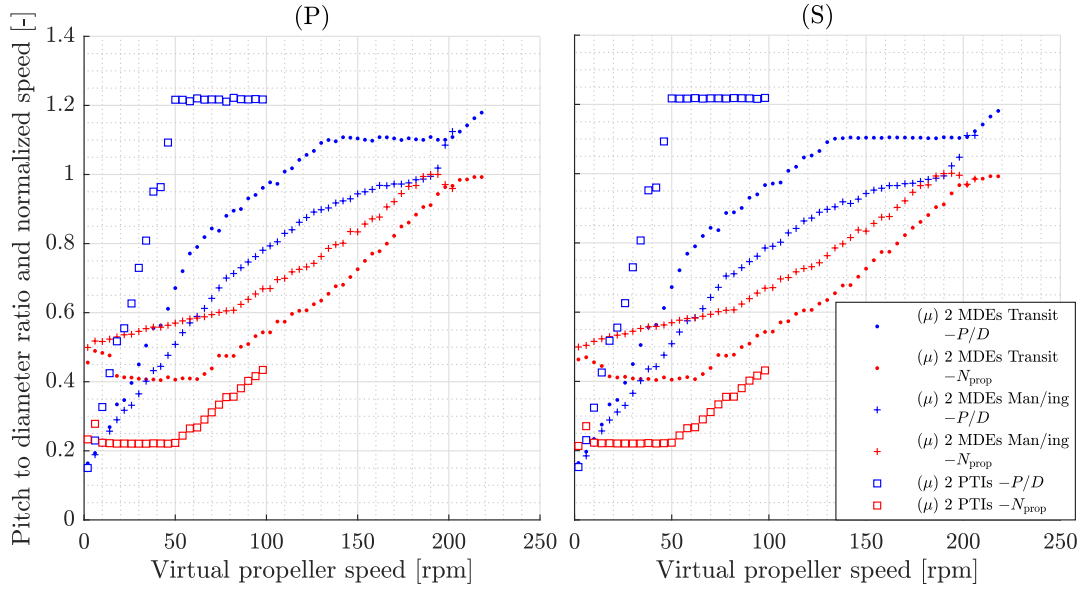
Figure 2.7: Mean value pitch to diameter and rotational speed over discretised virtual shaft speed of port (P) and starboard (S) propellers.
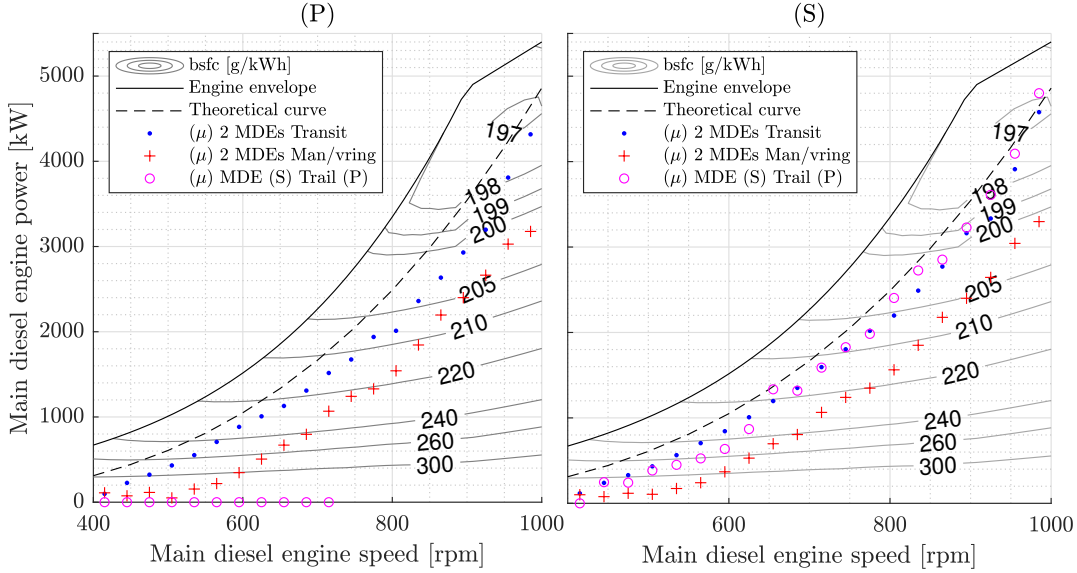
Figure 2.8: Working points of port (P) and starboard (S) main diesel engines, on 1 MDE trailing and 2 MDEs transit and manoeuvring modes.

advantage of our proposed methodology is the additional feedback it provides on the design and use of the different available operational modes, accounting for actual operational conditions.

2.4.3.1 *Description of the available operational modes*

The vessel can sail on one of the six different operational modes found in Table 2.3. Figure 2.7 provides the resulting combinator curves for the four operational modes used by the crew under normal mission requirements, and Figure 2.8 the resulting working points of the main diesel engines. Sailing on 2 MDEs manoeuvring mode
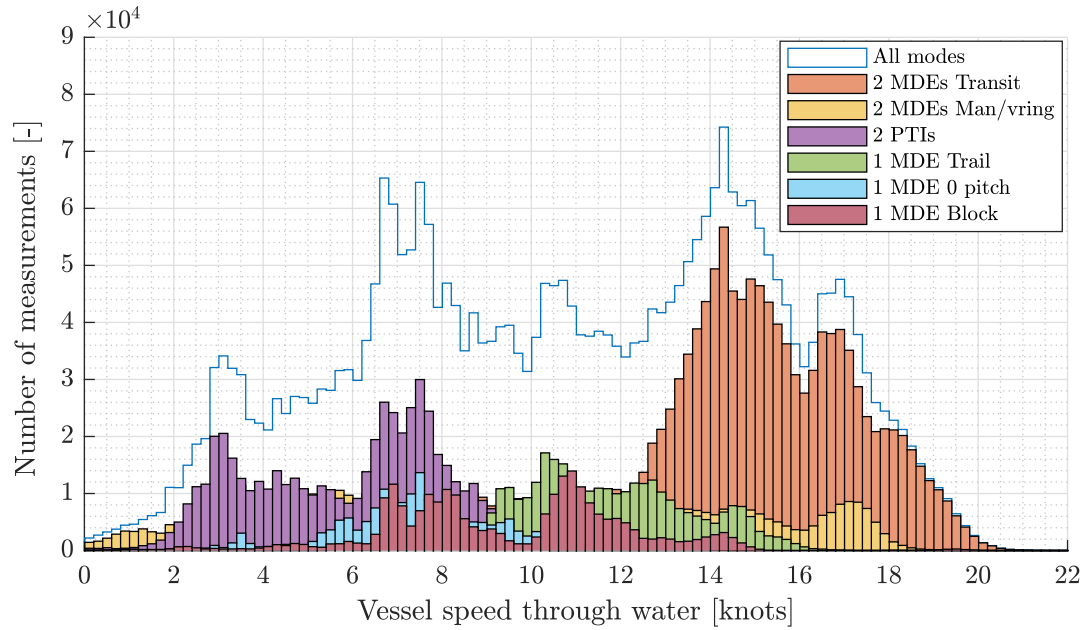
Figure 2.9: Vessel speed profile of all operational modes.

Table 2.3: Operational modes.

2 main diesel engines	transit
	manoeuvring
1 main diesel engine	trailing at full pitch
	shaft brake at 0-pitch
	blocked shaft at full pitch
2 electrical motors	

involves a conservative pitch strategy in comparison to transit mode, resulting in higher propeller speed. The decreased pitch value is a measure against diesel engine overloading, thus manoeuvring mode should be used mainly during operations with high manoeuvrability requirements, such as entering and leaving port, close-quarters operations and emergency manoeuvres. 2 PTIs mode on the other hand increases directly to maximum pitch, since the electrical motors can provide maximum torque without the risk of overloading. Moreover, 1 MDE trailing mode also involves a conservative pitch strategy compared to the 2 MDEs transit mode, as the whole load is provided by one engine. The trailing shaft is let to move freely at full pitch, although being restricted to maintain at least 50 rpm, thus not allowing sailing below 9 knots. Propelling on one main diesel engine offers another two options regarding the second shaft. 0-pitch mode includes the second propeller to reduce its speed by setting zero pitch. This mode normally precedes the final option of the blocked mode, when the shaft brake brings the second propeller to a full stop at full pitch. 0-pitch and blocked modes are usually selected when the vessel undergoes some kind of propulsion system maintenance. Furthermore, Figure 2.9 provides how often and at what speed are the operational modes used. 2 MDEs-transit is the most frequently used mode above 12 knots, while 2 PTIs mode is the most frequently used below 9 knots. 2 MDEs-manoeuvring mode is used across almost the whole
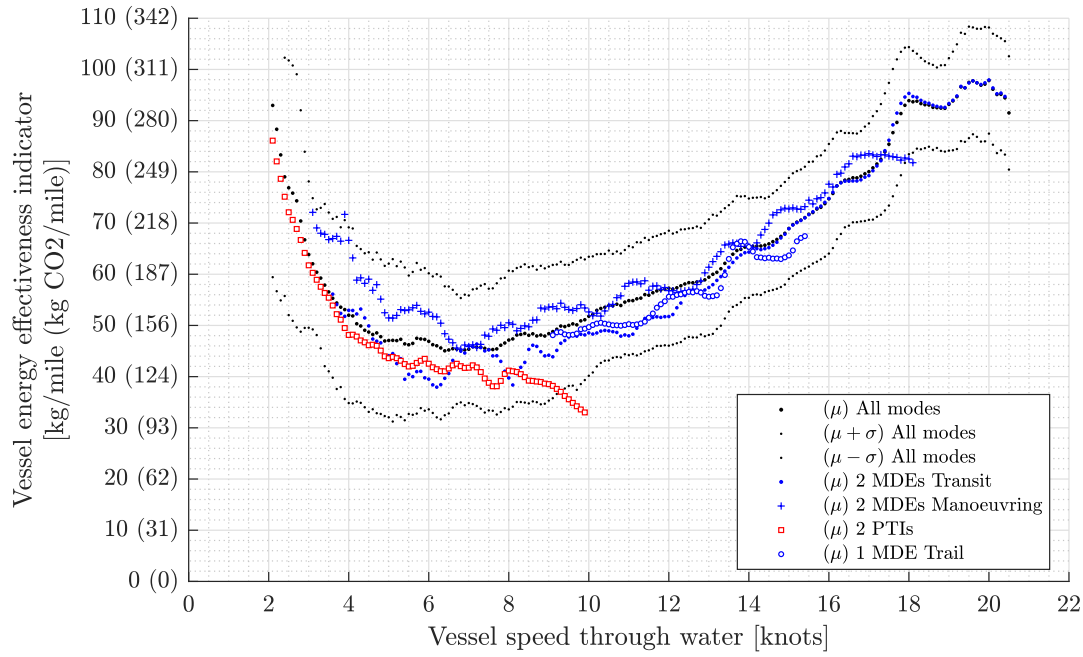
Figure 2.10: Mean value and standard deviation of the energy effectiveness indicator, over discretised vessel speed, on the main operational modes.

speed range, although not being the primary choice at any of them. Finally, one main diesel engine operation, especially on trailing mode, is used regularly between 9 and 16 knots.
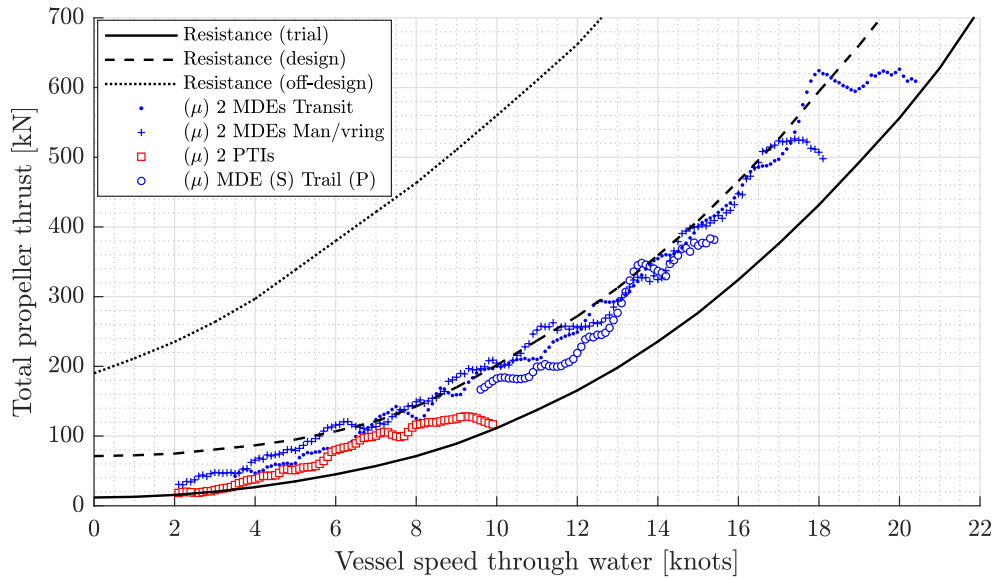
Figure 2.11: Mean value of the evaluated total propeller thrust on the main operational modes.

2.4.3.2   *Energy effectiveness on different operational modes*

Figure 2.10 presents the two dimensional distribution of vessel energy effectiveness indicator and the corresponding standard deviation curves. We observe that the effect of the non-uniformly distributed virtual shaft speed settings seen in Figure 2.4 is also visible in this figure, and that standard deviation varies between 15 kg/mile below 10 knots, and 10 kg/mile above 10 knots. This corresponds to 30% and 15% of mean value respectively, and it clearly suggests that the selection of operational mode and varying operational conditions can significantly affect the resulting energy performance of the vessel within short time windows.

Figure 2.10 also provides the mean energy effectiveness indicator curves for the four main operational modes. We observe that mean energy effectiveness indicator can vary significantly among the different modes. 2 MDEs transit mode appears to be the most effective mode above 10 knots with the exception of some short speed ranges. 2 MDEs manoeuvring mode on the other hand was clearly the less effective mode. 1 MDE trail mode shows a slightly better energy performance than the trasit mode above 13 knots and finally, 2 PTIs mode shows a similar energy performance with transit mode below 6.5 knots, and a clearly better performance between 6.5 and 10 knots.

2.4.3.3   *The effect of required thrust on energy effectiveness*

The mean energy effectiveness indicator when sailing on 2 PTIs was significantly lower than on all other modes above 6.5 knots, suggesting that electrical propulsion offers significant fuel savings. However, comparing mean total energy efficiency of the system, as discussed in the next section, reveals that transit mode was more efficient. The lower mean energy effectiveness indicator value is caused by the fact that running on the electrical motors was selected while sailing on a lighter propeller curve as seen in Figure 2.11, mainly under favourable weather conditions as supported by the corresponding actual wind histograms in Figure 2.12. In order
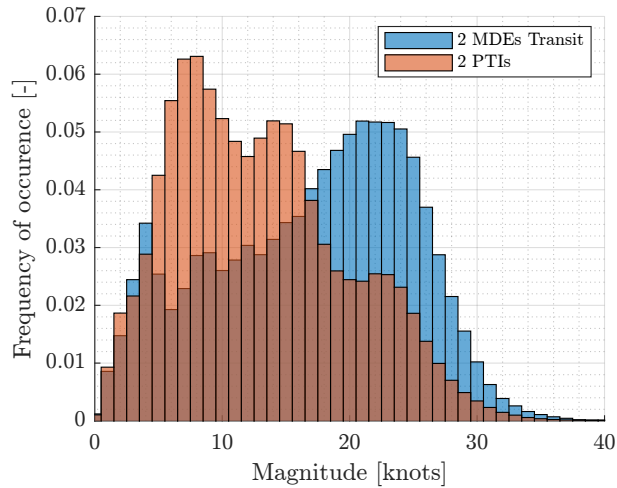
Figure 2.12: Histograms of actual wind speed in the longitudinal direction, where negative values correspond to head wind. Results bounded between 3.5 and 10 knots of sailing speed.

to understand this better, we need to examine the following equation on the relation of energy effectiveness indicator ζ with required propeller thrust T, total energy efficiency η_{tot}, and fuel calorific value h^L. Based on Equations 2.22 and 2.21, and furthermore by ignoring the typical weight W as discussed in Section 2.3.3:

$$\zeta = \frac{\dot{m}_{\text{f,tot}}}{v} = \frac{\dot{m}_{\text{f,tot}}\, h^L}{T\, v}\frac{T}{h^L} = \frac{1}{\eta_{\text{tot}}}\frac{T}{h^L}\,. \tag{2.30}$$

This equation suggests that the vessel's energy effectiveness while sailing at a certain speed is directly linked to the highly uncertain thrust requirement. Therefore, mean energy effectiveness indicator curves presented in Figure 2.10 describe the attained energy performance on the different operational modes, but they correspond to the operational conditions under which those modes were used. Already in Figure 2.11, we can find mean thrust for the examined modes. It is apparent that mean energy effectiveness curves qualitatively follow the mean thrust curves on each mode.

In order to make a more fair energy performance comparison among different operational modes, we examine the total energy efficiency of the system. Energy efficiency at a whole system and subsystem level is mainly determined by the component working points. While the working points shift due to changing thrust requirements for a given virtual shaft speed setting, the total energy efficiency change is indirect, and of a significantly lower scale than the thrust level change itself.

2.4.3.4 *Energy efficiency on different operational modes*

Figure 2.13 presents the comparison of the mean total system energy efficiency over discretised vessel speed for the different operating modes. This figure shows that the most energy efficient mode was the 2 MDEs transit one, with a maximum value of mean total energy efficiency equal to 28.5% at 18 knots. Manoeuvring mode was approximately 10 to 15% less efficient above 7 knots, and 1 MDE trail mode was 10 to 20% less efficient. Subsystem and component efficiency plots, shown in Figures 2.14, 2.15 and 2.16, indicate the main cause in both cases was the inferior propeller efficiency. Figure 2.7 suggests that this happens because of the the reduced pitch of the manoeuvring mode required to ensure the main engine has more margin to support faster acceleration of the engine and ship, and by the increased propeller speed of the trailing mode in order to provide all thrust by a single shaft. Finally, Figure 2.8 also confirms that the engine is operated at a conservative operating strategy as stated in [46], as the mean operating points in transit mode are well below the theoretical propeller curve.

2.4.4 *Hybrid propulsion*

Hybrid propulsion was selected for the case study patrol vessel in order to prevent main engines fouling and improve energy efficiency at low speed, as diesel engines operating at low power risk fouling due to carbon build-up and show high specific fuel consumption. Figure 2.13, however, shows that the overall power system energy efficiency of running on the electric motors in 2 PTIs mode was 15 to 25% worse than on the 2 MDEs transit mode. The subsystem efficiencies, presented in Figures 2.14

and 2.15 and the component efficiencies in Figure 2.16 provide insight into the cause of the poor efficiency of the 2 PTIs mode. Figures 2.14 and 2.15 clearly show that despite mean propulsion efficiency on the electrical motors improves compared to the 2 MDEs transit mode by up to 10% above 6 knots, mean power supply efficiency is significantly lower by 15% to 25%. Nevertheless, if mission requirements allow low speed transit, it is still advisable to sail near the maximum power of the electrical motors as long as engine fouling is still prevented, since the energy effectiveness in that speed range is low and the amount of fuel consumed is comparably less than at higher speeds.

First, we examine the components of the power supply subsystem. Mean diesel generators energy efficiency was between 32 and 35% when running on the electrical motors, compared to 34% on 2 MDEs transit mode. This is already 3% lower than the mean main diesel engine energy efficiency. We also need to consider that an electrical motor's nominal energy efficiency is usually equal to 94-97% [91]. The optimal power allocation of the diesel generators could bring significant energy efficiency gains, as running on three instead of two generators causes the efficiency to drop by 5 to 10%, as seen in Figure 2.17. This is also the case though when not running on the electrical motors, as the diesel generator efficiency can be improved by 10%, from 36% to 40%, by running one diesel generator instead of two diesel generators as soon as the risk of total electrical failure due to generator failure is acceptable.

On the propulsion subsystem efficiency, gearbox losses on the electrical motors are very high, equal to 7% at 9 knots and 12% at 6 knots, which is 5% less efficient than in transit mode. This is caused by the extra-stage double reduction gearbox needed to reduce the 1 800 rpm to 105 rpm. This additional reduction stage could have been prevented by selecting an electric motor with a nominal speed of 450 rpm, with 8 pole pairs instead of 2. If the electric motor had been fitted directly on the shaft, all gearbox losses could have been omitted completely. However, this would have required a significantly larger and more expensive electric motor.

2.5 CONCLUSIONS AND FUTURE RESEARCH

Maritime industry must reduce its greenhouse gas emissions in the coming decades. While indices and indicators as the EEDI and EEOI are useful in the energy performance assessment of cargo vessels, they do not provide sufficient insight into the operation of multifunction vessels with diverse operational profiles. In order to provide this insight, operational uncertainties need to be addressed, so as to improve both the design and the use of vessels for the actual operational conditions. In this direction, this chapter proposed a novel operational data-driven methodology, that uses logged measurements of a ship's automation system, which was applied on the energy performance and environmental footprint assessment of an ocean patrol vessel belonging to the Royal Netherlands Navy.

Ships equipped with mechanical, electrical and hybrid propulsion can benefit from the following conclusions and recommendations on the methodology:
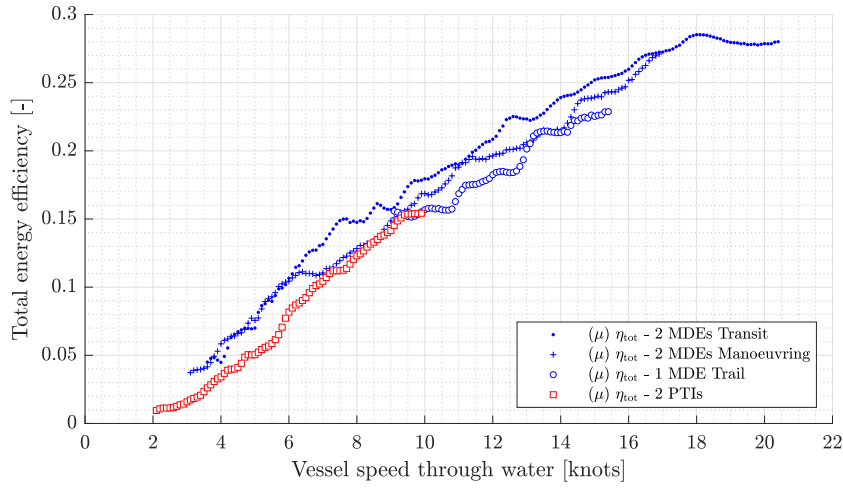
Figure 2.13: Mean total energy efficiency over discretised vessel speed on the main operational modes.
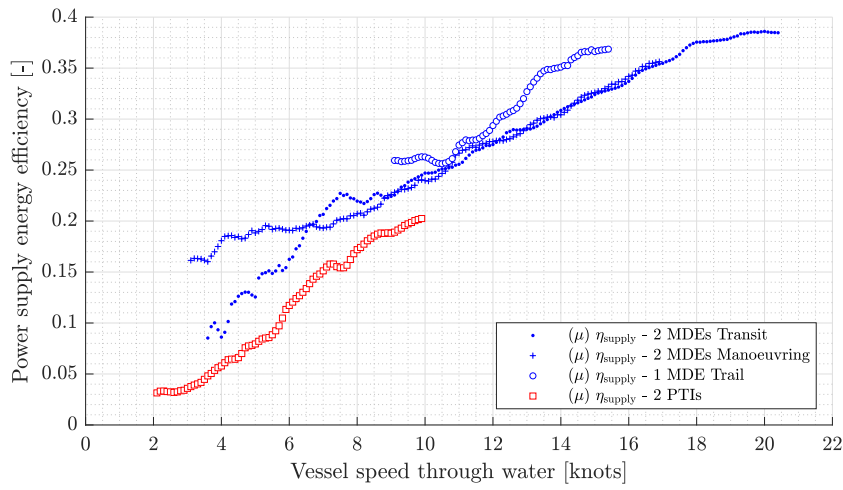
Figure 2.14: Mean power supply energy efficiency on the main operational modes.
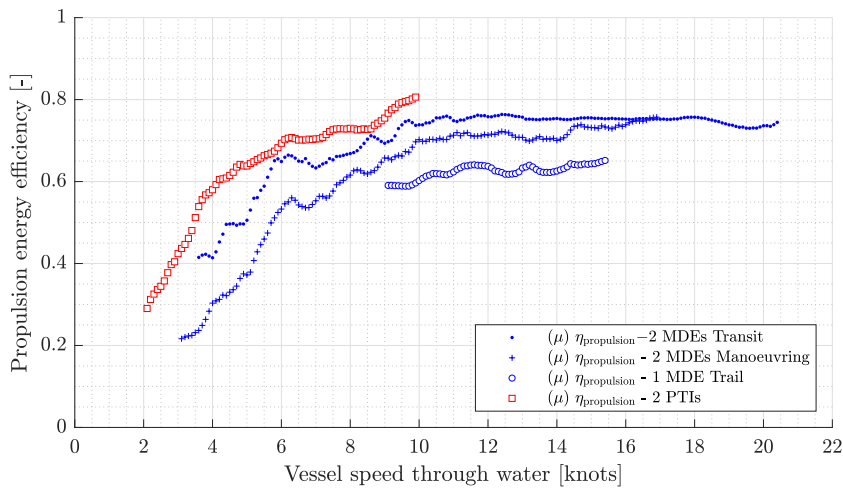
Figure 2.15: Mean power propulsion energy efficiency on the main operational modes.
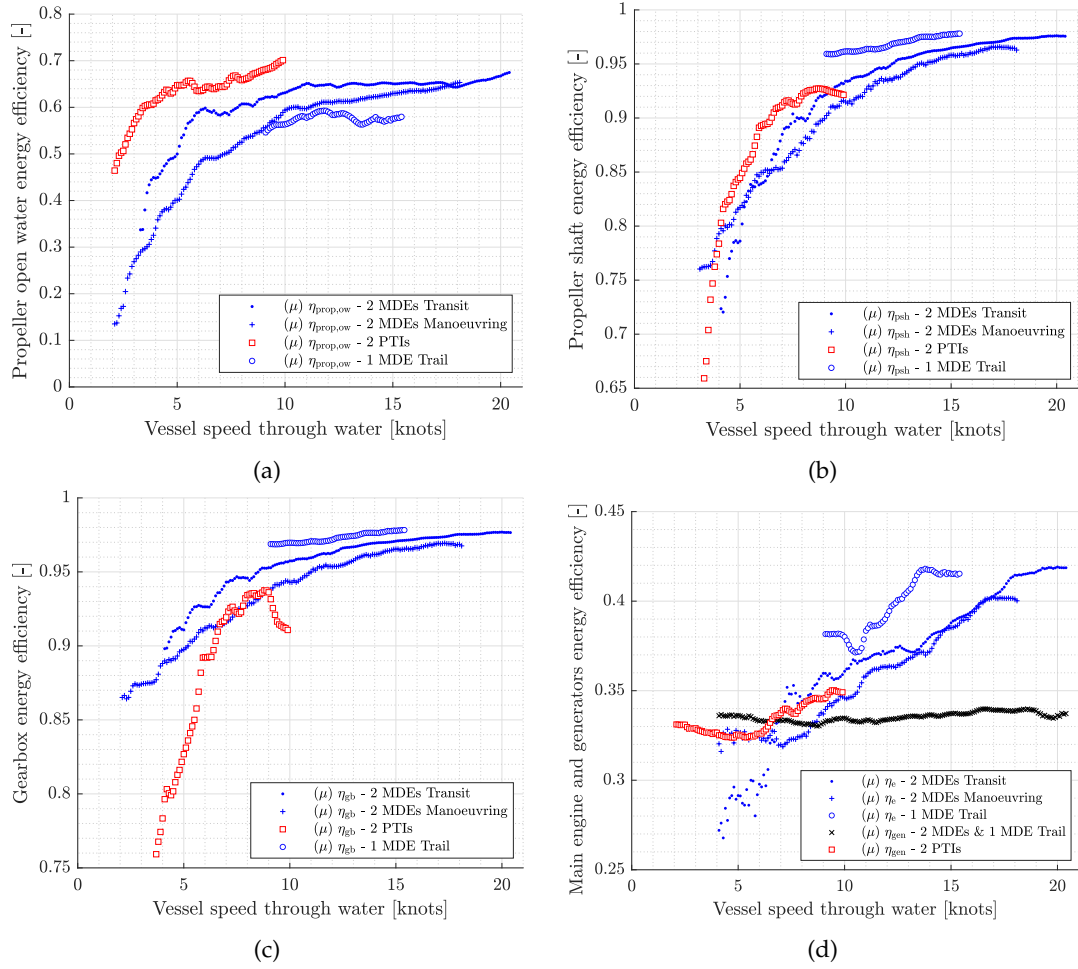
Figure 2.16: Component level mean energy efficiencies over discretised vessel speed on the main operational modes.

- Operational conditions such as weather conditions, loading conditions, hull fouling and manoeuvring cause extensive variation of propeller thrust over its mean value at a given vessel speed.

- Mean energy effectiveness indicator for all operational modes combined, as introduced in this chapter, is a good measure for the assessment of the achieved energy performance and carbon footprint, and for life cycle fuel consumption and carbon analyses. It provides the operator with insight into the most effective sailing speed, and the cost of sailing faster, but it should not be used to compare the energy performance of different operational modes as it can be distorted due to diverse thrust levels.

- The two dimensional histogram of discretised energy effectiveness indicator over ship speed, and the corresponding standard deviation curves indicate the uncertainty in the vessel's energy performance, caused by discrete operator settings and the varying operational conditions.

- Mean total energy efficiency can be used to compare different operational modes due to its small variation over varying thrust levels.
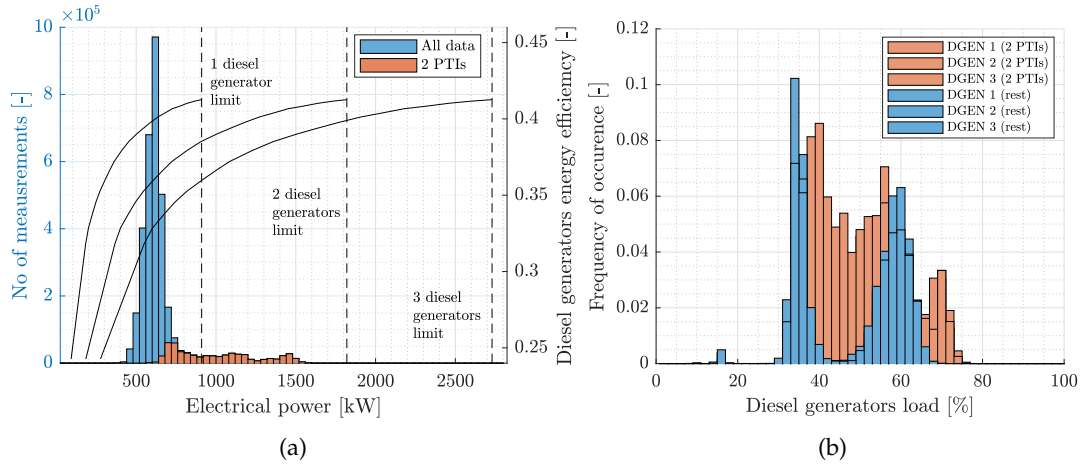
Figure 2.17: The difference of electrical propulsion on diesel generators electrical power supply, allocation and energy efficiency. (a) Combined electrical power supply histogram and energy efficiency of the diesel generators, with and without running on the electrical motors. (b) Diesel generators load histogram with and without running on the electrical motors.

- System, subsystem and component level mean energy efficiency evaluation can provide the designers with feedback on the design choices over the complete vessel operating profile in actual and uncertain operating conditions.

- Life cycle fuel consumption prediction will most likely be inaccurate without a reliable operational profile prediction.

The proposed methodology provides the following feedback to the operators of the vessel:

- Crew decisions, as the selection of operational mode and the selection of vessel speed, have a similar impact on overall energy performance as design decisions.

- Despite the high energy efficiency of most components at high sailing speed, the vessel consumes less fuel per mile in the range of 30 to 40% of nominal speed.

- Mean energy effectiveness indicator change for a 1 knot speed change is a good advisor for sailing speed selection.

- The operators appear to have a strong preference for certain discrete speed settings.

- While using electrical propulsion can be less efficient than mechanical propulsion, it can prevent fouling of the diesel engines at low loads. Therefore, for long transits at low speeds, running on the electrical motors is still advisable. Similarly, if speeds above the motors maximum speed are required, sailing on one engine can also reduce maintenance, if the one-shaft reduced manoeuvrability is acceptable.

The proposed methodology provides the following feedback to the designers of the vessel:

- Reducing the electrical motors speed with two reduction stages leads to significant gearbox losses. Fuel savings can be achieved by reducing the speed of the motors, thus the number of reduction stages, if the increased size of the motors is acceptable, and by optimally selecting the number and size of the diesel generators.

- While designers often consider gearbox and shaft losses insignificant, losses at part load are significant and can impact design choices.

- The effect of part load component losses causes total energy efficiency of the system to drop by almost 50% at half vessel speed compared to the nominal speed. Therefore, the use of numerous design points in order to reduce the fuel use and CO_2 emissions of vessels is recommended.

Future work could focus on a number of aspects to be investigated. First, in order to draw safer conclusions on the energy performance of different operational modes, we recommend the use of first principle models in examining all options under the same operational conditions. Moreover, the application of this methodology on a dataset which includes propeller thrust and torque, and main diesel engine torque sensor readings would make it possible to examine main diesel engine energy efficiency degradation, and propeller and hull fouling. Finally, while mean energy effectiveness provides useful insight for general trends for journey planning, route optimisation algorithms require fuel consumption prediction for the specific conditions the vessel is sailing in. The data analysis proposed in this work is not applicable for this type of analysis. Either first principle models, or machine learning algorithms would be required to identify the effect of specific operational conditions. However, the enriched dataset proposed in this work can be used by such machine learning algorithms.

The proposed methodology, using operational data from continuous monitoring, provides insight into the impact of operator and design choices for ships, and it allows the better assessment of technical and operational measures. For the case study, a 2 knots increase of the sailing speed between 8 and 14 knots causes a 14% increase of the CO_2 emissions, and a 27% increase above 14 knots. Similarly, an improved design including better auxiliary power allocation and the use of less or no gearbox reduction stages, can additionally save approximately 15 to 20% on CO_2 emissions, thus mitigating the environmental impact of ship operations.

3

A DIGITAL TWIN APPROACH FOR MARITIME CARBON INTENSITY EVALUATION ACCOUNTING FOR OPERATIONAL AND ENVIRONMENTAL UNCERTAINTY

This chapter is reproduced from [92]:

ABSTRACT

Maritime industry has set ambitious goals to drastically reduce its greenhouse gas emissions by stipulating and enforcing a number of energy assessment measures. Unfortunately, measures like the EEDI, EEXI, SEEMP and CII do not account for the operational and environmental uncertainty of operations at sea, even though they do provide a first means of evaluating the carbon footprint of ships. The increasing availability of high-frequency operational data offers the opportunity to quantify and account for this uncertainty in energy performance predictions. Current methods for evaluating and predicting energy performance at a whole energy system level do not sufficiently account for operational and environmental uncertainty. In this work, we propose a digital twin that accurately predicts the fuel consumption and carbon footprint of the hybrid propulsion system of an Ocean-going Patrol Vessel (OPV) of the Royal Netherlands Navy under the aggregate effect of operational and environmental uncertainty. It combines first-principle steady-state models with machine learning algorithms to reach an accuracy of less than 5% MAPE on both mechanical and electrical propulsion, while bringing a 40% to 50% improvement over a model that does not utilise machine learning algorithms. Results over actual voyage intervals indicate a prediction accuracy of consumed fuel and carbon intensity within 2.5% accounting for a confidence interval of 95%. Finally, the direct comparison between mechanical and electrical propulsion showed no clear energy-saving benefits and a strong dependency of the results on each voyage's specific operational and environmental conditions.

3.1   INTRODUCTION

Human influence has unequivocally warmed the atmosphere and oceans, and the current speed of climate change and its impact on the living environment for mankind is unprecedented [7]. To reduce the impact of shipping on the environment, the International Maritime Organization (IMO) adopted mandatory energy efficiency measures textcolorredalready back in 2011 [11]. However, adopting these measures did not prevent a further 9.6% increase of green house gas emissions from shipping between 2012 and 2018 [12]. Therefore, additional measures are urgently needed to reach a 40% reduction of carbon emissions per transport work by 2030 compared to 2008 [13].

Literature provides a wide range of technological and operational solutions to comply with these measures [36], [37], [93], [94]. The main difficulty in their energy performance assessment, though, is the high uncertainty level of the required power for propulsion, mission, and auxiliary loads at the different design and operational phases [54]–[57]. This uncertainty is mainly caused by the heterogeneous operational and environmental conditions ships operate in, as demonstrated by Parkes, Sobey and Hudson [53] for merchant vessels and by Vasilikis, Geertsma and Visser [21] for multi-function service vessels.

Current IMO regulations and regulations in preparation by international authorities such as IMO and the European Union require ships to comply with reference limits of indices and indicators that, in principle, indicate the amount of carbon dioxide (CO_2) emissions per transport work. Their calculation is done either on a single sailing point as in the case of EEDI [17] and EEXI [18] or by averaging the carbon footprint over a year of operations as in the case of CII [19]. However, Lindstad, Borgen, Eskeland *et al.* [24] demonstrated that one sailing point does not consider the operational and environmental uncertainty at sea. Moreover, balancing out the effect of this uncertainty over the course of similar voyages does not provide substantial feedback on the operational and design decisions, especially in the case of multi-function vessels that do not perform the same type of operations over time [21]. Therefore, this work aims at developing a digital twin that accounts for both operational uncertainty and unpredictability in environmental conditions.

The use of actual operating profiles or multiple operating conditions can improve the accuracy of the assessment of lifetime energy savings when comparing the impact of novel operational procedures and energy efficiency measures or design solutions [26], [63], [64]. The advent of new technological advances in collecting, storing, and transferring data has the potential to support the maritime industry to evaluate operational and design measures over more realistic operating conditions [61], [62]. The increasing availability of high frequency operational data in contrast to bias-sensitive noon reports and research on data-driven techniques makes it possible to quantify operational and environmental uncertainties and accurately assess the energy efficiency of real-time operations [60]. In this work, we thus provide a novel methodology to account for realistic operating conditions in evaluating operational procedures leveraging digital twin technologies that utilise high frequency operational data.

3.1.1   *Related Work*

Uncertainties in operational and environmental conditions significantly affect the energy efficiency of power and propulsion systems [58], [59]. Operational uncertainty is the result of differences in loading condition, rudder activity, hull, and propeller fouling, but also of the selected vessel speed and acceleration. Alternatively, environmental uncertainty is mainly related to wind and wave conditions, currents, and ambient air and sea temperatures. Many authors account for those uncertainties differently by formulating their problem accordingly.

Some studies examine the efficiency of the whole energy conversion chain of ships' power supply and propulsion systems. Shi, Grimmelius and Stapersma [78] and Sui, Stapersma, Visser *et al.* [47] evaluate fuel consumption over the whole vessel speed range, accounting for one resistance curve that is assumed representative of the ship's operation. Other studies provide results for multiple resistance curves in order to demonstrate the effect of different weather and hull fouling conditions [46], [49]. Another practice is to provide the total fuel consumed over certain sailing time periods. For example, Sui, Vos, Stapersma *et al.* [48] estimated energy gains over three voyages that each involved three parts of different sailing speeds and sea margins and a number of maneuvers. Moreover, Trivyza, Rentizelas and Theotokatos [26], [65] used actual vessel speed distributions, and finally, some authors examined actual vessel speed time profiles for energy management applications [2], [66]. While these approaches partly consider the effect of diverse conditions on system-level energy performance with multiple single-point conditions, they do not account for the full spread of actual conditions.

Another set of studies focuses on individual operational and environmental parameters. They usually use hindcast data of monitored weather, vessel speed, and loading parameters. The main applications are on weather routing problems [95]–[97], on operational parameters optimisation as trim [69] and vessel speed [98], but also on identifying hull fouling [70]. Monte Carlo simulations have also been used to quantify uncertainty on attained energy efficiency [99], [100]. Furthermore, there is a third branch of studies that examine the energy performance of individual components and subsystems. They use statistical distributions of the main engine, auxiliary engine, and thermal power for thermodynamic cycle optimisation [58], [79], [80] or a number of typical steady state operating conditions [101]. A similar strategy uses these power profiles in the time domain to examine different system configurations [102]–[104]. The work proposed in this chapter differs from these studies as it examines the aggregate effect of different operational and environmental conditions over selected voyages of the complete energy system rather than each parameter or subsystem separately.

Fuel consumption prediction of ships usually requires the development and use of simulation models of their energy systems [44], [45]. Literature provides many examples of such models, which usually consider different system limits and fidelity level. In general, simulation models can be categorised into first-principle models, that provide insight in the underlying physical processes, semi-empirical models, that use the experience of similar systems, and empirical models, that are built using the preceding knowledge of the examined system's operation. Another way to categorise different models is a division into dynamic and steady-state models,

based on whether they consider dynamic phenomena or not. Finally, simulation models can also be categorised into stochastic and deterministic models, depending on whether they consider the uncertainty of the input and output parameters or not. The application scope determines what would be a suitable model type and what should be the necessary fidelity level.

This trade-off between model type, application scope, and fidelity level has been discussed by many authors [42], [46], [47]. Energy performance prediction of ship energy systems usually utilises steady state models [26], [47], [48], [65], [66], [78]. This is a practice followed in automotive applications as well [105]–[107]. Those models usually consist of two or three-dimensional look-up tables provided by component manufacturers or they are the result of regression analysis over a certain amount of available data. Some models use constant energy efficiencies to model different components too. In general, the modelled components include the main propulsion engines, gearboxes, shafts, and propellers. In some cases, auxiliary power generation is modelled too. Control strategy applications on the other hand require the use of dynamic models [46], [108], [109]. In the specific case of energy management applications, both steady state [66] and dynamic [2], [73], [110] models of the energy system can be used.

Prediction of fuel consumption in certain environmental and operational conditions usually follows two modelling strategies. The first combines steady state energy system models with semi-empirical resistance prediction models [111] or more advanced computer fluid dynamics models [95]. The second uses statistical models to predict fuel consumption in a one step calculation as in [69] or in a two step main shaft propulsion power and fuel consumption prediction [98]. A review of statistical models and methods used in the fuel consumption prediction of ships can be found in [112], [113]. The modelling strategy in this chapter differs from this practice as the main aim is to preserve the first principle understanding of the system components.

Finally, energy performance analysis and optimisation at a component and sub-system level is also dominated by the use of steady state models, although these models can vary in their level of detail. For example, applications in finding optimal configurations use look-up tables [102]–[104], but applications on optimising thermodynamic working cycles require much more detailed models based on energy efficiency analysis [101] or even exergy analysis [58], [79], [80]. Those studies focus on the low-level examination of the system, nevertheless, they confirm the general practice of sacrificing time dependency for more detailed models and a higher number of simulations.

3.1.2 *Gaps*

Actual operational and environmental conditions are used coupled with empirical models to examine energy efficiency gains from optimising operational decisions such as weather routing, vessel speed selection, and optimal loading of vessels. When the focus lies on alternative system configurations and settings, technological innovations are tested on scenarios that are not representative of the actual conditions at sea. Hence, a methodology on the aggregate effect of actual operational and environmental conditions is missing. Moreover, ship energy systems consist

of a large number of interacting components that show non-linear behaviour [42]. Modelling discrepancies of those components result in accumulating prediction errors. On the occasion that large datasets of operational data are available, calibration and validation of the whole energy system model become challenging too. At a component level, there is a number of examples of calibrating, validating, and enhancing the accuracy of different models as in the case of main diesel engines [51], [52], [114]. However, such methodologies at a whole system level are lacking due to different sensor availability of monitoring platforms and diversity in system architecture.

3.1.3   *Aim and contribution*

This chapter presents an accurate and computationally low-cost operational data-driven methodology that can predict the fuel consumption and carbon footprint of ship operations under the aggregate effect of diverse and uncertain operational and environmental conditions and use this methodology to establish optimal settings and evaluate future design alternatives. The contribution of this chapter can be summarised as follows:

- It provides a methodology to build a digital twin of ship energy systems that can be used to evaluate operational decisions, design changes, and contribute to enhanced future designs.

- It proposes a novel methodology to account for realistic operational and environmental conditions.

- It proposes a systematic methodology to validate models of the whole energy system in the presence of large operational datasets.

- It proposes statistical modelling techniques to compensate for uncertainty related to sensor measurements and the limited availability of information from shipbuilders and component manufacturers.

- It provides a case study that demonstrates the capability of steady-state models coupled with data-driven techniques in accurately predicting fuel consumption over actual dynamic and quasi-static sailing conditions.

- It provides a direct comparison between electrical and mechanical propulsion over actual sailing profiles.

The rest of this chapter is organised as follows. Section 3.2 presents the main characteristics of the examined vessel and the used datasets. Section 3.3 presents our proposed methodology to build and utilise a digital twin of the vessel's energy system. Section 3.4 provides a description of the data-driven techniques applied. Section 3.5 provides all accuracy metrics for the developed models. Section 3.6 presents our results and Section 3.7 the drawn conclusions.

3.2   CASE STUDY VESSEL AND DATASET DESCRIPTION

The case study vessel in this chapter is a *Holland class* Ocean Patrol Vessel (OPV) of The Royal Netherlands Navy (RNLN). Appendix A provides a more detailed description of this class of vessels that are equipped with hybrid propulsion, including a schematic representation of the energy system, component specifications and performance diagrams provided by component manufacturers and the shipbuilder. The proposed methodology utilises operational data logged by the automation system of the vessel. Cleaning and pre-processing was done as in [115], but vessel speed was selected as the prime parameter and the top and bottom 0.1% percentile was used to discard outliers instead of standard deviation. The used dataset is characterised by a sampling frequency of 3 seconds and covers a time window of 15 months. The main parameters used in this chapter are reported in Table 3.1. These parameters are all measured by the automation system, except for the thrust parameter, which is estimated based on the dataset enrichment methodology described in the authors' earlier work [21].

The examined vessel uses a number of operational modes in order to serve its multifunction mission. The focus of this study lies in the two main operational modes. The first one is designed for sailing on two main diesel engines while in transit, from now on referred to as Mechanical Mode (MM). The second main mode is designed for patrolling or low speed transits up to 10 knots on the two electric motors, from now on referred to as Electrical Mode (EM). Figure 3.1 provides the distribution of the dataset parameters for the examined two propulsion options. Vessel operation below 5 knots is discarded as part of manoeuvring which does not have an important impact on attained energy performance and carbon footprint.

Table 3.1: Dataset parameters.

Parameter	Unit
Vessel speed through water	[knots]
Propeller pitch to diameter	[-]
Propeller thrust	[kN]
Propeller shaft speed	[rpm]
Propeller shaft torque	[kNm]
Electrical motors power	[kW]
Generated electrical power	[kW]
Main diesel engines fuel consumption	[kg/h]
Diesel generators fuel consumption	[kg/h]
Ambient air temperature	[degree]
Time	[sec]
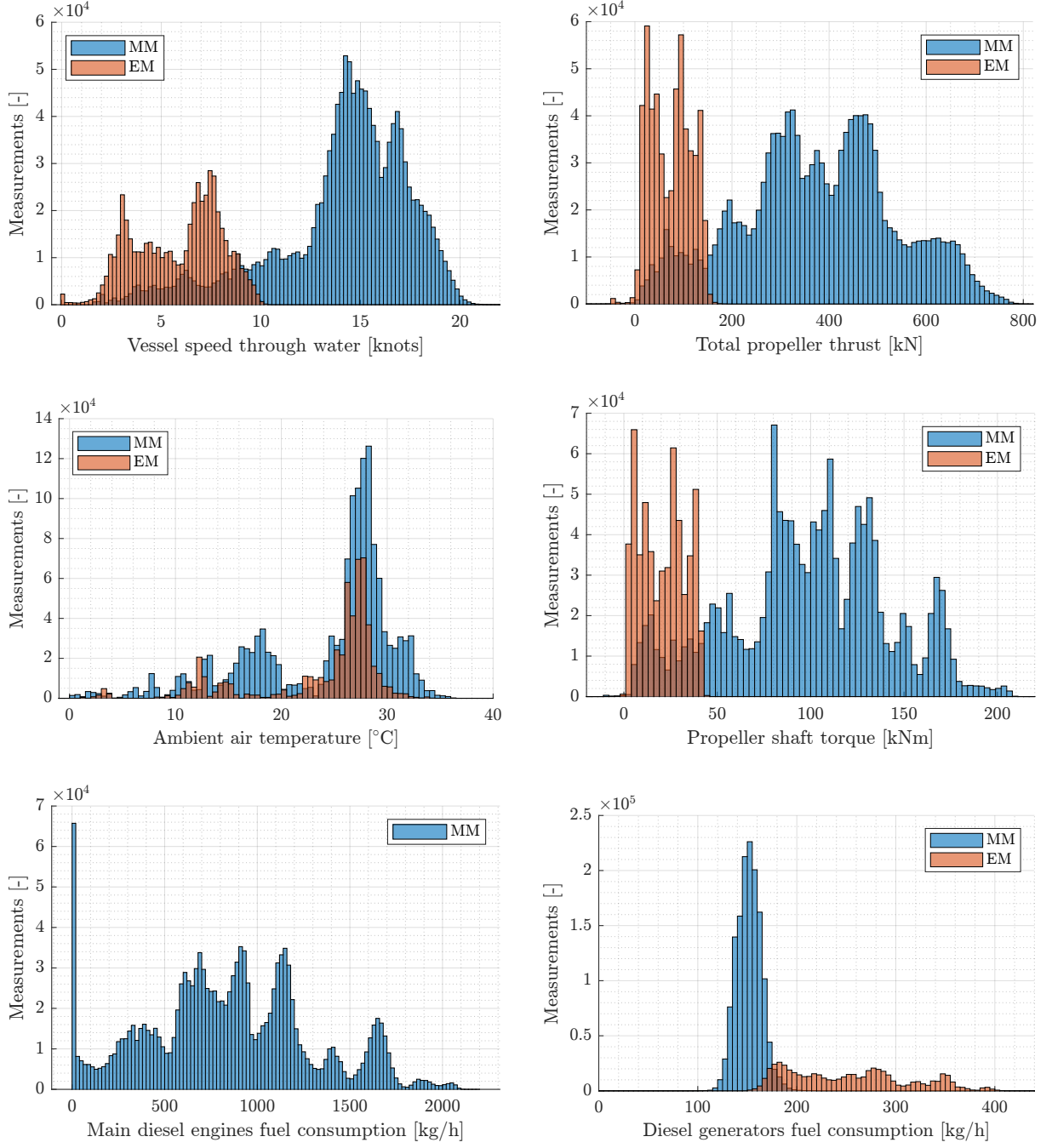
Figure 3.1: Dataset parameters distribution.
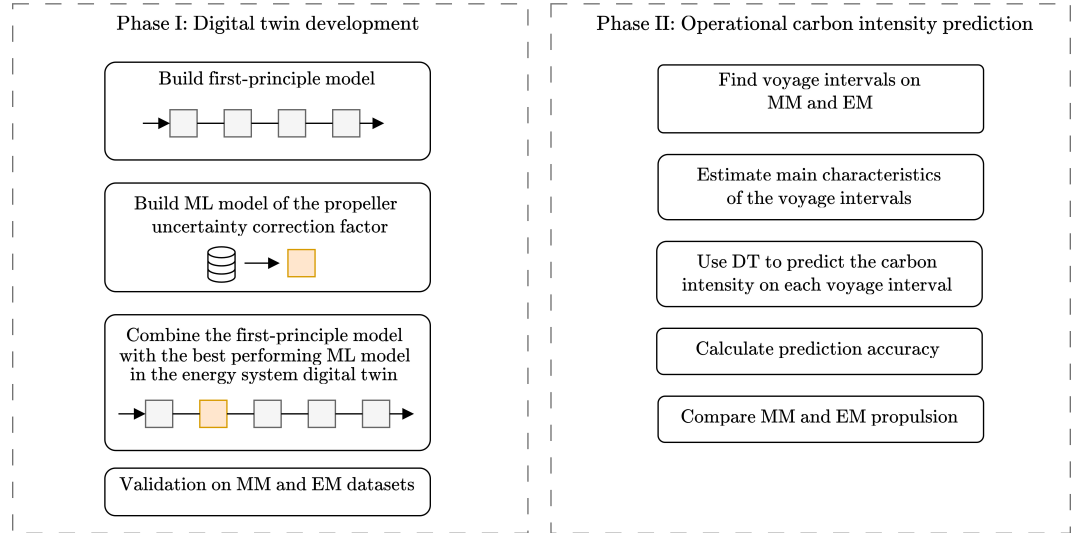
Figure 3.2: Schematic representation of the proposed methodology.

3.3 METHODOLOGY

The methodology of this chapter proposes a two-phase approach to accurately predict the energy performance of complex ship energy systems under realistic operational and environmental conditions, by leveraging steady-state first-principle models [21], [47], [99] and the high-frequency operational data described in Section 3.2, as follows:

- **Phase I**: a DT [116], [117] of the vessel's hybrid energy system is developed to capture the quasi-static behaviour of the vessel in terms of energy, fuel consumption, and emissions. Due to the hybrid approach of using data-driven and first-principle techniques, we can achieve accurate predictions that capture the aggregate effect of operational and environmental uncertainty. The description of this DT is reported in Section 3.3.1 and its validation in Section 3.5.

- **Phase II**: the developed DT is employed in predicting the energy performance (i.e., fuel consumption) and carbon intensity of the vessel over a number of actual voyages, and it also provides a direct comparison between Mechanical Mode (MM) and Electrical Mode (EM).

A schematic representation of the methodology can be found in Figure 3.2.

3.3.1 *Phase I: Digital Twin Development*

The developed DT predicts the fuel consumption of main diesel engines and generators and the propeller shaft torque for tuples of different vessel speed, propeller thrust, and ambient temperature. For
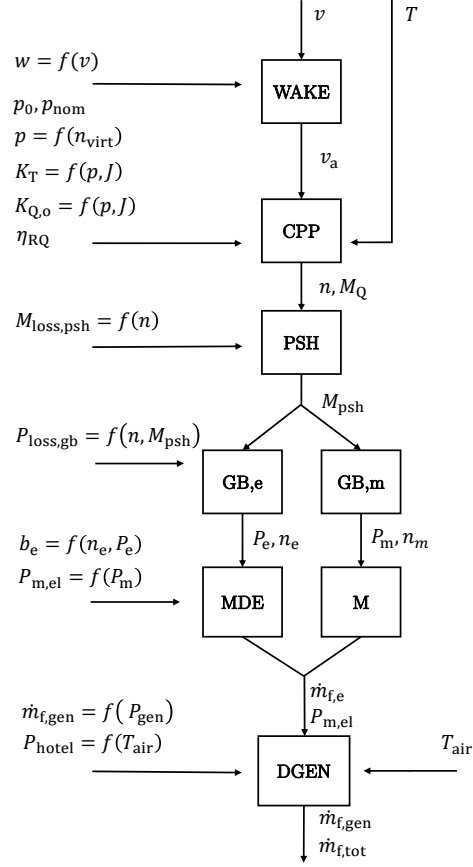
Figure 3.3: Flowchart of the Digital Twin

each component depicted in Figure 3.3, a short description of the modelling approach follows in the next subsections.

First, the model evaluates water speed in the ship's wake v_a from vessel speed v:

$$v_a = (1 - w)\, v\,, \tag{3.1}$$

using Taylor's wake fraction w which is provided by towing tank tests (Figure A.3 in Appendix A). Next, it evaluates rotational speed n and pitch p of the controllable-pitch propeller based on an iteration algorithm described in Figure 3.4. This algorithm iterates to the pitch setting for the given vessel speed using the fixed-pitch propeller matching algorithm and the ship's combinator curve as reported in [68] to estimate rotational speed. Propeller's thrust coefficient $K_{T,ship}$ curve is provided by:

$$K_{T,ship} = \frac{T}{\rho\, v_a^2\, D^2}\, J^2\,, \tag{3.2}$$
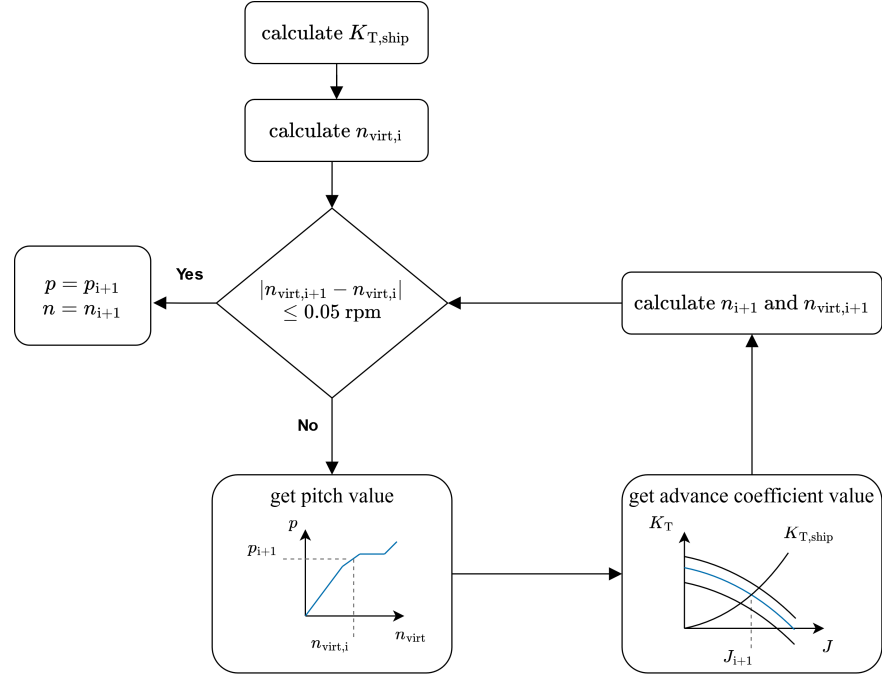
Figure 3.4: Controllable pitch propeller pitch and rotational speed evaluation algorithm.

where T is propeller thrust, ρ is water density, D is propeller diameter and J is the advance coefficient. The initial value for virtual shaft speed $n_{\text{virt,i}}$ is assumed a linear function of vessel speed:

$$n_{\text{virt,i}} = c_1 \, v - c_0, \qquad v > 2\text{knots} . \tag{3.3}$$

Propeller pitch is provided as a function of virtual shaft speed n_{virt} using the corresponding combinator curve for the selected operational mode in Figure 3.5. Thrust coefficient curves K_{T} are established with
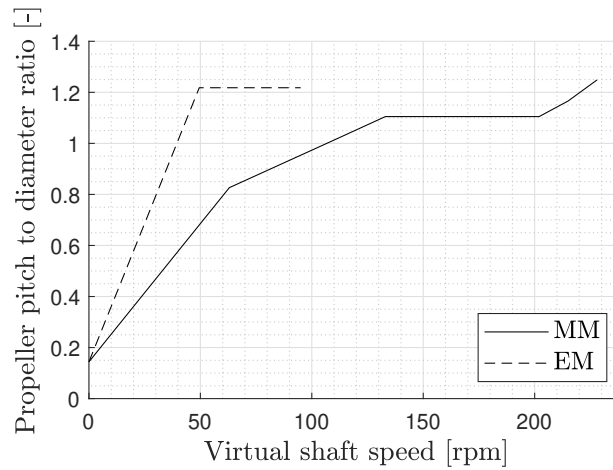
Figure 3.5: Combinator curves.

the propeller open water diagrams, as shown in Figure 3.6. Propeller
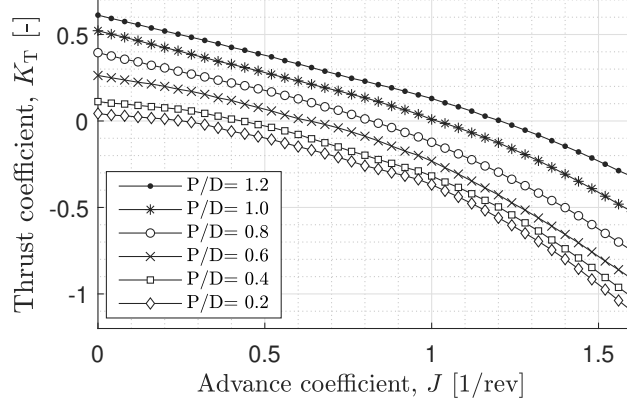
Figure 3.6: Thrust coefficient open water diagram.

speed is evaluated using the advance coefficient as follows:

$$n = \frac{v_a}{J D} \, . \tag{3.4}$$

Virtual shaft speed n_{virt} is provided by:

$$n_{\text{virt}} = \frac{p - p_0}{p_{\text{nom}} - p_0} \, n \, , \tag{3.5}$$

where p_0 is zero thrust pitch and p_{nom} is nominal pitch. Following the successful convergence of the iteration procedure, the pitch value and the advance coefficient are used in to establish the torque coefficient in open water conditions $K_{Q,o}$ using Figure 3.7. Propeller torque in
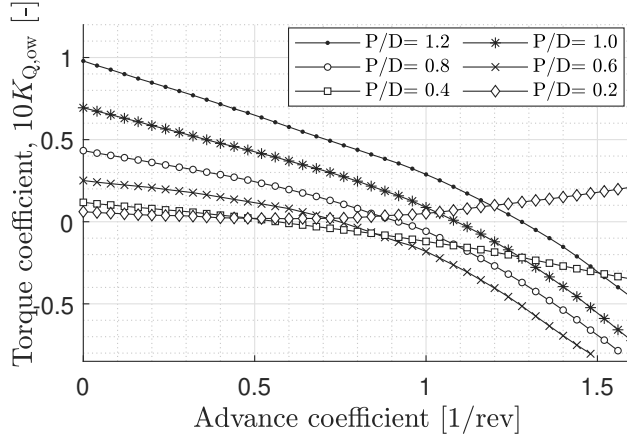
Figure 3.7: Torque coefficient open water diagram.

open water conditions $M_{Q,o}$ is then estimated from:

$$M_{Q,o} = K_{Q,o} \, \rho \, n^2 \, D^5 \, , \tag{3.6}$$

while propeller torque M_Q is evaluated using the relative rotative efficiency η_{RQ}:

$$M_Q = \frac{M_{Q,o}}{\eta_{\text{RQ}}} \, , \tag{3.7}$$

the background of which is discussed in the following two paragraphs. The use of propeller open water diagrams in predicting propeller thrust, torque, and speed is based on decoupling the problem of the self-propelled ship into the problem of open water propeller operation and the problem of the towed ship [118]. It uses scale models in static operating points, while recently including the effect of control strategies and the scaling challenges this introduces have been demonstrated in [119]. Typically, a selection between thrust or torque identity is made by introducing relative rotative efficiency. It is usual to select the first option of thrust identity, suggesting that the thrust coefficient stays the same in actual and open water conditions [120]. Literature provides semi-empirical formulas for evaluating relative rotative efficiency as in [121]. The use of those formulas corresponds to nominal design conditions, and their accuracy on modern ships and off-design conditions has not been examined [122].

Nonetheless, the availability of operational data offers the opportunity to assess the accuracy of those formulas in design and off-design conditions. The utilised IPMS dataset includes measurements of propeller torque, pitch, rotational speed, and vessel speed. Equation 3.6 provides an estimation of propeller torque in open water conditions. In theory, the fraction of this torque value with measured torque provides an estimation of the relative rotative efficiency $\hat{\eta}_{RQ}$:

$$\hat{\eta}_{RQ} \ = \ \frac{M_{Q,o}}{M_Q} \, , \tag{3.8}$$

where the hat symbol is used to distinguish our estimation to the theoretical value η_{RQ}, as it involves uncertainty related to the accuracy of our measurements and of the diagrams used. Parameters like the thrust deduction factor t, wake factor w, and the relative rotative efficiency are usually used to compensate for this uncertainty [123]. In this chapter, the estimated relative rotative efficiency based on Equation 3.8, from this point called propeller uncertainty correction factor, is modelled as a statistical model following the procedure described on Section 3.4.

Furthermore, the model evaluates propeller shaft torque M_{psh} using the propeller torque and propeller shaft torque losses $M_{loss,psh}$ according to:

$$M_{psh} \ = \ M_Q + M_{loss,psh} \, , \tag{3.9}$$

where the latter is provided as a linear function of shaft speed by the manufacturer,

$$M_{loss,psh} \ = \ c_3 \, n \ + c_2 \, , \tag{3.10}$$

Consequently, propeller shaft power is evaluated from $P_{psh} = M_{psh}\, n\, 2\pi$. Main diesel engine power P_e and electrical motor power P_m are estimated based on gearbox losses $P_{loss,gb}$:

$$P_e = P_{psh} + P_{loss,gb}\,, \tag{3.11}$$

$$P_m = P_{psh} + P_{loss,gb}\,. \tag{3.12}$$

The linear torque losses model proposed in [85] is used. It is calibrated with the data provided by the gearbox manufacturer as a function of input power and speed:

$$P_{loss,gb} = \begin{cases} c_6\, P_e + c_5\, n_e{}^2 + c_4\, n_e & \text{(MM)}, \\ c_9\, P_m + c_8\, n_m{}^2 + c_7\, n_m & \text{(EM)}, \end{cases} \tag{3.13}$$

where n_e and n_m derive using the corresponding speed reduction ratios r_e and r_m:

$$n_e = r_e\, n\,, \tag{3.14}$$

$$n_m = r_m\, n\,. \tag{3.15}$$

Following the substitution of Equations 3.11 and 3.12, gearbox losses are given from:

$$P_{loss,gb} = \frac{c_6\, P_{psh} + c_5\, n_e{}^2 + c_4\, n_e}{(1 - c_6)}\,, \tag{3.16}$$

$$P_{loss,gb} = \frac{c_9\, P_{psh} + c_8\, n_m{}^2 + c_7\, n_m}{(1 - c_9)}\,. \tag{3.17}$$

Fuel consumption of the main diesel engines $\dot{m}_{f,e}$ is evaluated from the specific fuel consumption b_e as:

$$\dot{m}_{f,e} = \frac{b_e\, P_e\, 3600}{1000}\,, \tag{3.18}$$

which is interpolated using speed n_e and power P_e from Figure 3.8. This look-up table was built out of the brake specific fuel consumption contour curves provided by the manufacturer in [90], corrected with the available dataset according to Table 3.2.

Table 3.2: Original brake specific fuel consumption contour lines provided by the manufacturer and percentage correction.

b_e [g/kWh]	correction	b_e [g/kWh]	correction	b_e [g/kWh]	correction
236	-1.7 %	213	no	199	+1.5 %
230	-1.7 %	209	no	195	+1.5 %
217	no	204	no	193	+2.1 %
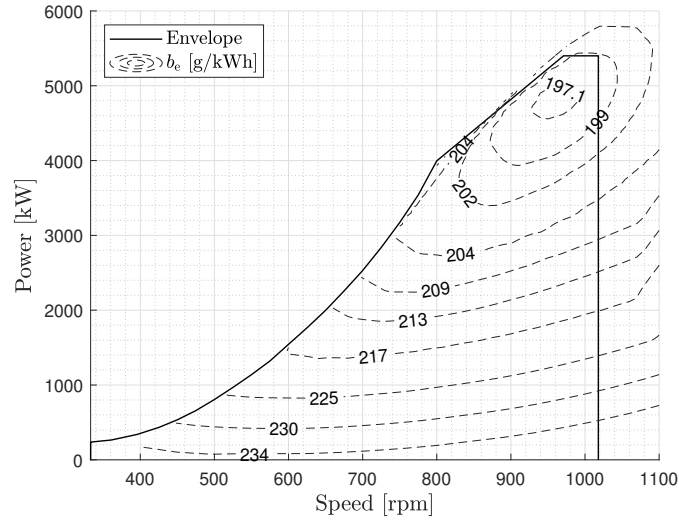
Figure 3.8: Brake specific fuel consumption map of the main diesel engines.

The electrical power delivered to the motors $P_{\mathrm{m,el}}$ is evaluated based on their energy efficiency η_{m} and delivered power P_{m}:

$$P_{\mathrm{m,el}} = \frac{P_{\mathrm{m}}}{\eta_{\mathrm{m}}} \,. \tag{3.19}$$

The energy efficiency of the motors is modelled as a function of the delivered power as:

$$\eta_{\mathrm{m}} = c_{12}\, z^2 + c_{11}\, z + c_{10} \,, \tag{3.20}$$

where

$$z = \log P_{\mathrm{m}} \,. \tag{3.21}$$

The constants are estimated based on the test results for an induction motor provided in Kalikatzarakis, Geertsma, Boonen *et al.* [2].
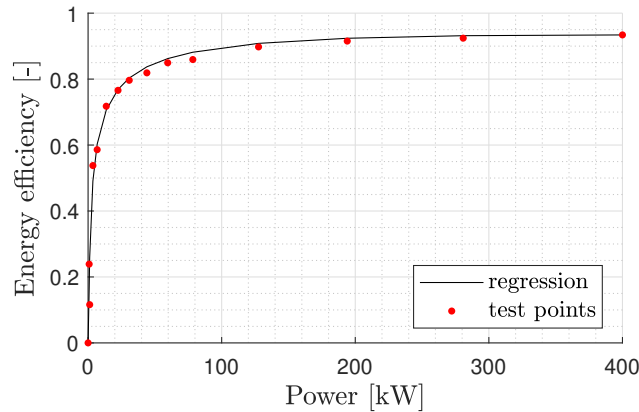
Figure 3.9: Electrical motor's energy efficiency against produced power.

Fuel consumption of the diesel generators $\dot{m}_{f,gen}$ is derived from the specific fuel consumption b_{gen} as:

$$\dot{m}_{f,gen} = \frac{b_{gen}\ P_{gen}\ 3600}{1000} . \tag{3.22}$$

Specific fuel consumption is modelled using the available dataset parameters as a function of the total generated electrical power P_{gen}:

$$b_{gen} = \frac{c_{14}}{P_{gen}} + c_{13} , \tag{3.23}$$

which is the sum of the hotel load P_{hotel} and the power provided to
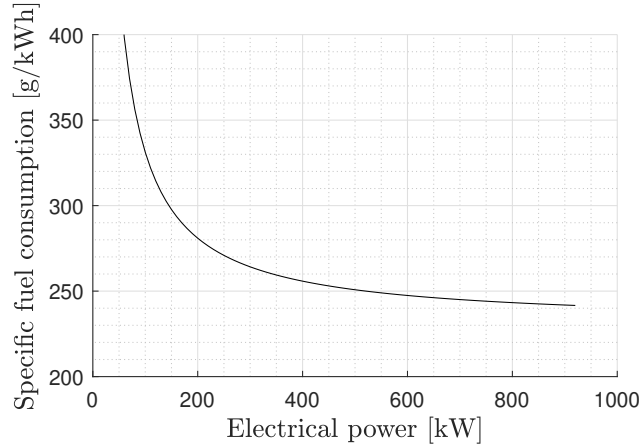
Figure 3.10: Diesel generators' specific fuel consumption against produced electrical power.

the electrical motors $P_{m,el}$:

$$P_{gen} = P_{hotel} + P_{m,el} . \tag{3.24}$$

The mission system and auxiliary electrical load clearly is influenced by many factors, such as the mission of the vessel that determines which sensor and weapon systems are active and the activities the crew are undertaking. From the dataset, we have established that the correlation with outside air temperature T_{air} is the strongest correlation for all parameters. This is caused by the fact that the electrical capacity of the chilled water plant for cooling of all systems is one of the largest electrical non-propulsion loads and directly influenced by the outside air temperature. Thus, hotel electrical load P_{hotel} is modelled as a quadratic function of the external air temperature T_{air} as derived from the analysis of the dataset:

$$P_{hotel} = c_{17}\ T_{air}^{2} + c_{16}\ T_{air} + c_{15} . \tag{3.25}$$

Ultimately, total fuel consumption of the vessel $\dot{m}_{f,tot}$ is provided by:

$$\dot{m}_{f,tot} = \dot{m}_{f,e} + \dot{m}_{f,gen} . \tag{3.26}$$

All model constants can be found in Table 3.3.
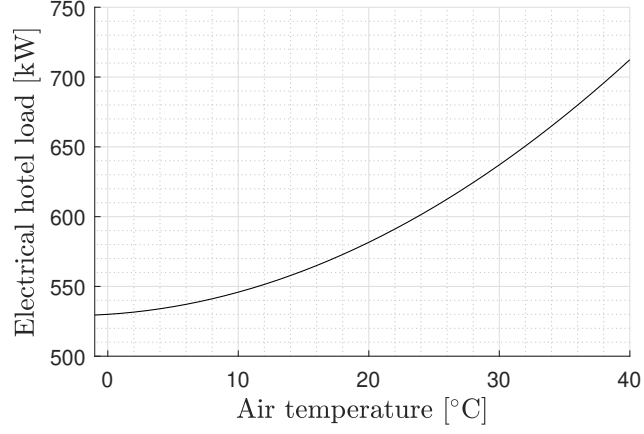
Figure 3.11: Electrical hotel load as a function of ambient air temperature.

Table 3.3: Model Constants

Initial Virtual Shaft Speed		Gearbox Losses (MM)		Electrical Motors	
c_0	11	c_4	0.0081	c_{10}	0.2161
c_1	7.9	c_5	9.002e-05	c_{11}	0.553
		c_6	0.0050	c_{12}	-0.1065
Propeller shaft losses		Gearbox Losses (EM)		Diesel Generators	
c_2	1.4	c_7	0.00297	c_{13}	230.7
c_3	0.0134	c_8	1.025e-05	c_{14}	10.05
		c_9	0.0050		
Ambient Temperature					
c_{15}	530	c_{16}	0.6	c_{17}	0.099

3.3.2 Phase II: Carbon Intensity Evaluation

The second phase of our methodology examines the hypothesis that the developed DT can accurately predict carbon emissions over a selection of actual voyage intervals in line with existing regulations [19]. The selection of those intervals involved finding periods of at least four hours of continuous sailing on the same operational mode. The total duration Δt, covered distance Δs, and total amount of consumed fuel $M_{f,tot}$ was approximated by midpoint rule numerical integration as follows:

$$\Delta t = \int dt \simeq \sum_{j=1}^{N} \delta t = N \, \delta t \,, \tag{3.27}$$

$$\Delta s = \int v_{log} \, dt \simeq \sum_{j=1}^{N} v_{log} \, \delta t \,, \tag{3.28}$$

$$M_{f,tot} = \int \dot{m}_{f,tot} \, dt \simeq \sum_{j=1}^{N} \dot{m}_{f,tot} \, \delta t \,. \tag{3.29}$$

Mean sea margin $\overline{SM}$ was evaluated as the mean difference of thrust and calm water resistance R_0:

$$\overline{SM} = \overline{(T - R_0)/R_0} \, . \tag{3.30}$$

Mean speed $\overline{v} = \Delta s / \Delta t$ and Carbon Intensity (CI) derive as:

$$CI = \frac{M_{f,tot} \, f_{CO2}}{\Delta s} \, , \tag{3.31}$$

where f_{CO2} is the carbon factor equal to 3.206 for diesel oil according to EEDI regulations [17]. The evaluated characteristics of the selected intervals can be found in Tables 3.8 and 3.9 in the case of mechanical and electrical propulsion, respectively. The prediction accuracy of the selected intervals is examined using the Mean Average Percentual Error (MAPE) of total fuel consumption $\dot{m}_{f,tot}$, and the Absolute Percentage Error (APE) of the predicted amount of consumed fuel $M_{f,tot}$, consequently carbon intensity.

The last step of phase II is the selection of non-dynamic intervals to simulate the energy performance of the vessel in MM and EM and provide a direct comparison between them.

3.4 DATA-DRIVEN MODELS

One of the objectives of this study is to develop a model for predicting the propeller uncertainty correction factor, denoted as $\hat{\eta}_{RQ}$, based on the input parameters outlined in Table 3.4. This model will utilize the data described in Section 3.2. Figure 3.12 illustrates the histogram of relative frequencies for the target feature in both MM and EM. This learning problem can be formulated as a supervised Ma-
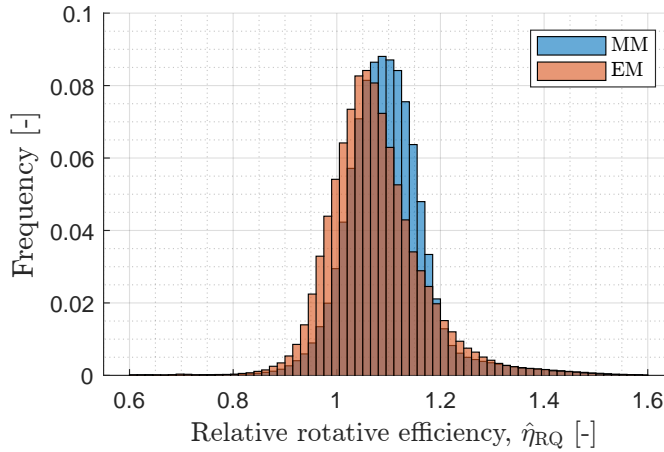
Figure 3.12: Propeller uncertainty correction factor $\hat{\eta}_{RQ}$ histogram of relative frequencies obtained from the IPMS dataset.

chine Learning (ML) problem, specifically a regression problem [124]. In regression analysis, an input space $\mathcal{X} \subseteq \mathbb{R}^d$ is comprised of d

Table 3.4: List of inputs and outputs of the ML models.

Space	Symbol	Description	Unit
Input	v	Vessel speed	[kn]
	T	Thrust	[kN]
	p	Pitch	[-]
	n	Shaft speed	[rpm]
Output	$\hat{\eta}_{RQ}$	Propeller uncertainty correction factor	[–]

features (in this case, the four parameters in Table 3.4). The output space, $\mathcal{Y} \subseteq \mathbb{R}$, corresponds to $\hat{\eta}_{RQ}$. A dataset of n examples, denoted as $\mathcal{D}_n = (x_1, y_1), \cdots, (x_n, y_n)$, represents input/output relationships where $x_i \in \mathcal{X}$ and $y_i \in \mathcal{Y}$ $\forall i \in 1, \cdots, n$. The aim is to learn the unknown input/output function $\mu : \mathcal{X} \to \mathcal{Y}$ based solely on $\mathcal{D}n$. An ML regression algorithm $\mathscr{A}$, characterized by its hyperparameters $\mathcal{H}$, selects a model f from a set of potential models $\mathcal{F}$ based on available data $\mathscr{A}\mathcal{H} : \mathcal{D}_n \times \mathcal{F} \to f$. The set $\mathcal{F}$ is typically unknown and depends on the choices of $\mathscr{A}$ and $\mathcal{H}$. Various ML algorithms exist in the literature [124]–[127]. However, according to the no-free-lunch theorem [128], there is no a priori method for determining the best ML algorithm for a specific application. Therefore, this study will consider an assortment of state-of-the-art ML algorithms.

The accuracy of model f in approximating μ is evaluated using a prescribed metric $M : f \to \mathbb{R}$. Multiple metrics are available for regression analysis in ML [129]. However, due to the physical significance of $\hat{\eta}_{RQ}$, this study will focus on four primary metrics: Mean Absolute Error (MAE), Mean Absolute Percentage Error (MAPE), Relative Error in Percentage (REP), and the Coefficient of Determination (R^2). To identify the most suitable ML algorithms and their corresponding optimal hyperparameters, as well as to evaluate the performance of the final model based on the desired metrics, a statistically consistent Model Selection (MS) and Error Estimation (EE) process was conducted. The methodology for this process is detailed in Section 3.4.2, following the recommendations presented in [130].

3.4.1   *Machine Learning Models*

This section provides a concise overview of the four algorithms employed in this study, highlighting the fundamental concepts, usage, and hyperparameters associated with each algorithm. The chosen algorithms represent the most effective approaches within the four primary families of ML regression algorithms [124]–[127]: Linear Methods[131], Kernel Methods [132], Ensemble Methods [133], and Neural Networks [125].

3.4.1.1 *Linear Methods*

Regularized Least Squares (RLS) is a regression method that introduces a regularization term to the traditional least squares problem to control the complexity of the model and prevent overfitting. The objective of RLS is to minimize the sum of squared residuals, similar to ordinary least squares, but with an additional penalty term that discourages large values of the model parameters. The regularization term is typically a function of the model parameters, such as the L2 norm (also known as Ridge regression) or the L1 norm (also known as Lasso regression). The L2 norm encourages small parameter values, leading to a more stable model with lower variance, while the L1 norm can lead to sparse solutions, where some parameters are exactly zero, effectively performing feature selection. The balance between the fit to the data and the regularization is controlled by the only hyperparameter of this algorithm λ. A larger λ increases the impact of the regularization term, leading to a simpler model, while a smaller λ allows the model to fit more closely to the data, potentially at the risk of overfitting.

3.4.1.2 *Neural Networks*

Neural Networks, inspired by human brain neurons, are complex networks built from numerous perceptrons [134]. Their structure consists of layers linked by weights, determined through backpropagation [135]. A network with a single hidden layer is a shallow neural network, while one with multiple hidden layers is a deep neural network. Deep networks excel in complex computations and learning high-level features, improving predictive accuracy. Despite Cybenko's Universal Approximation Theorem [136] suggesting equal representational capacities for both architectures, deep networks often outperform shallow ones in tasks like natural language processing and image analysis.

Given our study's limited sample size and unstructured features, we chose a shallow neural network to avoid overfitting [125], [137]. We used the Multilayer Perceptron Network (MLP) [125], [137] with Dropout architecture, which has a single hidden layer. The training process uses adaptive subgradient methods for dynamic learning rate adjustments. We optimized various hyperparameters during the MS phase [125], including the number of neurons in the hidden layer, dropout rate, batch size percentage, learning rate, fraction of gradient to retain, learning rate decay, and the activation function. By tuning these hyperparameters, we optimised the performance of our MLP model for the given task.

3.4.1.3 *Kernel methods*

Kernel Methods are algorithms that use the 'Kernel trick' to transform linear methods for non-linear problems [138]. They use kernel

functions to map input data into a higher-dimensional space, enabling linear separability for non-linear problems. This mapping allows the computation of inner products in the feature space without explicit high-dimensional computations, extending linear algorithms to work efficiently in the transformed space. Kernel methods balance empirical performance and model complexity [124], [132]. Empirical performance, measured by a pre-defined metric, assesses the model's fit and prediction reliability. Model complexity, evaluated by various measures, assesses the solution space complexity. Higher complexity can fit more functions but risks overfitting. Therefore, kernel methods aim to strike an optimal balance between these two aspects: achieving high performance on the data without over-complicating the model.

Support Vector Regression (SVR) is a well-known and efficient Kernel method technique. It uses Support Vector Machines (SVMs) principles and hyperparameters like the kernel function, often set to a Gaussian or Radial Basis Function (RBF) kernel for its flexibility in modeling complex, non-linear relationships [139]. The kernel hyperparameter, γ, controls the non-linearity of the decision boundary and the kernel function's shape and scale. A small γ leads to a more linear boundary, while a large γ creates a more complex, non-linear boundary. The regularization hyperparameter, C, balances model accuracy and solution complexity. A small C allows more misclassifications for a simpler boundary, while a large C aims for higher accuracy, potentially at the cost of a more complex boundary. Both γ and C are critical to the performance of the SVR model and need to be meticulously tuned during the MS phase to ensure optimal model performance.

3.4.1.4 *Ensemble methods*

Ensemble methods, like Random Forests, use the 'wisdom of the crowd' principle by integrating many simple, independent models to form a more complex and effective one. Random Forests are notable examples, using Decision Trees (DT) as their base models. A DT is a flowchart-like structure where each internal node represents a feature test, each branch shows the test's outcome, and each leaf node indicates the tree's output. A path from the root to a leaf represents a model rule. DT are built recursively to a specified depth, with each node constructed from the attribute and cut that best split the samples into two subsets, based on information gain. RF enhances bagging, a process where each DT is independently constructed using a bootstrap sample of the dataset, with random subset feature selection. This approach uses different bootstrap samples of the data for each DT and alters how DTs are constructed. RF splits each node using the best among a subset of predictors, randomly chosen at that node. The final prediction is derived from a straightforward majority vote. The accuracy of the final RF model primarily hinges on three factors: the number of trees in the forest, the accuracy of each tree, and the correl-

ation between them. As the number of trees in the forest increases, the accuracy for RF converges to a limit. Simultaneously, it improves as the accuracy of each tree increases, and the correlation between them diminishes. Several hyperparameters shape the performance of the final model, including the number of trees, the number of samples to extract during the bootstrap procedure, the depth of each tree, the number of predictors used in each subset during the growth of each tree, and finally, the weights assigned to each tree.

3.4.2 *Model Selection and Error Estimation*

MS and Empirical EE are critical tasks in the application of ML algorithms, focusing on hyperparameter tuning and performance evaluation. Resampling techniques, frequently used due to their effectiveness in various scenarios, will be implemented in this study. Though alternative methods exist within Statistical Learning Theory, they often underperform resampling techniques in practice. Resampling techniques work by resampling the original dataset $\mathcal{D}_n$ once or multiple times (n_r), either with or without replacement, to generate three independent datasets: the learning set $\mathcal{L}_l^r$, validation set $\mathcal{V}_v^r$, and test set $\mathcal{T}_t^r$, where $r \in 1, \cdots, n_r$. These datasets adhere to the following conditions:

$$\mathcal{L}_l^r \cap \mathcal{V}_v^r = \oslash, \qquad\qquad \mathcal{L}_l^r \cap \mathcal{T}_t^r = \oslash, \qquad (3.32)$$

$$\mathcal{V}_v^r \cap \mathcal{T}_t^r = \oslash \qquad\qquad \mathcal{L}_l^r \cup \mathcal{V}_v^r \cup \mathcal{T}_t^r = \mathcal{D}_n \qquad (3.33)$$

To perform MS, i.e., select the optimal combination of hyperparameters $\mathcal{H}$ from a set of possibilities $\mathfrak{H}$ for the algorithm $\mathscr{A}_\mathcal{H}$, we use the following procedure

$$\mathcal{H}^* : \quad \arg\min_{\mathcal{H} \in \mathfrak{H}} \sum_{r=1}^{n_r} M(\mathscr{A}_\mathcal{H}(\mathcal{L}_l^r), \mathcal{V}_v^r), \qquad (3.34)$$

Here, $\mathscr{A}_\mathcal{H}(\mathcal{L}_l^r)$ represents a model built using algorithm $\mathscr{A}$ with its set of hyperparameters $\mathcal{H}$ and data $\mathcal{L}_l^r$, and $M(f, \mathcal{V}_v^r)$ is the desired metric. $\mathcal{H}^*$ should minimize error on a dataset independent from the training set since $\mathcal{L}_l^r$ is independent from $\mathcal{V}_v^r$.

To perform EE, which assesses the performance of the optimal model $f^\mathscr{A} = \mathscr{A}_\mathcal{H}(\mathcal{D}_n)$, we use the following procedure

$$M(f_\mathscr{A}^*) = \frac{1}{n_r} \sum_{r=1}^{n_r} M(\mathscr{A}_{\mathcal{H}^*}(\mathcal{L}_l^r \cup \mathcal{V}_v^r), \mathcal{T}_t^r). \qquad (3.35)$$

Since the data in $\mathcal{L}_l^r \cup \mathcal{V}_v^r$ are independent of the ones in $\mathcal{T}_t^r$, $M(f_\mathscr{A}^*)$ is an unbiased estimator of the true performance, measured with the metric M, of the final model [130].

In this work, we will rely on Complete 10-fold cross-validation, which means setting

$$n_r \leq \binom{n}{k} \binom{n - \frac{n}{k}}{k},$$ (3.36)

$$l = (k - 2)\frac{n}{k},$$ (3.37)

$$v = \frac{n}{k},$$ (3.38)

and

$$t = \frac{n}{k}$$ (3.39)

and the resampling must be done without replacement [130]. The large size of the two utilized datasets, 1 331 972 and 338 918 elements in MM and EM respectively, guarantee sufficient representation of all parameters in the learning, validation and testing datasets. Finally, the performance of the models in terms of accuracy is measured in accordance with different metrics: four quantitative (MAE, MAPE, REP, and R^2) [140] and two qualitative such as the scatter plot actual versus predicted value and the histogram of the Absolute Percentage Error [141].

3.5 MODELS VALIDATION

This section provides the attained accuracy results of the four different ML algorithms of Section 3.4 used to model the propeller uncertainty correction factor, and the prediction accuracy of the developed digital twin.

3.5.1 *Propeller uncertainty correction factor*

In this section, we will report the performance of the ML models described in Section 3.4, using the validation approaches described in Subsection 3.4.2, and considering the different propulsive modes (i.e., MM and EM). In particular, we will compare the results of the different algorithms employed to build the models (RF, SVR, MLP, RLS). Table 3.5 reports the different metrics used to evaluate the performance for all algorithms employed and the different propulsive modes. Figure 3.13 provides a corresponding visual representation. Figure 3.14 and Figure 3.16 report the scatter plot for the best algorithm (RF) on each propulsive mode, while Figure 3.15 and Figure 3.17 report the absolute percentage error histogram of relative frequencies.

From Table 3.5 and Figure 3.13, it is possible to observe that: i) the selected RF algorithm outperformed the rest of the examined

algorithms on both propulsion modes, ii) the difference among the different algorithms was relatively bigger in EM compared to MM, with a 5.8% and 3.0% MAPE improvement, respectively. As expected, the RLS algorithm showed limited learning capability both on MM and EM. The inferior performance of the algorithms on EM compared to MM is possibly attributed to the pitch feature that stays almost constant on EM.

Table 3.5: ML models validation: quantitative metrics (MAPE, MAE, REP) employed to evaluate performance of all examined algorithms (RF, SVR, MLP and RLS), on both propulsive modes (MM and EM).

Mechanical Mode (MM)			
Algorithm	MAPE [%]	MAE [−]	REP [%]
RF	3.72 ± 0.04	0.041 ± 0.001	6.04 ± 0.02
SVR	3.97 ± 0.08	0.044 ± 0.001	6.41 ± 0.17
MLP	4.12 ± 0.05	0.045 ± 0.001	6.60 ± 0.10
RLS	6.71 ± 0.87	0.097 ± 0.013	9.75 ± 0.96
Electrical Mode (EM)			
RF	3.95 ± 0.01	0.043 ± 0.001	6.61 ± 0.03
SVR	4.94 ± 0.14	0.054 ± 0.002	7.86 ± 0.31
MLP	5.64 ± 0.04	0.061 ± 0.001	8.08 ± 0.06
RLS	9.78 ± 0.96	0.120 ± 0.002	12.61 ± 1.03

3.5.2 *Digital Twin*

The prediction accuracy of the developed DT over the two operational mode datasets is reported here using the metrics in Section 3.4.2. Table 3.6 shows the DT performances using the most performing ML model (RF), assessed over the IPMS operational data on both MM and EM. The prediction capability of the DT accounting for the effect of actual operational and environmental conditions is confirmed by total fuel consumption MAPE of 3.7% in EM and 4.9% in MM. MAE values of main diesel engines and diesel generators also stand below 2% of nominal values. The prediction accuracy of the other parameters lies below 5.5% MAPE as well. Considering that both datasets contain highly dynamic operating points and that the logging rate of 3 seconds did not average this behaviour, the prediction capability of the quasi-static approach used for the DT is confirmed.

Table 3.7 shows the DT performances without using an ML model. Relative rotative efficiency was estimated using the semi-empirical formula for twin-screw ships provided by Holtrop and Mennen [3]. This formula uses hull prismatic coefficient, longitudinal centre of buoyancy, and nominal propeller pitch to diameter ratio, resulting in a value equal to 0.976. Results demonstrate the significant improvement
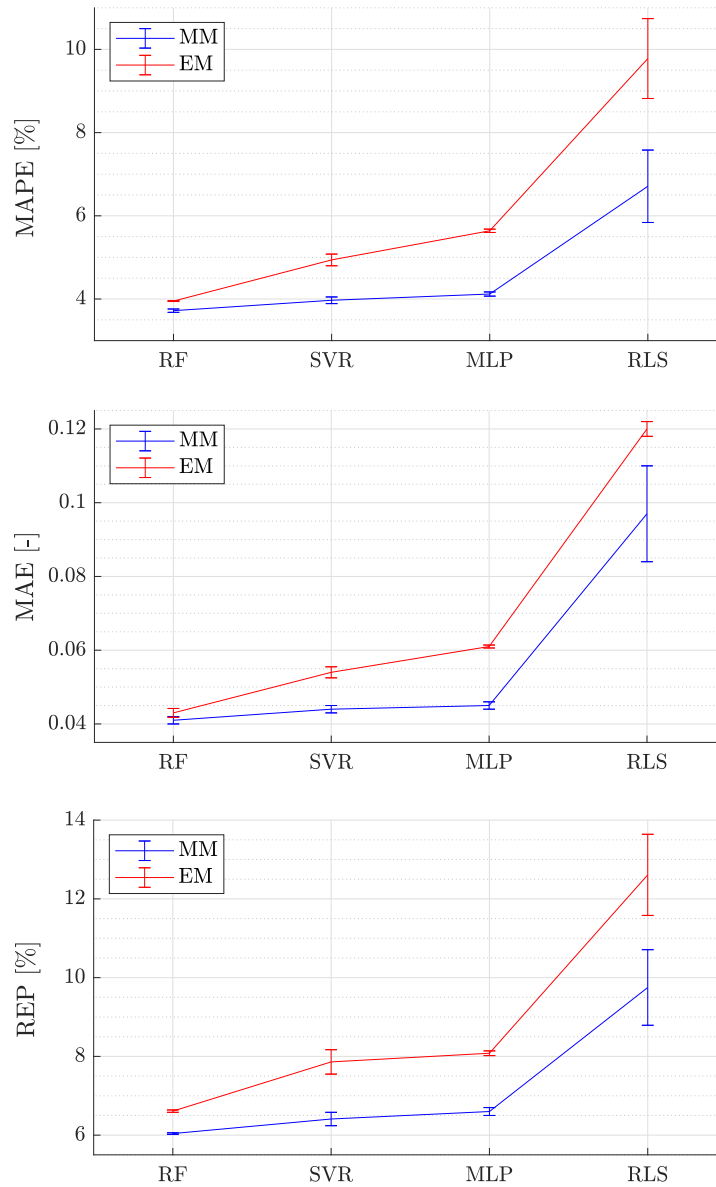
Figure 3.13: ML models validation: quantitative metrics (MAPE, MAE, REP) employed to evaluate the performance of all examined algorithms (RF, SVR, MLP, and RLS), on both propulsive modes (MM and EM).

in accuracy from integrating ML in our DT. The improvement becomes more apparent on MM as pitch value variates from the nominal value used by the semi-empirical formula. The smaller improvement from using ML on EM is explained by the nominal pitch value resulting from sailing mostly above 50 rpm virtual shaft speed as can be seen in Figure 3.5.
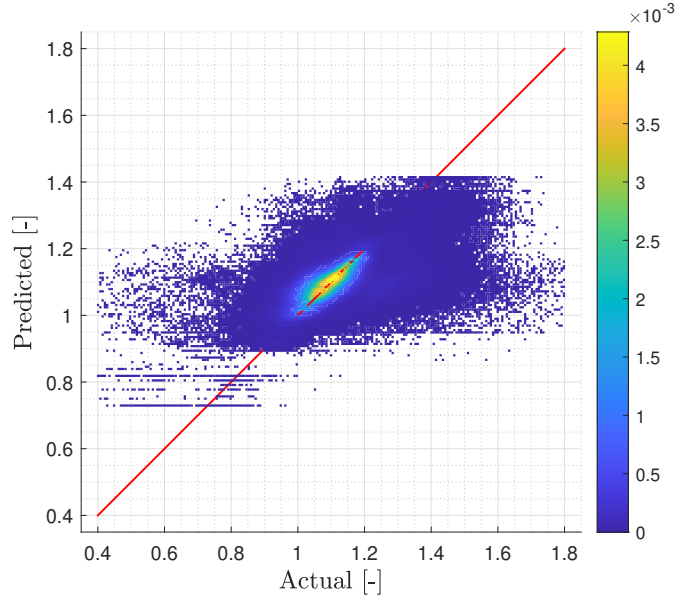
Figure 3.14: ML models validation: scatter plot for RF (the best algorithm identified in Section 3.5.1) on MM (see Table 3.5).
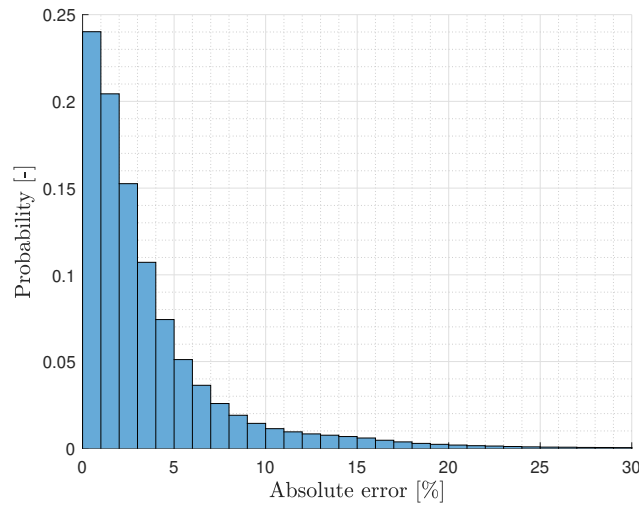
Figure 3.15: ML models validation: absolute percentage error histogram of relative frequencies for RF (the best algorithm identified in Section 3.5.1) on MM (see Table 3.5).

3.6 RESULTS

3.6.1 *Voyage intervals*

In the previous section, the capability of the digital twin to predict instant fuel consumption of the vessel and most logged parameters was confirmed. This section provides prediction results over the selected twenty two electrical propulsion and fifty mechanical propulsion voyage intervals that we selected for evaluating the method against real operating conditions. Figure 3.18 provides an example of five
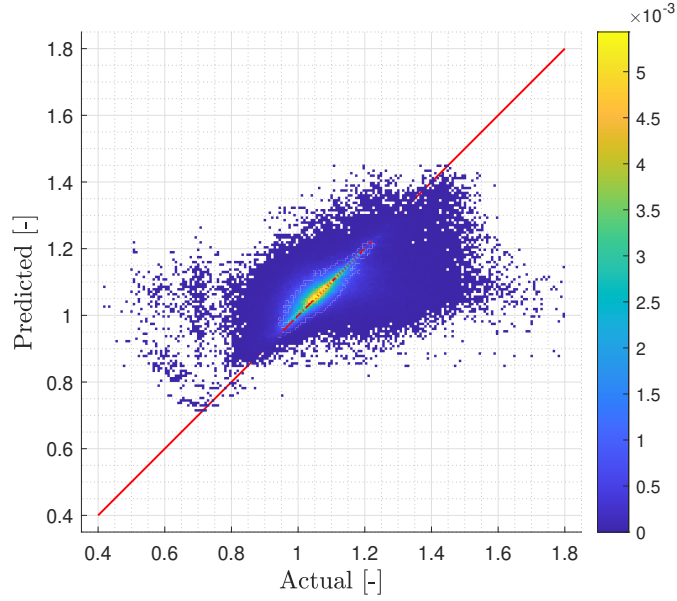
Figure 3.16: ML models validation: scatter plot for RF (the best algorithm identified in Section 3.5.1) on EM (see Table 3.5).
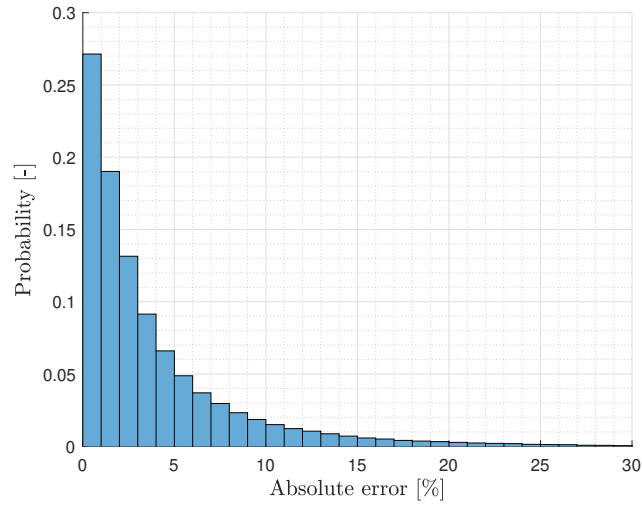
Figure 3.17: ML models validation: absolute percentage error histogram of relative frequencies for RF (the best algorithm identified in Section 3.5.1) on EM (see Table 3.5).

typical voyage intervals. It provides qualitative means to examine the variation of operational and environmental conditions, that can be assessed using the spread of vessel speed and propeller thrust in corresponding figures. The main characteristics of the selected voyage intervals as duration, average speed, total fuel consumption and carbon intensity, but also the achieved MAPE of the predicted instant fuel consumption and APE of consumed fuel and carbon intensity over the intervals can be found for MM in Table 3.8 and for EM in Table 3.9.

Results suggest that the average prediction accuracy over a voyage interval on EM, with a 95% confidence interval, is $1.65 \pm 0.49\%$. At the

Table 3.6: DT performances using the most performing ML model (RF), assessed over the two operational modes IPMS datasets.

Feature	MAPE	MAE	REP	R^2
Mechanical Mode (MM)				
$\dot{m}_{f,tot}$	4.9 %	40.1 kg/h	4.7 %	0.984
$\dot{m}_{f,gen}$	4.4 %	6.8 kg/h	6.0 %	0.452
$\dot{m}_{f,e}$	6.2 %	38.8 kg/h	5.2 %	0.985
eP_{gen}	4.2 %	25.1 kW	5.3 %	0.481
P_m	-	-		-
M_{psh}	4.4 %	3.8 kNm	5.3 %	0.977
p	0.5 %	0.004	2.2 %	0.862
n	0.4 %	0.6 rpm	1.2 %	0.995
Electrical Mode (EM)				
$\dot{m}_{f,tot}$	3.7 %	10.4 kg/h	4.7 %	0.913
$\dot{m}_{f,gen}$	3.7 %	10.4 kg/h	4.7 %	0.913
$\dot{m}_{f,e}$	-	-	-	-
eP_{gen}	3.6 %	40.2 kW	4.4 %	0.941
P_m	5.3 %	12.4 kW	6.3 %	0.966
M_{psh}	5.4 %	1.4 kNm	6.9 %	0.933
p	0.2 %	0.002	1.0 %	0.338
n	0.6 %	0.4 rpm	1.0 %	0.995

Table 3.7: DT performances using the Holtrop and Mennen [3] semi-empirical formula, assessed over the two operational mode IPMS datasets.

Feature	MAPE	MAE	REP	R^2
Mechanical Mode (MM)				
$\dot{m}_{f,tot}$	10.4 %	101.3 kg/h	11.0 %	0.918
$\dot{m}_{f,gen}$	4.4 %	6.8 kg/h	6.0 %	0.452
$\dot{m}_{f,e}$	13.1 %	102.1 kg/h	12.5 %	0.911
eP_{gen}	4.2 %	25.1 kW	5.3 %	0.481
P_m	-	-		-
M_{psh}	12.9 %	13.0 kNm	14.0 %	0.839
p	0.5 %	0.004	2.2 %	0.862
n	0.4 %	0.6 rpm	1.2 %	0.995
Electrical Mode (EM)				
$\dot{m}_{f,tot}$	5.6 %	16.2 kg/h	6.8 %	0.818
$\dot{m}_{f,gen}$	5.6 %	16.2 kg/h	6.8 %	0.818
$\dot{m}_{f,e}$	-	-	-	-
eP_{gen}	6.2 %	70.1 kW	7.1 %	0.849
P_m	9.9 %	26.5 kW	11.9 %	0.876
M_{psh}	10.6 %	2.8 kNm	12.2 %	0.788
p	0.2 %	0.002	1.0 %	0.338
n	0.6 %	0.4 rpm	1.0 %	0.995

same time, MAPE of instant fuel consumption is equal to $3.36 \pm 0.35\%$. This shows that increased prediction errors for individual samples of a voyage have a smaller overall impact on a voyage time scale, due to the random sampling behaviour, which is cancelled out over a high

amount of samples. This observation is also confirmed for MM with an average prediction accuracy over a voyage of $2.16 \pm 0.35\%$ and an instant fuel consumption MAPE of $3.79 \pm 0.52\%$. These errors are of the same scale with the accuracy of many fuel consumption sensors at $\pm 1\%$ [51], which means that the prediction accuracy is partially limited by the accuracy of the sensors.
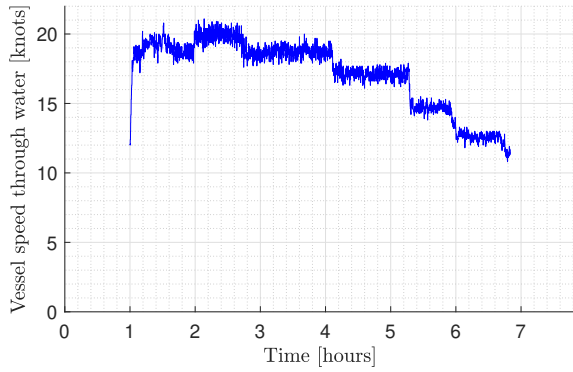
(a) Interval No 3 (MM), speed over time.
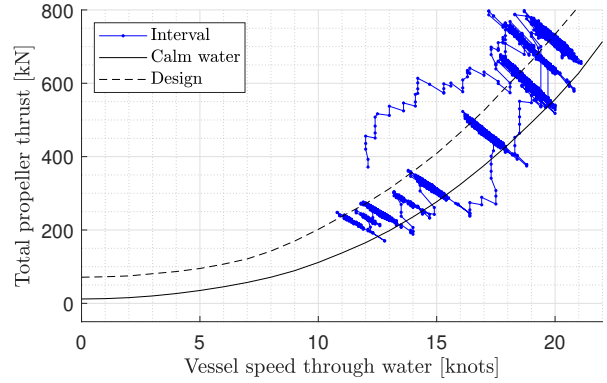
(b) Interval No 3 (MM), thrust over speed.
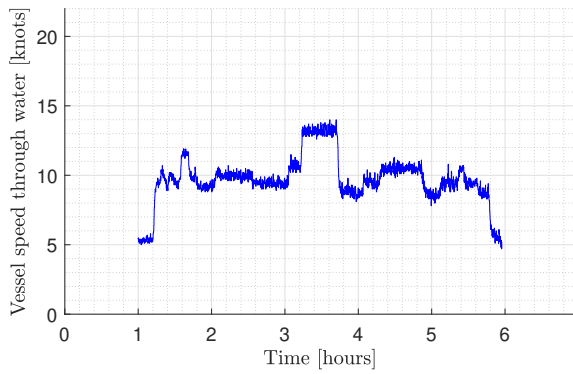
(c) Interval No 4 (MM), speed over time.
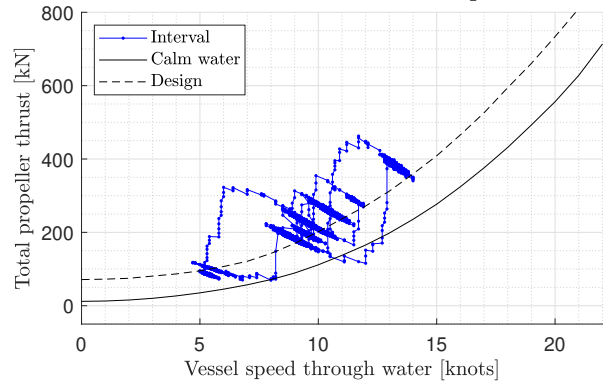
(d) Interval No 4 (MM), thrust over speed.
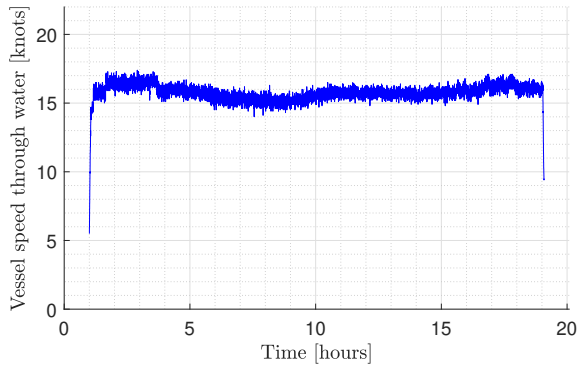
(e) Interval No 15 (MM), speed over time.
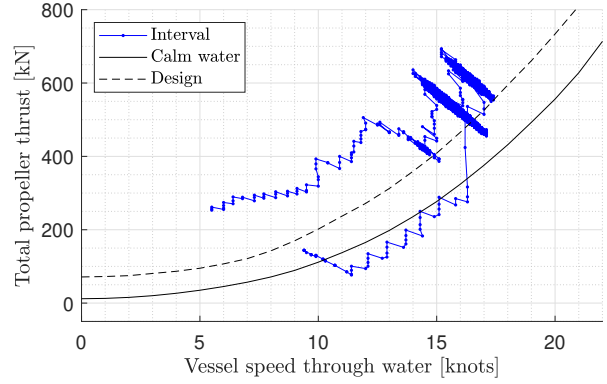
(f) Interval No 15 (MM), thrust over speed.
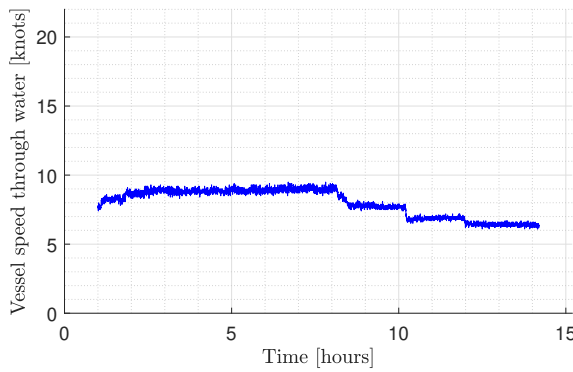
(g) Interval No 6 (EM), speed over time.
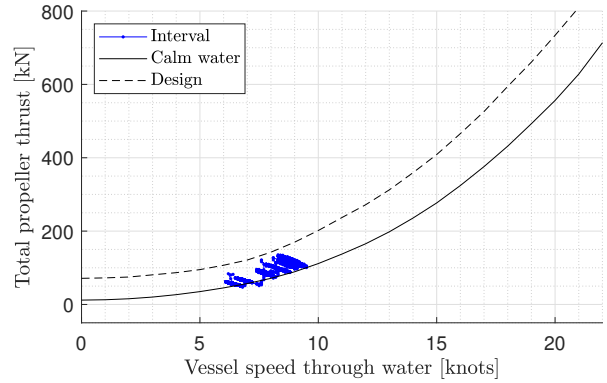
(h) Interval No 6 (EM), thrust over speed.

Figure 3.18: Typical voyage intervals.

3.6.2 *Comparison of electrical and mechanical propulsion*

In this section, we provide the results of comparing mechanical and electrical propulsion over ten voyage intervals characterised by non-dynamic conditions when the ship transits between 5 and 10 knots without manoeuvring. During these voyage intervals, the operator can run on either MM or EM. Alternatively, during manoeuvring intervals, which are excluded in this comparison, the operator often has to select MM to have sufficient power available for the manoeuvres. The main constraint of running in EM is the electrical motor's maximum power, which limits the maximum ship speed for these voyage intervals to 10 knots.

The comparison of the fuel consumption prediction between MM and EM is presented in Table 3.10. Figure 3.19 provides a visual representation of the result and main influencing parameters. According to the simulation comparison, MM would be, on average, 1.2 ± 1.7% less efficient than EM, and the vessel would consume just 0.67% more fuel in those ten voyage intervals combined. Nevertheless, it appears that higher mean sea margin and speed favors MM. It is interesting to compare these results with the results of previous work by Vasilikis, Geertsma and Visser [21]. In the data analysis performed on the same vessel's data, electrical propulsion appeared less efficient, but this was the case for the specific operational and environmental conditions for each mode selected, thus not comparing under similar conditions. Hence, we conclude that simulation of the vessel's energy performance on the exact same voyage intervals demonstrates that there are no clear energy efficiency benefits from sailing on one of the two operational modes, while many other influencing parameters can have a more significant impact on attained energy performance.

3.7 CONCLUSIONS AND RECOMMENDATIONS

This work proposes a method to evaluate and predict carbon intensity in true operational and environmental conditions. This method can be used to provide insight and guidance to improvements in the operation and design of ship propulsion and power systems to achieve more energy efficient designs and reduce the carbon intensity of ship operation over the lifetime of a vessel. This chapter proposes a novel digital twin that accurately predicts the fuel consumption and carbon intensity of mechanical, electrical, and hybrid propulsion systems under the aggregate effect of operational and environmental uncertainties. A combined approach with first principle steady state models and machine learning models allows us to predict instantaneous fuel consumption with an accuracy of less than 5% MAPE and carbon intensity over voyage intervals within 2.5% at a confidence interval of
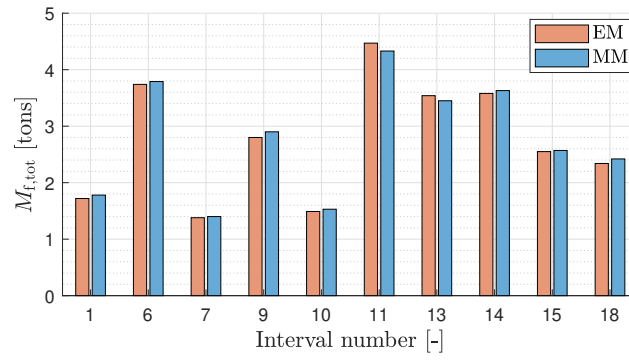
(a) Total fuel consumption.
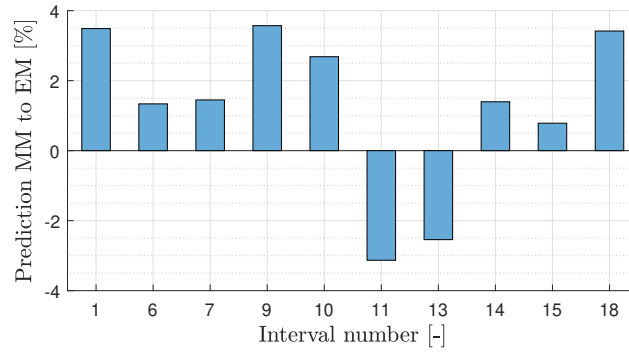
(b) Prediction difference between MM and EM.
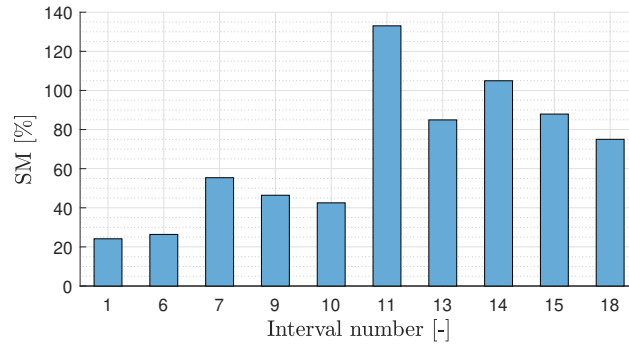
(c) Mean sea margin.
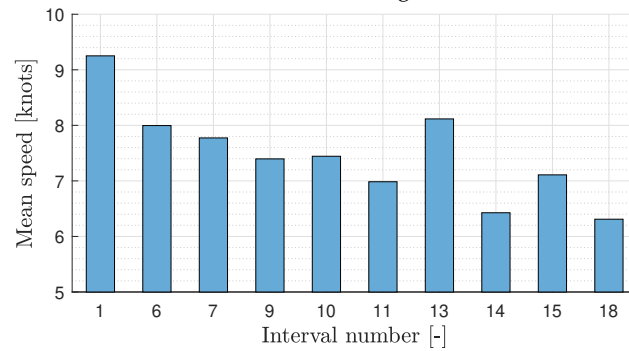
(d) Mean speed.

Figure 3.19: Comparison of MM and EM energy performance on the selected ten EM voyage intervals.

95% for the case study OPV. The use of machine learning algorithms contributes to improving prediction accuracy on the scale of 35 to 50%.

This work provides proof that steady state models can accurately predict fuel consumption and carbon footprint during both dynamic manoeuvring and constant speed operations. The prediction accuracy of the total amount of consumed fuel and carbon intensity over a sufficiently long voyage is higher than the point wise accuracy of the model. A combination of first principle and machine learning models can be used to overcome uncertainty due to inaccurate sensor readings and manufacturers' data, the scale effect of hull and propeller measurements, true operational conditions, and dynamic operational decisions. We expect using data from a thrust sensor can provide even more accurate predictions, as thrust measurement enables separating the effect of uncertainty due to the environmental conditions and scale effects from the effect of uncertainties in the efficiency of the propulsion plant due to inaccurate manufacturers' data and sensor readings.

The proposed method can be used to make accurate comparisons between different operating modes for real operating profiles represented by typical voyages under various conditions. The case study patrol vessel's results indicate that electrical propulsion does not provide statistically significant fuel and carbon savings, even though electrical mode can prevent the main diesel engines from running at low speed and can reduce noise levels. This result emphasises the need to evaluate and predict carbon intensity with models that account for operational and environmental conditions. In future work, we intend to demonstrate how the method can be applied to the evaluation of propulsion and power systems configuration modifications, but also to the evaluation of alternative design options for ships with a similar operating profile.

Table 3.8: Comparison between the MAPE of the instant fuel consumption and the APE of the amount of fuel and carbon intensity over the selected mechanical mode (MM) voyage intervals.

	Duration [hours]	Mean speed [knots]	$M_{f,tot}$ [tons]	Carbon intensity [kg$_{CO_2}$\nm]	MAPE $\dot{m}_{f,tot}$ [%]	APE $M_{f,tot}$ / CI [%]
1	10.2	12.2	6.2	160.9	5.82	2.73
2	6.2	15.7	6.2	201.8	4.62	3.82
3	5.8	17.2	8.1	258.8	4.40	2.54
4	5.0	9.7	2.4	159.4	11.18	1.74
5	8.8	10.3	4.8	169.9	7.07	0.69
6	5.8	18.7	11.5	342.5	2.77	1.41
7	5.4	17.0	7.3	254.4	4.30	4.06
8	9.1	18.7	16.4	308.8	3.32	3.00
9	13.5	17.9	21.8	289.4	2.80	2.03
10	7.0	13.6	5.4	182.8	2.81	0.91
11	16.4	17.5	24.7	274.8	3.20	2.65
12	9.0	17.8	16.3	325.2	2.21	1.85
13	13.6	16.3	17.9	258.9	1.99	0.97
14	18.5	15.2	22.2	253.2	2.79	1.72
15	18.1	15.8	24.1	271.7	2.26	1.60
16	5.0	11.5	3.3	182.5	9.56	1.53
17	16.3	13.6	16.6	238.8	4.79	1.49
18	8.3	13.0	7.3	214.1	3.06	0.59
19	25.8	13.4	24.1	224.1	3.52	2.30
20	10.8	15.7	15.1	284.6	2.83	0.97
21	14.5	14.4	14.8	227.0	2.00	0.92
22	3.9	14.8	4.3	241.1	1.97	0.92
23	12.3	15.1	13.6	234.0	2.08	1.81
24	11.7	14.9	12.7	233.8	2.30	1.62
25	13.3	12.9	9.4	175.7	4.61	2.29
26	10.8	13.3	7.4	165.7	5.23	2.58
27	9.6	15.5	9.8	211.5	3.37	2.65
28	11.4	17.1	14.5	239.8	1.89	0.33
29	7.7	14.4	6.1	178.8	2.78	0.82
30	10.6	16.4	13.6	251.8	2.83	1.40
31	10.6	15.9	14.0	267.8	4.36	4.25
32	13.4	14.3	13.2	222.3	6.73	4.05
33	7.9	15.8	8.6	220.1	3.58	2.07
34	20.0	14.4	16.9	188.0	3.29	0.24
35	25.2	18.2	39.3	275.2	2.82	2.56
36	15.8	14.0	11.7	170.0	4.24	3.90
37	23.0	15.0	20.9	194.5	3.48	2.70
38	24.5	15.2	22.1	190.7	2.50	1.94
39	14.6	15.9	15.2	210.6	3.37	2.16
40	12.4	16.6	16.2	252.5	3.21	3.00
41	4.7	16.8	6.1	247.6	1.95	0.61
42	17.8	16.7	23.1	249.7	2.08	0.39
43	15.7	17.1	21.2	254.0	2.40	1.42
44	23.2	16.9	29.0	236.3	4.47	4.42
45	12.2	16.4	13.9	220.9	4.81	4.79
46	8.3	14.9	7.6	196.1	4.39	4.37
47	16.9	14.7	14.8	190.6	4.43	3.79
48	15.7	13.9	13.0	191.3	3.71	1.59
49	28.1	15.1	27.8	209.3	4.63	1.96
50	10.0	18.8	16.8	285.0	4.69	3.87
Average					3.79 ± 0.52	2.16 ± 0.35

Table 3.9: Comparison between the MAPE of the instant fuel consumption and the APE of the amount of fuel and carbon intensity over the selected electrical mode (EM) voyage intervals.

	Duration [hours]	Mean speed [knots]	$M_{f,tot}$ [tons]	Carbon intensity [kg$_{CO_2}$\nm]	MAPE $\dot{m}_{f,tot}$ [%]	APE $M_{f,tot}$ / CI [%]
1	5.3	9.3	1.7	110.1	4.02	3.23
2	9.1	6.2	1.9	109.2	3.88	1.19
3	7.1	7.3	1.9	119.8	3.75	0.46
4	8.0	7.9	2.2	109.8	3.95	3.46
5	10.5	7.4	3.0	123.2	4.08	3.14
6	13.2	8.0	3.7	111.0	2.91	2.27
7	4.7	7.8	1.3	119.3	3.20	2.25
8	9.8	5.3	2.1	127.9	4.75	3.42
9	10.1	7.4	2.7	118.2	2.58	2.29
10	5.3	7.4	1.5	118.2	2.54	1.82
11	13.1	7.0	4.5	157.6	1.92	0.83
12	21.2	8.0	7.5	142.5	4.43	3.25
13	10.1	8.1	3.5	138.7	4.31	0.14
14	12.6	6.4	3.5	140.0	3.38	1.31
15	8.5	7.1	2.5	134.7	2.32	0.90
16	6.8	6.8	2.0	136.3	2.88	1.83
17	11.3	4.9	2.5	143.2	3.77	0.93
18	9.2	6.3	2.3	129.6	3.59	0.23
19	11.4	5.9	2.9	135.5	3.24	1.03
20	22.6	6.2	5.8	132.7	2.77	0.73
21	21.0	7.1	5.6	120.5	3.55	0.85
22	13.7	8.0	4.2	124.7	2.03	0.69
Average					3.36 ± 0.35	1.65 ± 0.49

Table 3.10: Total fuel consumption prediction on mechanical (MM) and electrical mode (EM) on selected electrical propulsion voyage intervals.

	Mean Speed [knots]	Mean SM [%]	Actual EM [tons]	Predicted EM [tons]	MM [tons]	MM to EM [%]
1	9.3	24	1.67	1.72	1.78	+3.1
6	8.0	26	3.65	3.74	3.79	+1.6
7	7.8	55	1.35	1.38	1.40	+1.3
9	7.4	46	2.74	2.80	2.90	+3.4
10	7.4	43	1.46	1.49	1.53	+2.6
11	7.0	133	4.51	4.47	4.33	- 3.3
13	8.1	85	3.54	3.54	3.45	- 2.6
14	6.4	105	3.53	3.58	3.63	+1.5
15	7.1	88	2.53	2.55	2.57	+1.0
18	6.3	75	2.35	2.34	2.42	+3.3
Total			27.33	27.61	27.80	+0.7
Average						$+1.2 \pm 1.7$

4

A ROBUST MULTI-OBJECTIVE OPTIMISATION FRAMEWORK FOR THE DESIGN OF SHIP ENERGY SYSTEMS

This chapter is an extended version to the single objective methodology presented in [142]:

N. Vasilikis, R. Geertsma, L. Oneto *et al.*, 'A design by optimisation approach for hybrid propulsion systems sizing using actual sailing profiles', *Proceedings of the ASME 43rd International Conference on Ocean, Offshore & Arctic Engineering (OMAE)*, 2024

ABSTRACT

Mitigation of climate change requires the transportation sector to reduce its carbon footprint, hence improve its energy efficiency. In that direction, electrification of ships is taking place at a fast pace. In particular, ships with hybrid propulsion and power supply are considered promising alternatives to ships with typical diesel mechanical propulsion. Nevertheless, an increased number of parameters crucially influences the energy performance and carbon footprint of hybrid ships. Such parameters are the electrical hotel load, individual sailing profiles, selection of component maker, volume and weight restrictions, but also the additional financial cost, both capital and operational. The energy performance of new designs for most ship types in the maritime industry is examined with the regulated Energy Efficiency Design Index (EEDI). However, its limited consideration of one design point in calm water conditions, determined by the installed rated power of the main propulsors, is characterised as insufficient, if not dangerous. The automotive and aviation industries have already adopted measures that assess the energy performance of new designs over defined operating cycles, such as the Worldwide harmonised Light-duty vehicles Test Cycle (WLTC) or the Landing and Take-Off cycle (LTO). This chapter proposes a new methodology for the sizing of hybrid propulsion systems, and demonstrates it in the use case of the 'Holland class' ocean patrol vessels of the Royal Netherlands Navy. This methodology uses

high-frequency operational data logged by the vessel's automation system to get the actual sailing profiles of three individual vessels. A state-of-the-art digital twin approach leveraging data-driven and first principle models of the vessels' energy system, developed by the authors in a previous stage, is used to predict fuel consumption and carbon intensity of ship operations under actual operational and environmental conditions. The developed optimisation methodology is compared to the benchmark methodology that integrates common assumptions at the design stage and regulated procedures. The solution of the resulting multi-objective optimisation problem demonstrates a carbon intensity improvement in the scale of 5% and an operational expenditure one in the scale of 10%, while actual sailing profiles are needed to reach safer conclusions.

4.1   INTRODUCTION

The maritime industry still delivers more than 80% of global trade, overcoming fluctuations caused by the COVID-19 pandemic [9]. Despite the large scale of operations, the International Maritime Organisation (IMO) decided in its updated greenhouse gases (GHGs) reduction strategy not only to cut those emissions in half by 2050 [13], but to aim for net-zero emissions around the same period [14]. In many cases, electrification of ships has been appointed the way forward, though a pure electrical propulsion system suffers from a number of disadvantages with the increased conversion losses near top ship speed being the most prominent [40]. Hybrid propulsion systems are considered a promising alternative, though the right sizing and selection of components is not a simple design problem, due to the exploding size of the design space [54].

The energy performance of the majority of new ships is regulated with the Energy Efficiency Design Index (EEDI) [17]. Although the name implies assessing the vessel's energy efficiency, this index provides carbon emissions per transport work, or carbon intensity, on a single sailing point determined by the rated power of main propulsors and a vessel's resistance in calm water conditions. As a consequence, it does not examine part-load energy savings of different hybrid propulsion systems and it does not consider the operational and environmental uncertainty at sea [24]. Additionally, its use in the design of ships instead of actual operating profiles of real ships tends to underestimate the lifetime energy savings of different energy solutions [26]. Other transportation fields like the automotive and aviation point in the same direction, evaluating carbon emissions and fuel economy on driving cycles and flight profiles accordingly [27], [28].
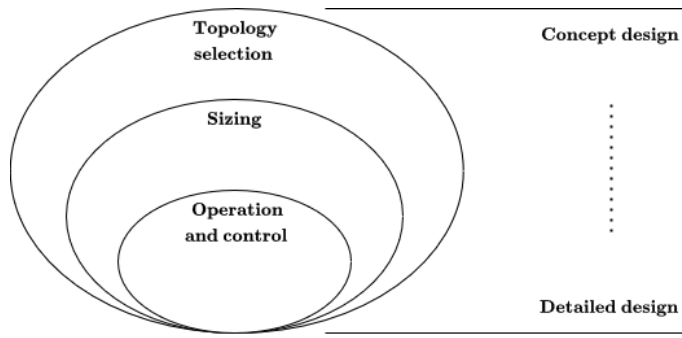
Figure 4.1: Optimisation of ship energy systems.

Design of ship energy systems involves additional difficulty due to a large number of components, their non-linear behaviour, and interconnection [42]. Recently increased requirements on ship energy performance impose the design of more complex ship energy systems than in the past as well [40]. A usual practice is to design ships according to sets of empirical rules [143]. However, ship design by optimisation has already established its superior performance [41], with the detail and type of problems addressed changing at different design phases [54] as suggested in Figure 4.1.

As early as in concept design, energy performance analysis and optimisation problems include topology selection and sizing of propulsion and power supply components [20]. At a later stage, problems involve sizing and energy management [144], [145]. Different fuel types are examined for the energy transition and maritime decarbonisation as well [65]. Finally, another branch of optimisation problems focuses on the optimal design and operation of specific components like propellers [64], [94], [146], engines [147], and subsystems [58], [101]. Regardless of the application, the usual objectives of the considered optimisation problems can be categorised as environmental, social, economic, and technical [43].

Environmental problems usually involve minimising greenhouse gas emissions, mainly carbon dioxide emissions, but also other exhaust gas pollutants, thermal pollution, noise pollution, and land deterioration. The examined time window also varies from static single-point calculations, as in the case of EEDI, to life-cycle assessments that evaluate gas emissions over the building, operation, and dismantling of ships [148]. Finally, the minimisation of carbon emissions should not be confused with maximising the energy efficiency of energy systems as demonstrated in Chapter 2 and in literature [20], or with reducing nitrogen (NO_x) and sulphur (SO_x) oxides, and primary particulate matter (PM) emissions.

Financial objectives include indicators such as capital expenditure (CAPEX), operational expenditure (OPEX), life-cycle cost (LCC), cost-benefit analyses, present worth value of costs (PWF), and years of investment return. Capital expenditure usually involves purchasing

costs, while operational expenditure consists mainly of fuel, lubrication, and maintenance cost [65], [101], [104]. Lately, with the increasing complexity of systems, the cost of replacing batteries is also considered [149]. Last but not least, technical objectives refer to reserved machine room volume and the total weight of the propulsion system.

As discussed in the previous paragraphs, carbon footprint assessment using the EEDI is criticised. Some studies consider carbon emissions over several static operating conditions as an alternative [150]. Chapter 3 discussed various input scenarios for the analysis and optimisation of ship energy systems. Those include the use of calm water and design resistance curves from towing tank tests, different vessel speed, mechanical, auxiliary, thermal and cooling power profiles, either as distributions or time-series. Mechanical profiles involve either shaft or propulsion power evaluated by vessel speed profiles and resistance curves or directly measuring shaft torque.

In this chapter, a decision was made to examine the optimal sizing and topology of a hybrid propulsion system using the attained carbon intensity, capital expenditure, operational expenditure, and total weight of the main system components. The proposed framework adopts actual sailing profiles from the continuous monitoring of three sister ships described by vessel speed and propeller thrust, for the following reasons:

- The increased thrust level over calm water resistance at corresponding speed captures the aggregate effect of different operational and environmental conditions.

- It allows the use of more detailed component maps integrating functioning over different shaft speed compared to power profiles, not only energy efficiencies dependent on power.

- Such vessel operational profiles can be used both with mechanical and electrical propulsion utilising different combinator curves.

The results of Chapter 3 suggest that this vessel speed and thrust consideration combined with a steady-state digital twin leveraging first-principle and operational data-driven techniques is accurate and computationally inexpensive in predicting carbon intensity over voyage intervals of at least 4 hours of continuous sailing. As a result, it is integrated in the design optimisation framework proposed in this chapter.

4.1.1 *Relative work*

Literature provides numerous studies on the design optimisation of ship energy systems [144], [145], [150]. Taking into account the elements of an optimisation problem, such as the number and nature

of objectives, the different simulation scenarios, the case study application itself, the selected mathematical formulation and solvers, classification can be done in different ways. Since our study focuses on a framework for the design optimisation of hybrid propulsion systems, we categorise literature examples based on application, as shown in Figure 4.1.

Purely on topology selection, Livanos, Theotokatos and Pagonis [151] compared techno-economic performance using LCC and environmental performance using EEDI for a number of alternatives to the original diesel engine plant of a Ferry/Ro-Ro vessel using steady state models. Again, on topology selection, though optimising the size as well, lies the work by Trivyza, Rentizelas and Theotokatos [65]. This study examines the simultaneous minimisation of three types of emissions and life cycle cost for a large number of available technologies. It utilises steady state models to simulate operation over a number of operating states and a non-dominated sorting genetic algorithm (NSGA-II) to solve the multi-objective combinatorial optimisation (MOCO) problem.

Solely focused on the sizing of components, Solem, Fagerholt, Erikstad *et al.* [152] optimised a diesel-electric system configuration over a number of working points while considering area size violation as a lost cargo profit in their cost objective. The examined options in their study are actual engine models of different manufacturers and they solve their problem using the branch and bound technique. Sakalis and Frangopoulos [101] optimise the size of main diesel engines by minimising present worth cost (PWC) using a genetic algorithm, although going deeper in modelling in detail exhaust heat treatment. Their analysis manifests the use of genetic algorithms in maritime energy system optimisation problems.

On energy management, Ancona, Baldi, Bianchi *et al.* [104] examined load allocation on a diesel mechanical and diesel hybrid system of a cruise ship. The objective function consists of the cost of fuel, maintenance, and the cost of buying electricity from the national grid. Furthermore, they introduce a regulatory, fictitious cost used to prioritise or penalise certain strategies. Their analysis uses mechanical, electrical, thermal, and cooling hourly power profiles over winter, summer, and spring/autumn. They also use a genetic algorithm and perform a deeper financial investment and environmental analysis on the optimal system obtained. Dedes, Hudson and Turnock [103] also optimised power allocation of main diesel engines, diesel generators and electricity storage means finding the global minimum of fuel consumption between charging and discharging mode. They additionally point out the importance of optimally sizing the system. Finally, Balsamo, Capasso, Lauria *et al.* [153] used dynamic programming to find the optimal battery current of a system that consists

of batteries and supercapacitors on a fast craft, in order to minimise charging/discharging fluctuations.

Another branch of studies works on both the sizing and energy management of components. Zhu, Chen, Wang *et al.* [66] optimised the size of diesel generators and batteries on a hybrid anchor handling tug supply vessel and the energy management rule-based parameters. The operation of the tug involves shore charging. Interesting in their methodology is the modelling of motors and generators performance of different size with the scaling technique of Willans line that uses principal dimensions, which they used as design variables. In their consequent work, they continued their single-objective optimisation work in a bi-objective optimisation problem [67]. Wang, Shipurkar, Haseltalab *et al.* [154] also worked on the optimal sizing and control of an examined hybrid system of an offshore support vessel utilising batteries and fuel cells, with the introduction of a double layer optimisation methodology. Specifically the upper layer optimisation involves the optimal sizing of main diesel engines, batteries and fuel cells, while the inner one the optimal load allocation. The used objectives in their work are CAPEX, OPEX, and emissions.

A different category of studies examines systems in more detail and focuses on optimising the working parameters of thermodynamic cycles. For example, Baldi, Larsen and Gabrielii [58] optimised the organic Rankine cycle of a suggested waste heat recovery (WHR) system of a product/chemical tanker. This work contributes to the substantial improvement of energy efficiency by accounting for part-load operation, comparing results on a single design point, a design and part-load point, and the actual power propulsion and auxiliary power profiles over one year. Shu, Liu, Tian *et al.* [80] reaches a similar conclusion with the comparison of optimal WHR operation based on six operating conditions and the most frequent (design) condition.

Finally, there is a last category of studies that focuses on the optimisation of the performance of certain components. For example, minimising the fuel consumption of a four-stroke turbocharged diesel engine by selecting the speed of turbocharger, start angle of injection, intake valve timing, and amount of injected fuel Tadros, Ventura and Soares [147] or the optimisation of the performance of diesel engines and propellers using two distinct optimisation modules Tadros, Ventura and Soares [155]. Design optimisation of propellers, especially controllable-pitch ones, has been the subject of many studies which recently focus on overall fuel consumption of propulsion systems rather than the energy efficiency of the propeller itself [64], [94], [146]. The scenarios examined in their design are usually sets of thrust and rotational speed, while genetic algorithms are mainly used as solvers.

Ultimately, a look at design optimisation in other transportation fields shows the aforementioned use of driving cycles and flight profiles in the evaluation of fuel efficiency. In automotive, fuel economy

and carbon emissions are evaluated on driving cycles as the World harmonised Light-weighted Testing Cycle (WLTC) [27]. These speed profiles refer to a combination of urban and highway driving and translate to certain speed torque tuples for a selected vehicle. In aviation, fuel economy and emissions are evaluated over flight profiles, such as the landing and take-off (LTO) and the cruise, climb, and descent (CCD) cycles. Although these procedures are already more detailed than EEDI, emission performance gaps have been observed between real world driving and laboratory testing [156], a gap that following the 'diesel gate' scandal was estimated at 30-40% [157], [158]. For this reason, research in both automotive and aviation moves into the direction of adopting more realistic running profiles through the statistical analysis of actual driving and flight profiles [159]–[161]. Latest maritime literature follows this approach with a number of publications either indicating the necessity or aiming to provide operational profiles for ships either as power profiles of main engines or vessel speed and draft profiles [162]–[164].

4.1.2 *Research gap*

The usual consideration in the design optimisation literature of ship energy systems is a limited number, if not only one operational condition to describe the complex effect of weather conditions and propeller and hull fouling. Moreover, the modelling framework using power profiles does not support the distinction and demonstration of the effect of those different conditions on the examined objectives as well. Finally, design optimisation at an energy system level usually uses the total cost of purchasing and operating a system. This consideration is sensitive to selected fuel, maintenance and unit capital costs, and it does not demonstrate the effect of capital investment on carbon footprint reduction and operational costs, important to maritime industry stakeholders.

4.1.3 *Aim and contribution*

The contribution of this work is summarised hereafter: It provides a complete and holistic optimisation framework for the hybrid propulsion topology selection and system sizing at the concept design stage. It uses the existing knowledge on actual operational and environmental conditions variation, result of monitoring vessels of existing classes that serve similar mission types, to find the necessary resolution of the examined scenarios. This holistic framework considers environmental, financial, and technical objectives and focuses on demonstrating competing mechanisms rather than case-specific individual solutions. Its computational efficiency and prediction accuracy allows the extended design space exploration that is not limited to the se-

lection of individual components but extends to the performance modelling of a continuous space of solutions, as described in Section 4.2. Finally, it demonstrates the stability and efficiency of the proposed optimisation problem formulation.

4.2   CASE STUDY

4.2.1   *Original design*

The case study design is the *Holland class* ocean patrol vessels designed by DAMEN group for the Royal Netherlands Navy (RNLN). A total of four vessels was built between 2008 and 2011. The vessels are equipped with hybrid propulsion. Two controllable pitch propellers are driven either mechanically by two main diesel engines or electrically by two electrical motors. Speed is reduced in two two-stage gearboxes and electrical power is produced by three diesel generators. A detailed description of the vessels is provided in Appendix A.

4.2.2   *Alternative designs*

The examined alternative designs include the resizing of the electrical power supply and propulsion of the vessels, adding the power take-off option which allows electrical motors to perform as shaft generators. The main parameter describing the size of the electrical system is the size of the two electrical motors. The vessel is equipped with two low speed induction motors rated at 400 kW. At this rating, the vessel can sail up to 10 knots in calm water conditions, preventing the main diesel engines from running at loads that are lower than 15%, an operating area that shows increased brake specific fuel consumption and results in additional maintenance cost. Electrical propulsion also offers the advantage of less noise nuisance. Larger electrical motors would allow vessels to sail on electrical propulsion at higher speeds, as shown in Figure 4.2. Larger electrical motors can be both high and low voltage up to approximately 2 200 kW and high voltage above that rating. High voltage motors for marine applications, typically utilise 3 300, 6 600, and 11 000 V, compared to 440 V and require additional modifications to the power system architecture, such as adding transformers for both the propulsion converters and the mission system and auxiliary loads. It is not the scope of this study a detailed design of the electrical system of the vessel, as this takes place at a more advanced part of the design process. This range of voltages refers to medium voltage shore applications. ABB offers a variety of high frequency electrical motors for marine applications, the weight and rating of which can be found in Figure 4.3. Furthermore, these electrical motors are able to run at lower speeds, comparable to main diesel engines' nominal speed of 1,000 rpm. This allows the motors and the main diesel engines to share the
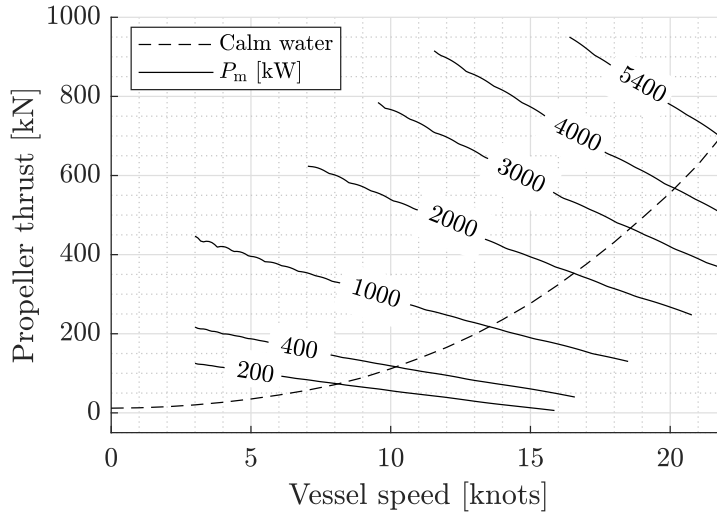
Figure 4.2: Thrust limit over vessel speed for electrical motors of different rated power.

same single reduction stage gearbox. On the electrical power supply, larger motors require larger electricity production. The total electricity production of the current design stands at 3x 910 kW. The specific fuel consumption and weight of different diesel generators available in the market can be found in Figures 4.4 and 4.5. Catalogue specific fuel consumption of diesel generators has a tolerance of +5% usually without engine driven pumps, it refers to fuel of lower calorific value 47 700 kJ/kg, ISO fuels, and ISO standard reference conditions, and it does not include the effect of ageing which can cause an increase of up to 2% [165], [166]. Engine driven pumps can add 2.5% as well [11]. As a consequence, our study considers a conservative increase of 8% over the catalog value to compensate for operation in actual working conditions and non-ISO fuels.

4.3 METHODOLOGY

This chapter provides an optimisation framework for the topology selection and sizing of the hybrid propulsion system of ships. This framework evaluates different systems from an environmental, financial, and technical perspective, accounting for realistic operational and environmental conditions. The simulation of the vessel's operation utilises a state-of-the-art digital twin approach for the modelling of the vessel's energy system leveraging first-principle and operational data-driven techniques as described in Chapter 3. This model, although computationally expensive to build, it is sufficiently inexpensive to use in design optimisation applications. The methodology is summarised in Figure 4.6, and it is fully described in this section.
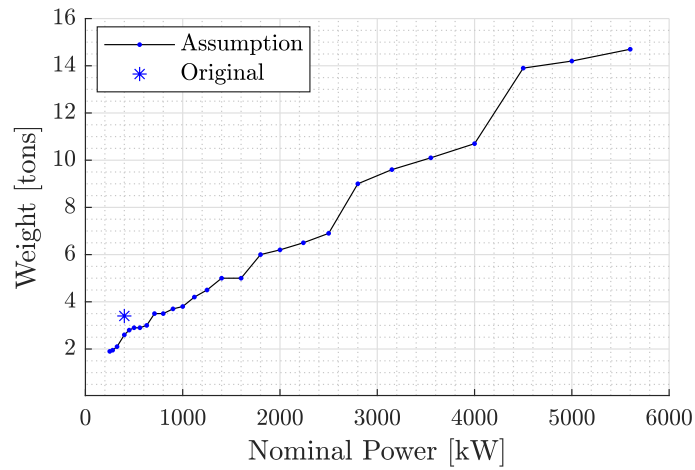
Figure 4.3: Weight of available electrical motors.
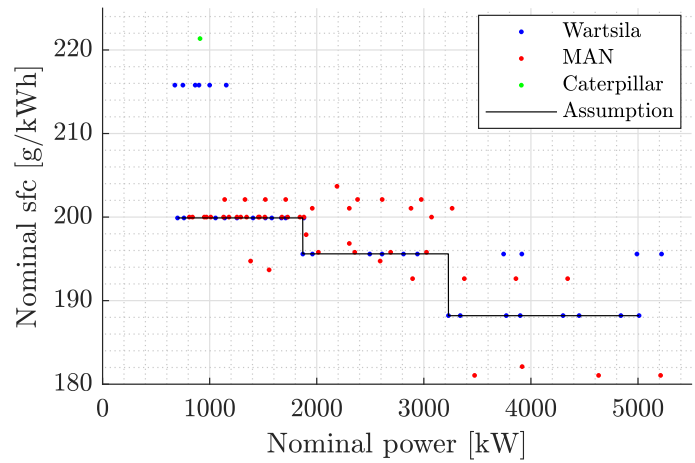
Figure 4.4: Catalogue nominal specific fuel consumption of available market diesel generators.
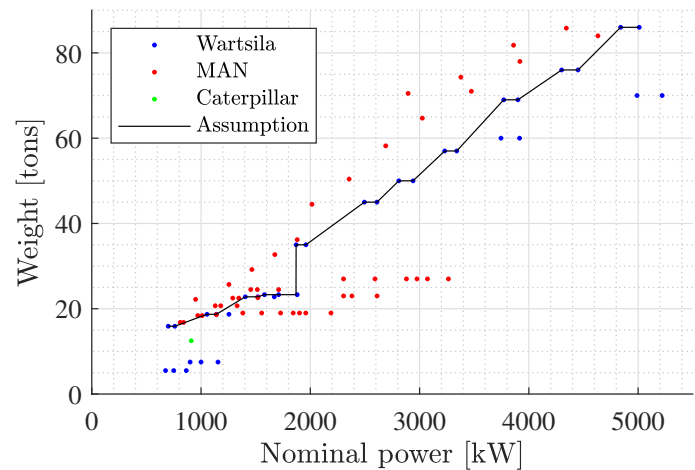
Figure 4.5: Weight of the different diesel generators.
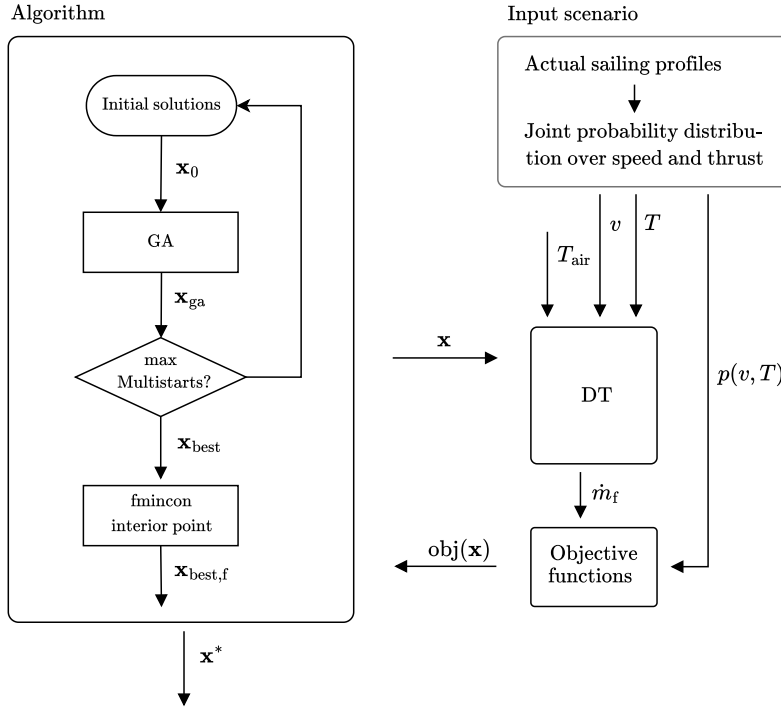
Figure 4.6: Design by optimisation framework.

4.3.1 *Problem Description*

As discussed in the introduction of this chapter, topology and sizing optimisation has emerged as an innovative technique in the design of ship energy systems, particularly for hybrid systems. It employs advanced computational methods to determine the most efficient and effective layout and size within a specific design space, aiming to achieve the best performance under given constraints. For marine power supply and propulsion systems, this means determining the optimal configuration of components – such as combustion engines, electric motors, energy storage systems, and transmission elements – to ensure seamless power delivery, reduce fuel consumption, and minimise environmental impact. This study concentrates on the optimal design of future classes of ships based on results of analysis and modelling over operational data available from the monitoring of three vessels of the same class that were operated under diverse operational and environmental conditions. A detailed description of the examined class of vessels can be found in Appendix A. Based on the number and type of components, it is possible to define a number of parameters that can be optimised. Some of them will be kept fixed, while some will be optimised as seen in Table 4.1. The examined problem focuses on the electrical propulsion system of the vessel, hence all new

Table 4.1: Original Powertrain design associated parameters' value.

Parameter	Symbol	Value	Unit	Optim-ized
Main diesel engine nominal power	P_e	5 400	[kW]	
Main diesel engine nominal speed	n_e	1 000	[rpm]	
Gearbox reduction stage 1	r_e	4.355	[-]	
Gearbox reduction stage 2	r_m	17.88	[-]	
Electrical motors nominal power	P_m	400	[kW]	✓
Electrical motors nominal speed	n_m	1788	[rpm]	
Number of type a diesel generators	N_a	2		✓
Power rating of type a diesel generators	P_a	910	[kW]	✓
Number of type b diesel generators	N_b	-		✓
Power rating of type b diesel generators	P_b	-	[kW]	✓

designs considered use the same main diesel engines, propellers, shaft lines and combinator curves. We further assume that both mechanical and electrical propulsion use the first reduction stage of the original two-stage reduction gearboxes. New designs will still involve two electrical induction motors. The main design parameters concern the size of the two electrical motors and the number and size of diesel generators. The number of different types of diesel generators is set to two based on common design practise, from now on type a and type b. The performance of different designs is examined on the design vessel speed profile under calm water and design conditions, but also on the actual operational and environmental sailing conditions encountered by the three vessels of the class.

4.3.2 *Optimisation problem formalisation*

The developed optimisation framework aims to minimise four objectives, be them carbon intensity CI, operational expenditure C_{opex}, capital expenditure C_{capex} and total weight W_{tot}, written as:

$$\min_{\mathbf{x}} \quad \text{CI} \quad (\mathbf{x}, \mathbf{p}, \mathbf{i}), \tag{4.1}$$

$$\min_{\mathbf{x}} \quad C_{opex} (\mathbf{x}, \mathbf{p}, \mathbf{i}), \tag{4.2}$$

$$\min_{\mathbf{x}} \quad C_{capex}(\mathbf{x}, \mathbf{p}), \tag{4.3}$$

$$\min_{\mathbf{x}} \quad W_{tot} \quad (\mathbf{x}, \mathbf{p}), \tag{4.4}$$

where $\mathbf{x}$ is the set of independent design variables:

$$\mathbf{x} = (P_m, N_a, P_a, N_b, P_b), \tag{4.5}$$

with P_m being the power rating of the electrical motors, N_a, P_a, N_b, P_b the number and power rating of the type a and type b diesel generators and:

$$P_m, P_a, P_b \in \mathbb{R} \text{ and } N_a, N_b \in \mathbb{I}. \tag{4.6}$$

p is the set of fixed parameters as discussed in the problem description and demonstrated in Table 4.1, and **i** is the optimisation input scenario described by vessel speed v, propeller thrust T, the probability of occurrence $p(v, T)$, and external air temperature T_{air}:

$$\mathbf{i} = \{ v, T, p(v, T), T_{air} \} . \tag{4.7}$$

The optimisation problem is subject to a number of boundary constraints (see Table 4.2):

$$P_m^l \leq P_m \leq P_m^u , \tag{4.8}$$

$$N_a^l \leq N_a \leq N_a^u , \tag{4.9}$$

$$P_a^l \leq P_a \leq P_a^u , \tag{4.10}$$

$$N_b^l \leq N_b \leq N_b^u , \tag{4.11}$$

$$P_b^l \leq P_b \leq P_b^u , \tag{4.12}$$

$$N_a + N_b \leq 5 . \tag{4.13}$$

Diesel generators power range lies between the smallest available engine by the manufacturers and engines that do not violate the height of the main diesel engines by more than 50%. Finally, the number of diesel generators of type a, b, and the total number of them is bounded based on the common practise in similar vessel type designs to comply with weight, space and maintenance spare parts limitations.

One technical constraint secures that sufficient electrical power is installed:

$$N_a\ P_a + N_b\ P_b \geq \left(\frac{2\ P_m}{\eta_m} + \max P_{hotel} \right) \frac{1}{L_{max}} , \tag{4.14}$$

where maximum electrical hotel power under typical operation is set at 710 kW, the maximum running load of the diesel generators L_{max} is equal to 0.85 and the nominal efficiency of the motors η_m is equal to 0.934.

Another technical constraint prevents the installation of unnecessary diesel generators:

$$N_a\ P_a + (N_b - 1)\ P_b \leq \left(\frac{2\ P_m}{\eta_m} + \max P_{hotel} \right) \frac{1}{L_{max}} , \tag{4.15}$$

or in the case of $N_b = 0$:

$$(N_a - 1)\ P_a \leq \left(\frac{2\ P_m}{\eta_m} + \max P_{hotel} \right) \frac{1}{L_{max}} . \tag{4.16}$$

Furthermore, there is a redundancy constraint as the maximum hotel load needs to be served by a single diesel generator, hence:

$$P_a, P_b \geq \frac{\max P_{hotel}}{L_{max}} . \tag{4.17}$$

Table 4.2: Design variables and lower/upper bounds.

Lower bound		Upper bound		Unit
Symbol	Value	Symbol	Value	
P_m^l	200	P_m^u	5 500	[kW]
N_a^l	1	N_a^u	5	[-]
P_a^l	700	P_a^u	4 529	[kW]
N_b^l	0	N_b^u	4	[-]
P_b^l	700	P_b^u	4 529	[kW]

4.3.3   *Objective functions*

4.3.3.1   *Carbon intensity*

In this work, CI is evaluated as the fraction of carbon dioxide emissions M_{CO2} and covered distance Δs over the examined period Δt:

$$CI = \frac{M_{CO2}}{\Delta s} \qquad (4.18)$$

Carbon dioxide emissions are evaluated as a double integral of speed v and thrust T:

$$M_{CO2} = \int\!\!\int^{v\,T} \dot{m}_f(v,T)\, f_{CO2}\, p(v,T)\, \Delta t \; dv\,dT \qquad (4.19)$$

$$\simeq \sum_v \sum_T \dot{m}_f(v,T)\, p(v,T)\, \Delta t\, f_{CO2}\, \delta v\, \delta T \,, \qquad (4.20)$$

where $p(v,T)$ is the probability of occurrence of a (v,T) tuple, f_{CO2} is the carbon coefficient f_{CO2} equal to 3.206 as in EEDI calculation [17] and $\dot{m}_f$ is the total fuel consumption estimated using the digital twin approach described in Chapter 3 for certain vessel speed v, propeller thrust T, and ambient temperature T_{air}. Covered distance is calculated in a similar manner as:

$$\Delta s = \int\!\!\int^{v\,T} v\, p(v,T)\, dv\,dT \simeq \sum_v \sum_T v\, p(v,T)\, \delta v\, \delta T \,. \qquad (4.21)$$

Fuel consumption of diesel generators and electrical motors of different size is simulated using the nominal specific fuel consumption values in Figure 4.4 and the normalised part load behaviour described in Figures 4.7 and 4.8.

4.3.3.2   *Operational expenditure*

Net present value of the operational expenditure C_{opex} is evaluated from the yearly amount $C_{opex,y}$:

$$C_{opex} = \sum_{y=1}^{N_y} C_{opex,y} \left(\frac{1 + i_f}{1 + i_m} \right)^y \,, \qquad (4.22)$$
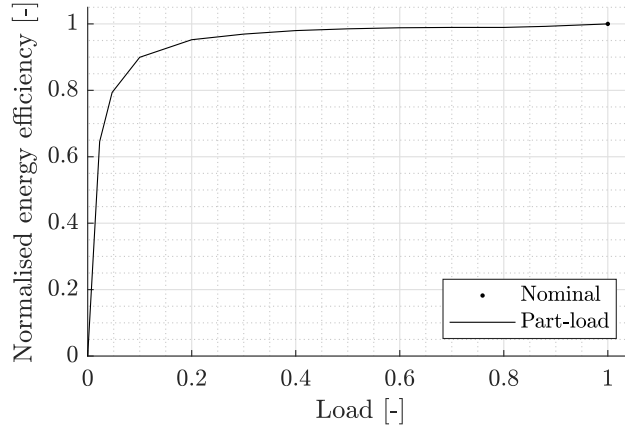
Figure 4.7: Normalised energy efficiency of the electrical motors [2].
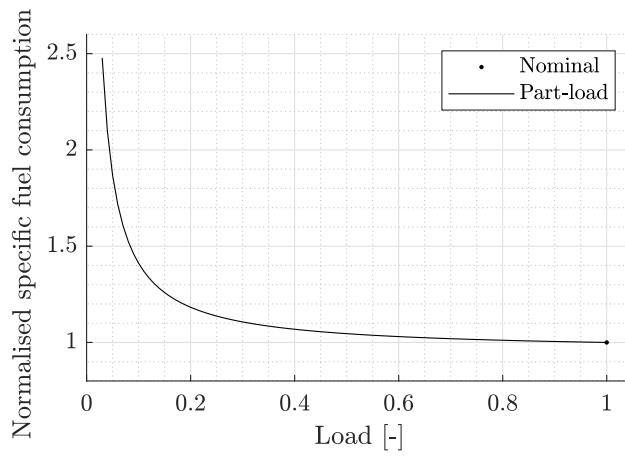
Figure 4.8: Normalised specific fuel consumption of the diesel generators.

accounting for inflation rate i_f, market interest rate i_m and years in consideration N_y. Example values from literature and the selection of this study can be found in Table 4.3. Operational expenditure in a

Table 4.3: Inflation rate i_f, market interest i_m and years under consideration N_y in this study and examples in literature.

	i_m	i_f	N_y
[151]	10%	-	20
[101]	8%	3%	-
[65]	7%	-	25
This study	8%	3%	25

certain year consists mainly of the fuel C_{fuel} and maintenance C_{maint} cost.

$$C_{opex,y} = C_{maint} + C_{fuel} , \qquad (4.23)$$

Fuel cost is given from:

$$C_{\text{fuel}} = \left(M_{\text{f,g}} + M_{\text{f,e}} \right) c_{\text{f}} , \qquad (4.24)$$

where

$$M_{\text{f,e}} = \int\int^{v\,T} \dot{m}_{\text{f,e}}(v, T)\, p(v, T)\, \Delta t\, dv\, dT , \qquad (4.25)$$

$$M_{\text{f,g}} = \int\int^{v\,T} \dot{m}_{\text{f,g}}(v, T)\, p(v, T)\, \Delta t\, dv\, dT , \qquad (4.26)$$

is the total fuel mass consumed by the main diesel engines and diesel generators respectively. Fuel price for marine diesel oil was selected at 630 €/ton. Maintenance cost C_{maint} is given from the maintence cost of main diesel engines $C_{\text{maint,e}}$, diesel generators $C_{\text{maint,g}}$ and electrical motors $C_{\text{maint,m}}$:

$$C_{\text{maint}} = C_{\text{maint,e}} + C_{\text{maint,g}} + C_{\text{maint,m}} , \qquad (4.27)$$

$$C_{\text{maint,e}} = \int\int^{v\,T} 2\, P_{\text{e}}\, c_{\mu,\text{e}}\, p(v, T)\, \Delta t\, dv\, dT , \qquad (4.28)$$

$$C_{\text{maint,g}} = \int\int^{v\,T} \sum P_{\text{g}}\, c_{\mu,\text{g}}\, p(v, T)\, \Delta t\, dv\, dT , \qquad (4.29)$$

$$C_{\text{maint,m}} = 2\, P_{\text{m}}\, c_{\mu,\text{m}} , \qquad (4.30)$$

where c_{μ} are maintenance cost coefficients providing the cost of a running hour per unit rated power. We use a value of 0.015 €/kWh both for diesel main engines and generators as in [104], and 1% of capital expenditure for the electrical motors [149].

4.3.3.3 *Capital expenditure*

Capital expenditure C_{capex} of the main components of the system consists of the capital costs of main diesel engines $C_{\text{capex,e}}$, diesel generators $C_{\text{capex,g}}$, and electrical motors $C_{\text{capex,m}}$:

$$C_{\text{capex,g}} = \sum P_{\text{g}}\, c_{\text{g}} , \qquad (4.31)$$

$$C_{\text{capex,e}} = 2\, P_{\text{e}}\, c_{\text{e}} , \qquad (4.32)$$

$$C_{\text{capex,m}} = 2\, P_{\text{m}}\, c_{\text{m}} . \qquad (4.33)$$

where c_{g}, c_{m}, and c_{e} are the purchase cost coefficients of the diesel generators, electrical motor, and main diesel engines respectively in euros per unit rated power (€/kW).

4.3.3.4 *Total weight*

Total weight of the main power supply and propulsion components W_{tot} is given from:

$$W_{\text{tot}} = 2\, W_{\text{e}} + 2\, W_{\text{m}} + \sum W_{\text{g}} , \qquad (4.34)$$

where W_a, W_b, W_m are the weights of the type a and b diesel generators and electrical motors that can be evaluated from Figures 4.3 and 4.5 respectively, and W_e is the weight of each main diesel engine which goes to zero in a fully diesel electric configuration:

$$W_e = \begin{cases} 36.1 & P_m \leq 5\,500\,\text{kW} \\ 0.0 & \text{otherwise} \end{cases} \tag{4.35}$$

4.3.3.5 *Redundancy terms*

The solution of the introduced optimisation problem provides the required electrical motors and diesel generators to serve sufficiently the examined operational scenarios. The actual energy system consists of one more diesel generator, able to serve the hotel load for redundancy purposes. We need to account for this with the following redundancy parameters on the capital expenditure:

$$C_{\text{capex,red}} = \begin{cases} \min(P_a, P_b)\, c_g, & \min(P_a, P_b) \leq P_{g,\text{thr}}, \\ 840\, c_g, & \min(P_a, P_b) > P_{g,\text{thr}}, \end{cases} \tag{4.36}$$

and total weight:

$$W_{\text{red}} = \begin{cases} \min(W_a, W_b), & \min(P_a, P_b) \leq P_{g,\text{thr}}, \\ 16.7, & \min(P_a, P_b) > P_{g,\text{thr}}. \end{cases} \tag{4.37}$$

The distinction below and above the power threshold $P_{g,\text{thr}}$ is used to balance prioritising a larger number of identical diesel generators to unnecessary installed power. In this work it was picked equal to 1 000 kW.

4.3.4 *Problem resolution*

The multi-objective optimisation problem reported in Equations 4.1-4.17 can be formulated and solved following a different number of strategies [167]. In this paper, we adopt a formulation of the problem into a single objective framework by converting the multiple objectives into a weighted sum of the normalised objectives, as detailed in [168]:

$$\min_{x} \quad \lambda_1\, \text{CI}(x, p, i) + \lambda_2\, C_{\text{opex}}(x, p, i) \\ + \lambda_3\, C_{\text{capex}}(x, p) + \lambda_4\, W_{\text{tot}}(x, p), \tag{4.38}$$

where $\lambda_i \in [0, 1]$ defines the importance of the different objectives, i.e., for $\lambda_i \to 1$, authors care more about the weight than the ultimate compressive strength and vice-versa for $\lambda_i \to 0$, and $\lambda_1 + \lambda_2 + \lambda_3 + \lambda_4 = 1$. Solving Equation (4.38) for different values of λ allows for the creation of the so-called Pareto frontier in a computationally efficient way [168].

4.3.5 *Optimisation algorithms*

Optimisation problems can be classified according to a number of criteria. A typical distinction is in constrained and unconstrained problems based on the presence or absence of linear or non-linear equality or inequality relations among decision variables, and in linear and non-linear problems based on the linearity of the objective function or functions. Another important aspect is whether decision variables are real or integer. Many of the mathematical optimisation algorithms discussed in the following paragraphs are originally developed for the case of real variables, making the solution of integer programming problems challenging [169]. Other classes of problems include deterministic and stochastic programming, separable, single or multi-objective programming, and finally, static, dynamic, and intertemporal static programming based on the way they handle time.

Solving algorithms in most textbooks fall under three main categories, search methods, calculus (gradient based) methods and stochastic or evolutionary methods [170]–[172]. Search methods and evolutionary methods do not guarantee global optimality of the result solutions. Optimisation problems that seek the optimal value of decision variables over time are usually making use of calculus of variations methods or if they include sequences of decisions, dynamic programming methods. In case of no time-dependency and discretisation, these problems are turned into multiple static optimisation problems. The solvers used depend on the nature of the examined problem.

Search methods or region elimination methods do not require the objective function to be continuous, they are also suitable in the case of discrete variables, it is sufficient though the functions to be unimodal [171]. The main philosophy behind those methods is the comparison of the objective function value at two different points. In the case of single variable functions, example methods are the Swann method and golden section search. In the case of multi-variable functions, example methods are the univariate method, simplex method and its improved version Nelder and Mead method, Hook and Jeeves method and its improved version Rosenbrock method, and Powell method.

Calculus (gradient) methods impose additional requirements on the objective function, as it needs to be unimodal, continuous and differentiable. Example methods in the single variable function case are Newton-Raphson method, Bisection method, and Secant method, while a well known method in the case of multi-variable functions is the generalised reduced gradient method. A special category that uses the benefits of gradient methods is the polynomial approximation methods, with sequential linear and quadratic programming methods (SLP & SQP) being two widely used examples.

A distinct class of algorithms simulates biological, molecular and neurological phenomena [173]. Examples are genetic and evolutionary

algorithms, simulated annealing, and Particle swarm optimization among others. Genetic algorithms are mainly used because of the nature of ship energy systems optimisation problems:

- no analytical description of objective functions is regularly the case

- non-continuous objective functions or first derivative function

- integer decision variables

4.3.6 *Selected algorithm*

The introduced multi-objective optimisation problem of Equations 4.1-4.17 and 4.38 has a non-linear and non-convex objective function and a series of non-linear constraints. Taking into account the integer nature of some of the decision variables in Equation 4.7, the introduced problem can be classified as a Mixed-Integer Non-Linear Programming (MINLP) problem. In order to solve it, different approaches can be exploited [174]. In fact, a series of no-free-lunch theorems [175] ensure that there is no way to choose a-priori the best optimisation algorithms for a particular problem, and the only option is to empirically test multiple approaches verifying which is actually the best one.

Recognising the challenges, heuristic approaches like Genetic Algorithms (GA) or Simulated Annealing (SA) can be considered viable solution strategies as reported in the relevant literature [168], [171]. These may not guarantee absolute optimality, but they have demonstrated prowess in delivering high-quality solutions within restricted time frames [171]. Nonetheless, with heuristic methods, managing constraints effectively is important, and penalty methods need to be employed to ensure the constraints are respected [176]. Since the convergence of all these algorithms is influenced by the starting point, multi-start strategies are followed [177].

In this study, as demonstrated in Figure 4.6, we use a genetic algorithm using the ga function of the Matlab 2022a[1] environment within a multi-start loop. As starting points, this methodology uses: (i) the original system configuration and size (ii) 100 in the case of single optimisation and 50 in the case of multi-objective optimisation, random points uniformly distributed in the domain induced by the constraints of Equations 4.8 - 4.17. Table 4.4 summarises the parameter settings of the implemented algorithm. The resulting best solution of the genetic algorithm is then provided to a gradient method like the interior-point algorithm.

---

1 https://www.mathworks.com/

Table 4.4: Parameters setting for the different optimisation algorithms.

Parameter	Value(s)
Population size	300
Elite count	250
Crossover fraction	0.7
Crossover function	"crossoverscattered"
Max generations to stall	30
Function tolerance	1e-4
Constraint tolerance	1e-4
UseParallel	"true"

4.3.7 *Optimisation scenarios*

The design by optimisation methodology described in this chapter uses the actual sailing profiles of three sister vessels, but generalises to using sailing profiles of vessels that serve similar missions. These scenarios are then compared with simple ones based on calm water resistance and design conditions commonly used at the concept design phase that are treated as benchmarks. Sailing profiles are described by vessel speed and propeller thrust, and a complete scenario in the context of this work consists of a sailing profile described with tuples of vessel speed v and thrust T, the frequency of occurrence of each tuple $p(v, T)$, and the external air temperature T_{air} that is statistically correlated to the electrical hotel load as seen in Figure 3.11. Figures 4.9b, 4.9d and 4.9f provide the joint probability distribution of vessel speed and thrust in the case of the the three OPVs. Benchmark scenarios use a typical speed profile of an OPV (see Subfigure 4.9g), and three cases for ship resistance (see Subfigure 4.9h). A calm water resistance curve based on scale model towing tank tests, a fixed percentage increase in resistance over calm water conditions, and a design resistance curve that is the result of sea keeping tank tests at certain environmental conditions.

All elements can be found in Figure 4.9, and they are summarised in Table 4.5. The time spent at sea was assumed as 20% of a calendar year (see Table A.4).
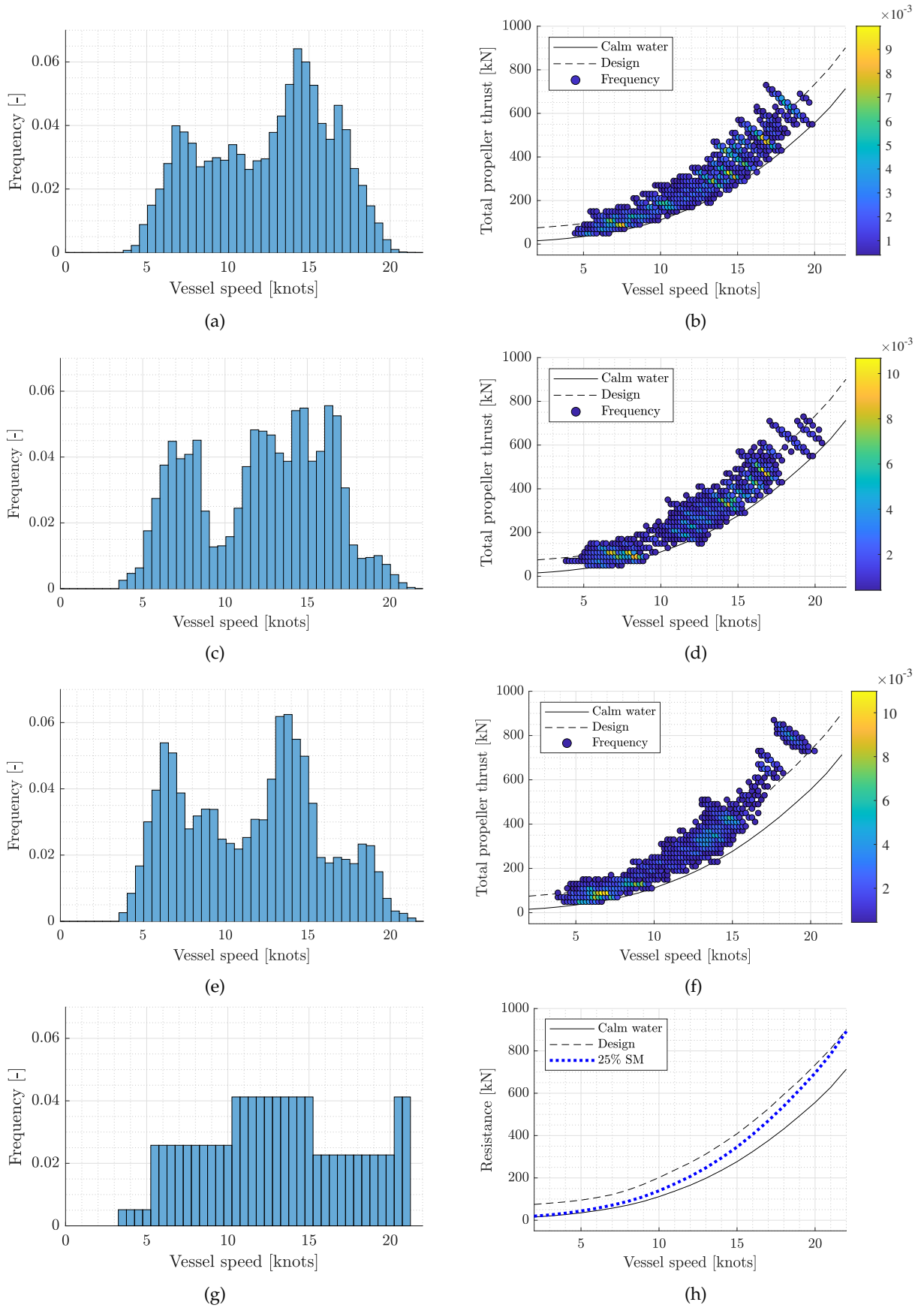
Figure 4.9: Elements of optimisation scenarios.

4.4   RESULTS

4.4.1   *Single-objective optimisation*

This section discusses the results of the four single-objective optimisation problems described by Equations 4.1 - 4.4. The result of these problems is useful in understanding the individual influence of each objective on the optimal design of the examined system. Being simpler than the multi-objective problem, they make it possible to identify the influence of the different optimisation scenarios on the optimal solutions as well. Mathematically, these problems derive from Equation 4.38 setting $\lambda_i = 1, \lambda_j = 0, \forall\, i, j \in [1, 4], j \neq i$. Carbon intensity and operational expenditure required the simulation of the energy system's operation over the examined operating scenarios, while total weight and capital expenditure were just calculated over different feasible solutions. The original design mentioned in the results refers to the original size of electrical motors, diesel generators, and manufacturers, though with a gearbox of a single reduction stage rather than two on electrical mode.

The decisive factor for carbon intensity minimisation is the nominal specific fuel consumption curve found in Figure 4.4. Table 4.7 provides the results for the carbon intensity optimisation problem in the case of calm water and design conditions, and sailing profiles of three class vessels. It comes not as a surprise that the size of diesel generators that appears in different solutions is 1 870 or 3 230 kW. Slightly smaller diesel generators have a worse nominal specific fuel consumption, and slightly bigger ones operate at a lower load for the same specific fuel consumption which based on Figure 4.8 indicates an overall higher fuel consumption. The size of the electrical motors is driven by the fuel efficiency of the diesel generators. Carbon intensity is proportionally related to fuel consumption hence the result is one big engine compared to multiple small ones.

Operational expenditure consists of the cost of fuel and maintenance. The assumption in this work is that the maintenance cost in €/hour depends on the nominal power of the engine. According to this assumption, running smaller and cheaper to maintain per hour diesel generators is better than bigger engines. The same applies to running on electrical propulsion instead of main diesel engines at lower speeds, as their maintenance cost per running hour is higher, proportional to rated power. Table 4.8 provides the results of the operational expenditure minimisation problem. Savings in the scale of one million euros in net present value are established in all scenarios. Again calm water with sea margin and design conditions overestimate savings, but also the height of operational expenditure as well in a 25 year horizon.

Table 4.5: Optimisation scenarios.

	$v,\ T,\ p(v,T)$	T_{air} [°C]	P_{hotel} [kW]
Calm	Figure 4.9g & 4.9h	25.0	605
Calm +25%	Figure 4.9g & 4.9h	25.0	605
Design	Figure 4.9g & 4.9h	25.0	605
Vessel 1	Figure 4.9b	23.4	600
Vessel 2	Figure 4.9d	22.3	590
Vessel 3	Figure 4.9f	20.8	585

The mathematical optimisation solution is trivial in the case of capital expenditure and total weight of the energy system. This happens because the increase in the size of electrical motors is not followed by a decrease in the size of main diesel engines. Therefore, the optimal solution is the smallest electrical propulsion part.

A general observation on the results of both the CI and OPEX problems is that the different environmental and operational conditions established by each vessel influence the optimal solution of the problem and the achieved height of savings. As an example, power take-off has marginal effect for the heavier conditions that vessel 3 sailed into. Improvement of CI was smaller compared to OPEX in all input scenarios as well.

Table 4.6: Objectives value in the case of the original design.

Input	Decision variables			Objectives	
	pto [-]	P_m [kW]	P_{gen} [kW]	CI [kg_{CO_2}/nm]	OpEx [x10^3 €]
Calm	no	2x 400	2x 910	179.7	-
Calm +25%	no	2x 400	2x 910	210.8	16 853
Design	no	2x 400	2x 910	236.0	18 724
Vessel 1	no	2x 400	2x 910	203.7	14 610
Vessel 2	no	2x 400	2x 910	199.0	13 761
Vessel 3	no	2x 400	2x 910	215.0	13 189
				CapEx [x10^3 €]	W_{tot} [tons]
-	no	2x 400	2x 910	3 681	116.5

4.4.2 *Capital expenditure and total weight*

Capital expenditure and the total weight of the system are both parameters of significant importance in the design of a system. Especially in the way modelled in this work, they also seem to have an almost linear correlation as can be seen in Figure 4.10. This figure demonstrates an example of one thousand randomly built system designs, demonstrating an R^2 value of 0.97. This correlation allows us to move

Table 4.7: CI minimisation results including percentage the improvement to benchmark case.

Input	Decision variables						Objective	
	pto	P_m	N_a	P_a	N_b	P_b		CI
	[-]	[kW]	[-]	[kW]	[-]	[kW]		[kg$_{CO_2}$/mile]
Calm	no	2x 1 420	1x	3 245	2x	895	(-3.5 %)	173.3
	yes	2x 1 366	1x	3 230	2x	904	(-4.6 %)	171.4
Calm +25%	no	2x 1 698	1x	3 230	3x	880	(-2.7 %)	205.2
	yes	2x 1 276	1x	3 230	1x	952	(-3.4 %)	203.6
Design	no	2x 1 260	1x	840	1x	3 230	(-2.4 %)	230.3
	yes	2x 1 383	1x	3 291	2x	891	(-3.1 %)	228.7
Vessel 1	no	2x 1 350	1x	824	2x	3 230	(-2.9 %)	197.9
	yes	2x 1 370	1x	3 271	2x	839	(-3.9 %)	195.8
Vessel 2	no	2x 1 175	2x	835	1x	3 230	(-2.9 %)	193.2
	yes	2x 1 250	1x	3 234	1x	839	(-3.9 %)	191.2
Vessel 3	no	2x 700	4x	835	-	-	(-2.9 %)	208.8
	yes	2x 1 406	1x	3 231	2x	855	(-3.5 %)	207.5

Table 4.8: Net present value of OPEX including the percentage improvement to benchmark case.

Input	Decision variables						Objective	
	pto	P_m	N_a	P_a	N_b	P_b		OpEx
	[-]	[kW]	[-]	[kW]	[-]	[kW]		[x10^3 €]
Calm	no	2x 1 823	3x	1 004	2x	1 233	(-10.9 %)	13 118
	yes	2x 1 741	1x	1 901	4x	835	(-12.4 %)	12 894
Calm +25%	no	2x 1 770	2x	837	3x	1 213	(-9.1 %)	15 323
	yes	2x 1 800	1x	1 873	4x	884	(-10.0 %)	15 164
Design	no	2x 2 125	3x	835	2x	1 870	(-8.2 %)	17 181
	yes	2x 2 128	1x	3 254	4x	897	(-9.2 %)	17 008
Vessel 1	no	2x 2 151	3x	839	2x	1 881	(-9.5 %)	13 229
	yes	2x 2 195	1x	3 232	4x	830	(-11.0 %)	13 004
Vessel 2	no	2x 2 423	2x	1 876	3x	1 072	(-9.2 %)	12 495
	yes	2x 2 170	1x	3 236	4x	863	(-10.5 %)	12 317
Vessel 3	no	2x 2 254	2x	1 875	3x	934	(-9.2 %)	11 983
	yes	2x 2 191	2x	1 871	3x	878	(-9.7 %)	11 908

on the optimisation procedure accounting for one of the two, in this case capital expenditure, and report the value of total system weight. Hence, we proceed with $\lambda_4 = 0$.

4.4.3 *Multi-objective optimisation*

Multi-function ships are complex ships that need to serve many types of missions. This means that their design unavoidably requires a per-

Table 4.9: Computational efficiency of the genetic algorithm over 100 algorithm starts: (K) Average number of generations per start, (L) Average number of fitness function calls per start, (M) Average running time per start.

		CI problem			OpEx problem		
	pto	K	L	M	K	L	M
	[-]	[-]	[-]	[sec]	[-]	[-]	[sec]
Calm	no	40	8 003	252	41	8 334	300
	yes	38	7 680	225	51	10 326	439
Calm +25%	no	37	7 450	232	45	9 132	379
	yes	39	7 942	273	55	11 059	559
Design	no	41	8 259	339	47	9 358	482
	yes	37	7 536	308	48	9 638	413
Vessel 1	no	38	7 637	322	47	9 498	532
	yes	38	7 644	315	55	10 954	772
Vessel 2	no	36	7 349	572	47	9 420	1 015
	yes	37	7 566	734	46	9 191	1 103
Vessel 3	no	40	7 991	876	49	9 768	1 360
	yes	37	7 493	659	49	9 839	532
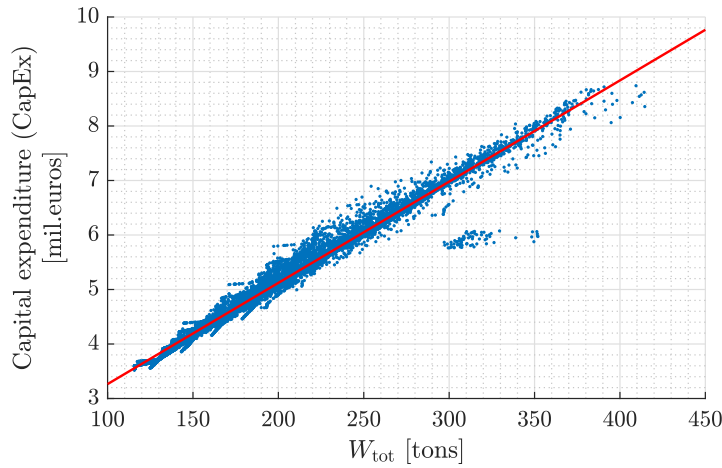
Figure 4.10: Linear correlation of capital expenditure (CapEx) and total weight of the system W_{tot} for 10 000 randomly generated designs.

formance trade-off evaluated with a number of objectives. This section provides the results of the multi-objective optimisation problem and solving strategy introduced in Section 4.3. The result of the optimisation algorithm is a number of solutions that form the so-called Pareto front. Figure 4.11 provides a visual representation of the Pareto front, and Tables 4.10 and 4.11 provide details of different solutions. The input scenario in the case of the multi-objective optimisation problem is the actual sailing profile of vessel 1. Power take-off is also considered in problem solutions.

Figure 4.12 allows the examination of the Pareto front from different angles. We pay attention to the qualitative characteristics of

these figures, as absolute values are influenced by the values used for different costs. It is clear that carbon intensity can improve at the cost of additional capital expenditure, but there is a limit after which it increases again. The same applies to carbon intensity against operational expenditure. On the trade-off between capital and operational expenditure, we observe that increased investment brings improved operational costs, though this improvement rate slows down with additional investment.

Another observation on those results is that based on the influence of each objective, the optimal solution varies (see Figure 4.13). The electrical motor size of the original design at 400 kW forms a lower bound, while motors that are five or six times larger at 2 200 kW form an upper bound. In more than half of cases, only type *a* diesel generators are used. Moreover, in the majority of solutions only one type *a* diesel generator is used, while type *b* ones can vary significantly in number. We also observe that type *b* generators are usually smaller in rated power compared to type *a*.

4.4.4 *Computational efficiency*

Table 4.9 provides metrics on the computational efficiency of the algorithm in the case of single objective optimisation problems of CI and OpEx. Tables 4.12 and 4.13 provide the same metrics in the case of the multi-objective optimisation problem. Genetic algorithms are considered computationally demanding algorithms [150]. Results show that each start of the algorithm requires thousands of fitness function calls. We observe that the CI problem requires around 30% less calls than the OpEx problem. Fitness function calculation times of more than a couple of seconds, and the lack of parallel computing would lead to solving times much higher than a single day for each one of the 83 different problems solved to form the Pareto front. It is also important to notice the significant increase in computational time from the use of the actual sailing profiles of the vessels. Despite this challenge, the selected optimisation framework delivered quality results within the limits of computers capable of supporting parallel running of at least five workers.

4.5 CONCLUSIONS

This chapter provided a design by optimisation framework for the optimal design of the energy system of multi-function vessels from an environmental, financial and technical perspective. This framework is based on the actual sailing profiles of vessels following similar missions, and utilises an accurate and computationally inexpensive digital twin approach for the prediction of the ship's operation. This methodology can generalise in the case of retro-fitting existing ves-
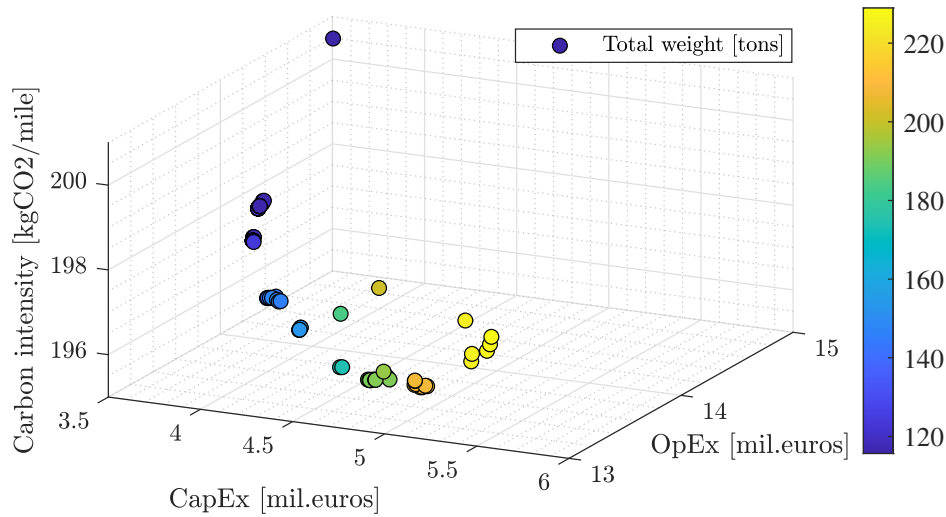
Figure 4.11: Multi-dimensional Pareto front.

sels, though constraints on the dimension of system components are expected to be stricter. It can also generalise in the case of different propulsion or power supply systems, or for ships of different type, although it is expected to benefit more ships that sail under diverse operational and environmental conditions.

This chapter demonstrates this framework on the topology selection and sizing of the hybrid propulsion system of an ocean patrol vessel. The electrical propulsion system of the case study vessels can be used as an alternative to mechanical propulsion, but it can not operate simultaneously with it. For this reason only the electrical propulsion and electrical power supply system is resized, demonstrating the potential in reducing carbon emissions and operational costs.

The main conclusions extracted are summarised hereafter:

- The different solution and attained environmental, financial and technical performance for the different actual sailing profiles of the three vessels of the same class indicate the difficulty in identifying the best trade off among different designs in actual operation.

- Calm water conditions or design conditions resulting from a sea margin superposition can be misleading leading to overestimated energy savings and not optimal designs.

- The proved accurate steady-state modelling approach adopted in this optimisation framework allows the use of joint probability distributions of vessel speed and thrust to describe operational profiles, significantly reducing computational time offering the opportunity of exploring a wider design space.

- Jump discontinuities in nominal specific fuel consumption and weight attributed to different diesel generator families reduce
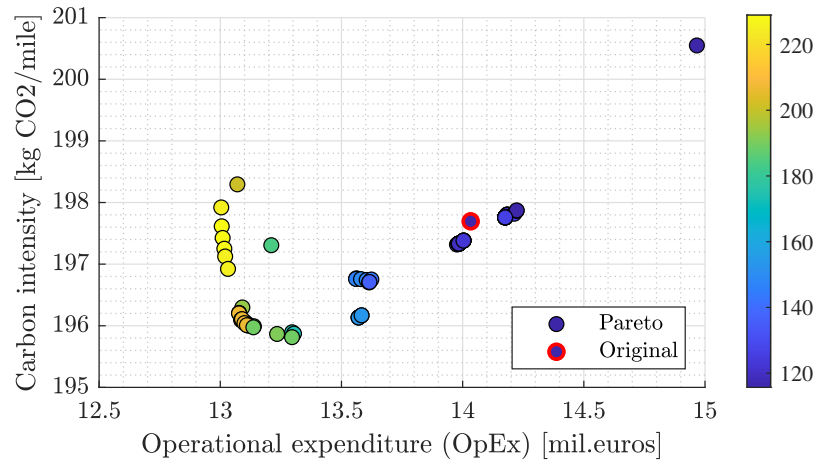
(a)
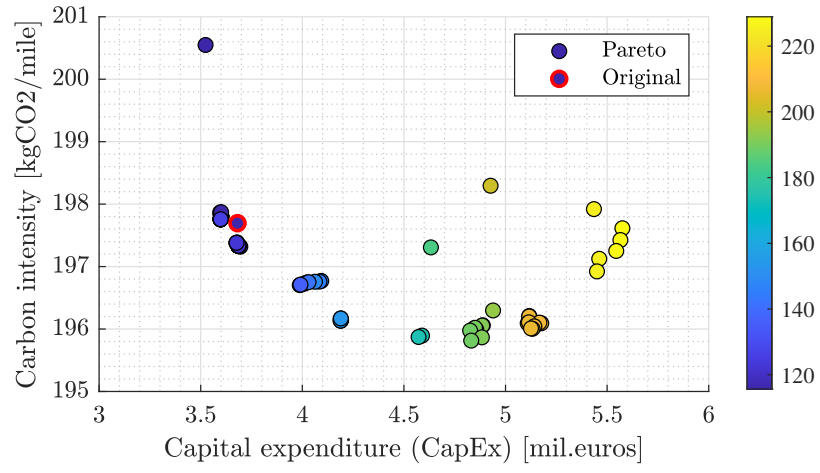
(b)
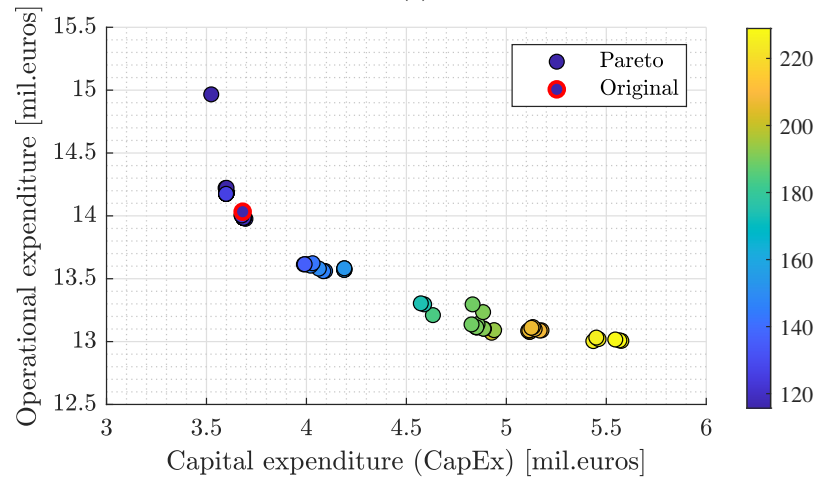
(c)

Figure 4.12: Two dimensional views of the Pareto front with solutions coloured on the total system weight in tons.
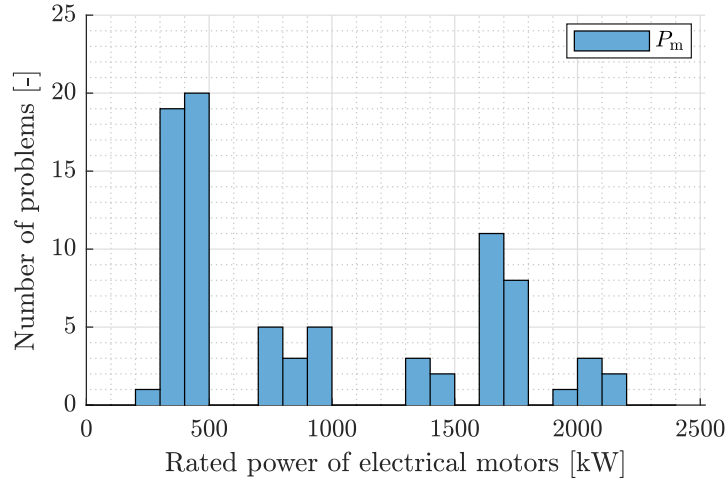
(a)
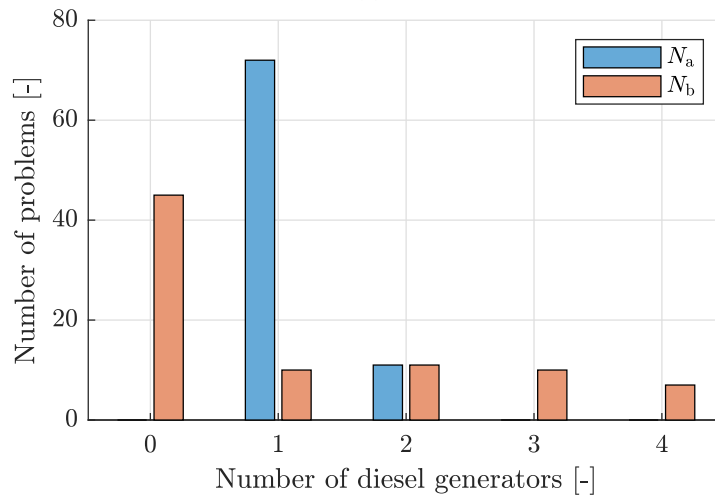
(b)
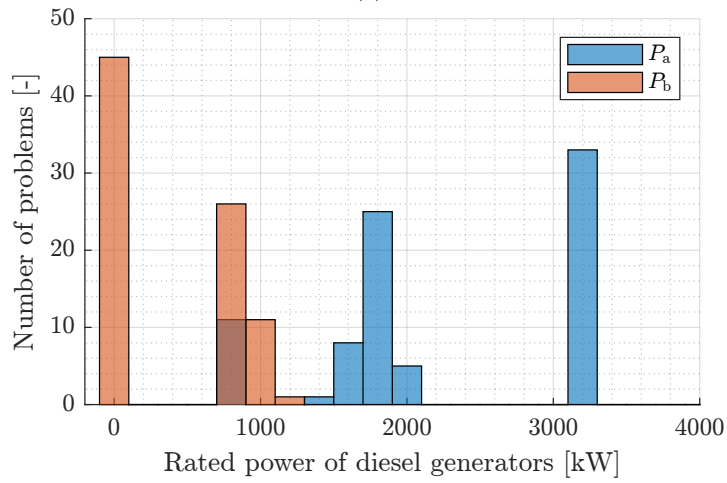
(c)

Figure 4.13: Histograms of the independent design variables of the multi-objective optimisation problem solution.

the effect of different operational and environmental conditions on the optimal problem solution.

- A percentage increase over calm water conditions is not representative of the actual environmental and financial life-cycle footprint of ship operations.

- Designs with an increased electrical motor size coupled with multiple small diesel generators lead to a decreased life-cycle operational cost.

- The use of electrical propulsion has the potential to reduce maintenance cost if propulsion power is provided by diesel generators that are relatively small compared to the main engines, and which have a lower maintenance cost per running hour.

- Designs with an increased motor size coupled with a smaller number of large diesel generators lead to improved carbon intensity due to improved fuel efficiency, though at the expense of higher capital and operational cost, and additional weight.

- Power take-off option improves attained carbon intensity in all operating scenarios resulting to different optimal solutions in most of the examined cases.

- Increasing capital investment reduces operational costs at a decreasing rate before stabilising. This is not the case for carbon intensity, where the initial decrease is followed by an increase indicating a certain capital investment that minimises carbon footprint.

Table 4.10: Solution of the multi-objective optimisation problem.

	λ_1 [-]	λ_2 [-]	λ_3 [-]	λ_4 [-]	P_m [kW]	N_a [-]	P_a [kW]	N_b [-]	P_b [kW]	CI [kgCO2/mile]	OPEX [x10³ €]	CAPEX [x10³ €]	W_tot [tons]
-	1.000	0.000	0.000	0.000	1352	1x	3257	2x	862	195.8	13296.1	4831.2	189
-	0.000	1.000	0.000	0.000	2196	1x	3236	4x	835	197.9	13004.0	5435.1	225
-	0.000	0.000	1.000	0.000	250	1x	1468	-	-	200.5	14966.4	3523.8	116
1	0.100	0.900	0.000	0.000	2120	1x	3235	4x	918	197.6	13005.9	5575.2	229
2	0.087	0.783	0.130	0.000	1720	1x	1870	4x	835	198.3	13070.5	4926.4	201
3	0.071	0.643	0.286	0.000	1415	1x	1870	3x	848	197.3	13210.5	4632.7	184
4	0.059	0.529	0.412	0.000	747	1x	1870	1x	857	196.7	13615.4	4002.4	148
5	0.040	0.360	0.600	0.000	410	1x	1877	-	-	197.4	14003.6	3677.0	122
6	0.200	0.800	0.000	0.000	2091	1x	3234	4x	914	197.4	13009.7	5565.4	229
7	0.174	0.696	0.130	0.000	1740	1x	3233	2x	1003	196.3	13091.0	4938.7	194
8	0.143	0.571	0.286	0.000	840	1x	1873	1x	1114	196.8	13561.8	4093.3	146
9	0.118	0.471	0.412	0.000	430	1x	1924	-	-	197.3	13976.6	3694.8	124
10	0.080	0.320	0.600	0.000	410	1x	1873	-	-	197.4	14003.2	3675.8	126
11	0.300	0.700	0.000	0.000	2063	1x	3236	4x	903	197.3	13016.7	5544.9	228
12	0.261	0.609	0.130	0.000	1663	1x	3230	2x	906	196.1	13102.1	4888.2	192
13	0.214	0.500	0.286	0.000	840	1x	1873	1x	1089	196.8	13560.0	4084.3	146
14	0.176	0.412	0.412	0.000	420	1x	1898	-	-	197.3	13983.9	3685.3	120
15	0.120	0.280	0.600	0.000	330	2x	835	-	-	197.8	14175.3	3598.2	126
16	0.350	0.650	0.000	0.000	2041	1x	3232	4x	857	197.1	13020.1	5461.2	226
17	0.304	0.565	0.130	0.000	1640	1x	3260	2x	863	196.0	13112.7	4851.9	190
18	0.250	0.464	0.286	0.000	817	1x	1870	1x	1033	196.8	13580.6	4062.2	149
19	0.206	0.382	0.412	0.000	420	1x	1899	-	-	197.3	13984.0	3685.6	120
20	0.140	0.260	0.600	0.000	330	1x	1675	-	-	197.8	14183.6	3601.5	116
21	0.400	0.600	0.000	0.000	1999	1x	3231	4x	852	196.9	13031.9	5450.1	225
22	0.348	0.522	0.130	0.000	1642	1x	3276	2x	858	196.0	13113.7	4853.0	190
23	0.286	0.429	0.286	0.000	770	1x	1962	1x	835	196.7	13604.0	4020.6	147
24	0.235	0.353	0.412	0.000	420	1x	1899	-	-	197.3	13984.0	3685.6	120
25	0.160	0.240	0.600	0.000	330	2x	835	-	-	197.8	14175.3	3598.2	126
26	0.450	0.550	0.000	0.000	1747	1x	3231	3x	839	196.2	13077.8	5116.7	207
27	0.391	0.478	0.130	0.000	1661	1x	3234	2x	902	196.1	13102.3	4885.4	192
28	0.321	0.393	0.286	0.000	740	1x	1926	1x	871	196.8	13623.2	4030.8	143
29	0.265	0.324	0.412	0.000	420	1x	1898	-	-	197.3	13983.9	3685.3	120
30	0.180	0.220	0.600	0.000	330	2x	835	-	-	197.8	14175.3	3598.2	126
31	0.500	0.500	0.000	0.000	1743	1x	3230	3x	839	196.2	13077.2	5116.3	207
32	0.435	0.435	0.130	0.000	1640	1x	3288	2x	849	196.0	13115.3	4846.7	190
33	0.357	0.357	0.286	0.000	740	1x	1872	1x	835	196.7	13613.9	3987.4	145
34	0.294	0.294	0.412	0.000	420	1x	1899	-	-	197.3	13984.0	3685.5	120
35	0.200	0.200	0.600	0.000	330	2x	835	-	-	197.8	14175.3	3598.2	126
36	0.550	0.450	0.000	0.000	1701	1x	3262	3x	875	196.1	13089.5	5175.8	208
37	0.478	0.391	0.130	0.000	1610	1x	3264	2x	867	196.0	13138.5	4855.9	190
38	0.393	0.321	0.286	0.000	740	1x	1882	1x	835	196.7	13615.4	3990.9	136
39	0.324	0.265	0.412	0.000	420	1x	1899	-	-	197.3	13984.0	3685.5	120
40	0.220	0.180	0.600	0.000	330	1x	1674	-	-	197.8	14183.5	3601.1	116
41	0.600	0.400	0.000	0.000	1701	1x	3231	3x	835	196.1	13086.0	5109.2	207
42	0.522	0.348	0.130	0.000	1640	1x	3270	2x	857	196.0	13114.6	4849.8	190
43	0.429	0.286	0.286	0.000	420	1x	1899	-	-	197.3	13984.0	3685.6	120
44	0.353	0.235	0.412	0.000	420	1x	1899	-	-	197.3	13984.0	3685.6	120
45	0.240	0.160	0.600	0.000	330	1x	1672	-	-	197.8	14183.2	3600.3	116
46	0.650	0.350	0.000	0.000	1700	1x	3236	3x	875	196.1	13088.0	5166.7	208
47	0.565	0.304	0.130	0.000	1370	1x	3271	1x	1035	195.9	13296.3	4588.9	174
48	0.464	0.250	0.286	0.000	420	1x	1900	-	-	197.3	13984.1	3685.8	120
49	0.382	0.206	0.412	0.000	420	1x	1899	-	-	197.3	13984.1	3685.7	120
50	0.260	0.140	0.600	0.000	330	2x	835	-	-	197.8	14175.3	3598.2	126

Table 4.11: Solution of the multi-objective optimisation problem. (continue).

	λ_1 [-]	λ_2 [-]	λ_3 [-]	λ_4 [-]	P_m [kW]	N_a [-]	P_a [kW]	N_b [-]	P_b [kW]	CI [kg$_{CO_2}$/mile]	OPEX [x10^3 €]	CAPEX [x10^3 €]	W_{tot} [tons]
51	0.700	0.300	0.000	0.000	1 702	1x	3 245	3x	836	196.1	13 089.6	5 114.9	207
52	0.609	0.261	0.130	0.000	1 350	1x	3 259	1x	1 004	195.9	13 304.2	4 572.2	174
53	0.500	0.214	0.286	0.000	420	1x	1 900	-	-	197.3	13 984.1	3 685.7	120
54	0.412	0.176	0.412	0.000	410	1x	1 883	-	-	197.4	14 004.3	3 679.3	118
55	0.280	0.120	0.600	0.000	330	2x	835	-	-	197.8	14 175.3	3 598.2	126
56	0.750	0.250	0.000	0.000	1 664	1x	3 230	3x	860	196.0	13 099.9	5 141.6	207
57	0.652	0.217	0.130	0.000	950	1x	3 245	-	-	196.1	13 571.6	4 190.6	153
58	0.536	0.179	0.286	0.000	420	1x	1 906	-	-	197.3	13 984.9	3 688.2	121
59	0.441	0.147	0.412	0.000	330	2x	835	-	-	197.8	14 175.3	3 598.3	126
60	0.300	0.100	0.600	0.000	330	1x	1 674	-	-	197.8	14 183.4	3 601.0	116
61	0.800	0.200	0.000	0.000	1 640	1x	3 298	3x	838	196.0	13 115.5	5 132.9	206
62	0.696	0.174	0.130	0.000	950	1x	3 241	-	-	196.1	13 570.7	4 189.0	153
63	0.571	0.143	0.286	0.000	420	1x	1 900	-	-	197.3	13 984.1	3 685.8	120
64	0.471	0.118	0.412	0.000	330	1x	1 675	-	-	197.8	14 183.6	3 601.5	116
65	0.320	0.080	0.600	0.000	330	2x	835	-	-	197.8	14 175.3	3 598.2	126
66	0.850	0.150	0.000	0.000	1 640	1x	3 239	3x	848	196.0	13 109.8	5 125.4	207
67	0.739	0.130	0.130	0.000	940	1x	3 243	-	-	196.2	13 582.8	4 189.3	153
68	0.607	0.107	0.286	0.000	420	1x	1 899	-	-	197.3	13 984.0	3 685.6	120
69	0.500	0.088	0.412	0.000	330	1x	1 677	-	-	197.8	14 183.7	3 602.0	116
70	0.340	0.060	0.600	0.000	330	2x	835	-	-	197.8	14 175.3	3 598.2	126
71	0.900	0.100	0.000	0.000	1 613	1x	3 272	2x	836	196.0	13 136.6	4 825.9	189
72	0.783	0.087	0.130	0.000	950	1x	3 239	-	-	196.1	13 570.4	4 188.6	153
73	0.643	0.071	0.286	0.000	420	1x	1 900	-	-	197.3	13 984.1	3 685.9	120
74	0.529	0.059	0.412	0.000	325	2x	835	-	-	197.8	14 213.1	3 597.9	126
75	0.360	0.040	0.600	0.000	325	1x	1 660	-	-	197.9	14 222.0	3 595.7	116
76	0.950	0.050	0.000	0.000	1 450	1x	3 259	2x	905	195.9	13 234.4	4 883.6	191
77	0.826	0.043	0.130	0.000	940	1x	3 244	-	-	196.2	13 583.0	4 189.6	153
78	0.679	0.036	0.286	0.000	410	1x	1 875	-	-	197.4	14 003.4	3 676.6	123
79	0.559	0.029	0.412	0.000	325	1x	1 673	-	-	197.9	14 223.2	3 600.4	116
80	0.380	0.020	0.600	0.000	330	2x	835	-	-	197.8	14 175.3	3 598.2	126

Table 4.12: Computational efficiency of the multi-objective optimisation problem solving algorithm over 50 algorithm starts.

	λ_1	λ_2	λ_3	λ_4	Average number of generations per start	Average number of fitness function calls per start	Average running time per start
	[-]	[-]	[-]	[-]	[-]	[-]	[min]
-	1.000	0.000	0.000	0.000	37	7 485	21
-	0.000	1.000	0.000	0.000	54	10 940	16
-	0.000	0.000	1.000	0.000	69	13 872	18
1	0.100	0.900	0.000	0.000	57	11 366	19
2	0.087	0.783	0.130	0.000	53	10 656	20
3	0.071	0.643	0.286	0.000	43	8 710	20
4	0.059	0.529	0.412	0.000	48	9 723	26
5	0.040	0.360	0.600	0.000	60	11 937	29
6	0.200	0.800	0.000	0.000	56	11 244	28
7	0.174	0.696	0.130	0.000	53	10 676	49
8	0.143	0.571	0.286	0.000	42	8 490	28
9	0.118	0.471	0.412	0.000	45	9 108	23
10	0.080	0.320	0.600	0.000	56	11 291	18
11	0.300	0.700	0.000	0.000	57	11 445	19
12	0.261	0.609	0.130	0.000	53	10 558	26
13	0.214	0.500	0.286	0.000	46	9 285	26
14	0.176	0.412	0.412	0.000	52	10 357	25
15	0.120	0.280	0.600	0.000	57	11 397	29
16	0.350	0.650	0.000	0.000	53	10 594	48
17	0.304	0.565	0.130	0.000	50	10 054	32
18	0.250	0.464	0.286	0.000	45	9 096	22
19	0.206	0.382	0.412	0.000	52	10 456	16
20	0.140	0.260	0.600	0.000	58	11 669	20
21	0.400	0.600	0.000	0.000	54	10 759	25
22	0.348	0.522	0.130	0.000	50	10 136	28
23	0.286	0.429	0.286	0.000	48	9 719	23
24	0.235	0.353	0.412	0.000	47	9 549	22
25	0.160	0.240	0.600	0.000	56	11 322	49
26	0.450	0.550	0.000	0.000	50	10 144	32
27	0.391	0.478	0.130	0.000	49	9 916	23
28	0.321	0.393	0.286	0.000	44	8 773	22
29	0.265	0.324	0.412	0.000	50	10 081	34
30	0.180	0.220	0.600	0.000	56	11 295	51
31	0.500	0.500	0.000	0.000	52	10 424	30
32	0.435	0.435	0.130	0.000	48	9 671	19
33	0.357	0.357	0.286	0.000	46	9 270	19
34	0.294	0.294	0.412	0.000	51	10 314	47
35	0.200	0.200	0.600	0.000	59	11 799	37
36	0.550	0.450	0.000	0.000	52	10 353	20
37	0.478	0.391	0.130	0.000	49	9 829	24
38	0.393	0.321	0.286	0.000	46	9 278	31
39	0.324	0.265	0.412	0.000	54	10 921	49
40	0.220	0.180	0.600	0.000	60	12 103	35
41	0.600	0.400	0.000	0.000	52	10 389	18
42	0.522	0.348	0.130	0.000	44	8 935	19
43	0.429	0.286	0.286	0.000	46	9 278	27
44	0.353	0.235	0.412	0.000	52	10 361	22
45	0.240	0.160	0.600	0.000	59	11 772	24
46	0.650	0.350	0.000	0.000	51	10 200	21
47	0.565	0.304	0.130	0.000	45	9 081	25
48	0.464	0.250	0.286	0.000	48	9 597	24
49	0.382	0.206	0.412	0.000	54	10 755	26
50	0.260	0.140	0.600	0.000	57	11 500	30

Table 4.13: Computational efficiency of the multi-objective optimisation problem solving algorithm over 50 algorithm starts. (continue)

	λ_1	λ_2	λ_3	λ_4	Average number of generations per start	Average number of fitness function calls per start	Average running time per start
	[-]	[-]	[-]	[-]	[-]	[-]	[min]
51	0.700	0.300	0.000	0.000	48	9 597	20
52	0.609	0.261	0.130	0.000	45	9 084	13
53	0.500	0.214	0.286	0.000	49	9 766	14
54	0.412	0.176	0.412	0.000	53	10 562	13
55	0.280	0.120	0.600	0.000	60	12 024	57
56	0.750	0.250	0.000	0.000	47	9 553	39
57	0.652	0.217	0.130	0.000	44	8 951	42
58	0.536	0.179	0.286	0.000	47	9 518	21
59	0.441	0.147	0.412	0.000	54	10 885	16
60	0.300	0.100	0.600	0.000	61	12 170	17
61	0.800	0.200	0.000	0.000	45	9 053	29
62	0.696	0.174	0.130	0.000	48	9 747	24
63	0.571	0.143	0.286	0.000	49	9 869	19
64	0.471	0.118	0.412	0.000	55	10 948	52
65	0.320	0.080	0.600	0.000	55	11 086	45
66	0.850	0.150	0.000	0.000	47	9 400	43
67	0.739	0.130	0.130	0.000	48	9 593	12
68	0.607	0.107	0.286	0.000	49	9 896	12
69	0.500	0.088	0.412	0.000	51	10 318	33
70	0.340	0.060	0.600	0.000	60	12 055	27
71	0.900	0.100	0.000	0.000	43	8 746	25
72	0.783	0.087	0.130	0.000	49	9 766	26
73	0.643	0.071	0.286	0.000	52	10 452	24
74	0.529	0.059	0.412	0.000	53	10 574	25
75	0.360	0.040	0.600	0.000	60	12 063	36
76	0.950	0.050	0.000	0.000	41	8 210	14
77	0.826	0.043	0.130	0.000	43	8 643	26
78	0.679	0.036	0.286	0.000	49	9 872	25
79	0.559	0.029	0.412	0.000	55	11 074	27
80	0.380	0.020	0.600	0.000	65	12 973	36

5

REFLECTION

Ship designers and operators receive feedback on their designs and decisions only on a limited number of occasions like in ship acceptance trials. This feedback corresponds to calm water conditions that are usually not representative of the actual conditions during operations in most geographical places and calendar months. Chapter 1 framed this issue, and it suggested the use of operational data with the following problem statement:

How can the collection, processing and use of operational data improve the operation and design of ships from an environmental, financial, and technical point of view?

In this direction, Chapter 2 provided a methodology to assess the energy performance of ship operations using high-frequency operational data, it provided feedback to ship designers and operators, and it described realistic operational and environmental conditions to be utilised in the design of new ship energy systems. Chapter 3 provided a steady-state digital twin approach for the carbon intensity prediction of ship operations leveraging first-principle and data-driven techniques. It accounted for the aggregate effect of both operational and environmental conditions, and it balanced computational cost and prediction accuracy. Chapter 4 provided a design by optimisation framework for ship energy systems. This framework utilised computationally efficient and accurate digital twin approaches as the one introduced in Chapter 3, and it sought the trade-off from an environmental, technical, and financial perspective. Finally, this chapter, Chapter 5, discusses the progress made towards the goal of this dissertation summarising and reflecting on the results and conclusions from Chapter 2 to 4, and identifying the conclusions, limitations and recommendations of this dissertation.

5.1   CONCLUSIONS

Distilled from the whole of this dissertation, this paragraph summarises the key findings of the work conducted as answers to the research questions introduced in Chapter 1.

5.1.1   *Energy performance assessment of ship operations*

How can we quantify and depict operational and environmental uncertainty using operational data analysis?

Operational and environmental uncertainty is addressed in all three main chapters of this dissertation. Chapter 2 proposes the qualitative depiction of its aggregate effect on the two-dimensional histogram of propeller thrust against vessel speed. Quantitative means evaluate mean thrust over discretised vessel speed and standard deviation, especially in comparison to the vessel's resistance in calm water conditions or design resistance curves. Chapter 2 also focuses on the influence of diverse conditions on the energy efficiency of different components that is usually overlooked in many pieces of work in maritime literature. Moreover, Chapter 3 demonstrates the result of those diverse conditions on the accuracy of the developed digital twin, and Chapter 4 their influence on the solution of different design optimisation problems.

What energy performance indicators can sufficiently describe ship operations and provide feedback to both designers and operators of the vessels?

At a whole system level, mean energy effectiveness indicator and total energy efficiency over discretised vessel speed can sufficiently describe attained energy performance, as described in Chapter 2. Specifically, the extra dimension provided in carbon intensity evaluation compared to Carbon Intensity Indicator (CII) calculation allows energy performance specialists and operators of the vessels to distinguish between the effect of sailing speed and that of sailing conditions. Feedback to the vessel designers was acknowledged to be misleading, as those indicators refer to the sailing conditions encountered by the vessel; thus, they cannot provide conclusions on the comparison of operational decisions such as sailing mode selection. As a result, simulations comparing energy performance under the same conditions are needed.

Which parameters influence the attained energy performance?

Literature provides examples of indicators aiming to describe the attained energy performance of ship operations. Until recently, these indicators expressed carbon intensity or in other words the carbon cost of a certain transport work, but future trends additionally consider the carbon footprint of fuel production. For a specific vessel

that consumes a specified type of fuel, a combination of operational and environmental decisions and uncertainties influences its energy performance. Selection of speed, operational mode, loading of the vessel, and selected route are important operational decisions driving resulting carbon intensity. Hull and propeller fouling decrease energy performance by a percentage that is difficult to measure, offering less opportunities for corrective actions as well. Ultimately, environmental conditions like wind and wave conditions, currents, and ambient air and sea temperatures influence energy performance by alternating ship resistance, hence propulsion power, needed electrical power and cooling of different components.

5.1.2 *Ship energy systems modelling*

Should we use first-principle, statistical, or hybrid models with large operational datasets?

First-principle models have been the main way of modelling ship energy systems in scientific literature. However, the recent increase in the availability of operational data, computational resources, and free libraries that can be used without fundamental knowledge of statistical inference has given rise to the development of many statistical models of ship energy systems. Those models though, demonstrate poor extrapolation performance. The latest trend in modelling ship energy systems involves hybrid models, which combine benefits of the two modelling approaches, while maintaining an understanding of the physical system and the effect of design and operational decisions on different components efficiency. This dissertation demonstrates an example of such an approach through the first principle modelling of components, and the use of statistical models to compensate for the uncertainty related to real scale propeller operation in the ship's wake, and uncertainty regarding the available healthy condition operation of system components.

What is a suitable prediction model formulation in terms of input, output and utilised parameters?

Models of ship energy systems usually follow two formulation approaches. The first one uses fuel consumption of different components as an input and the output is the vessel's speed based on the resistance of the vessel, as in the case of designing system controllers. The second one uses vessel speed as an input to predict the output which is fuel consumption of main consumers. Energy management, component sizing, topology selection applications use the second. The resistance of the vessel influences the results of both formulations. Calm water resistance, sometimes following the superposition of a sea margin is a typical assumption. Sometimes, a resistance curve as a result of specific conditions for wind, waves and hull fouling is used. In the

context of this dissertation that focuses on the topology selection and sizing of a hybrid propulsion system, vessel speed and thrust joint probability distribution is selected, as it describes the aggregate effect of operational and environmental conditions at sea over a certain time period of sailing in certain geographical areas. In this way, simulation is not done over the span of some hours, months, or even a year of operations that would result in computationally expensive simulations that are also relatively independent of the exact environmental conditions. Of course, such a formulation stands under the assumption of steady-state conditions that are not dependent on previous computational steps.

What is the selected time-dependency of a model calibrated and validated over large datasets and used in optimisation iterations? Are steady-state models used in automotive sufficient in maritime applications?

According to the validation results of the digital twin approach presented in Chapter 3, the average accuracy of a first-principle steady-state model in predicting carbon intensity over voyages of a couple hours of continuous sailing is in the scale of 10-12%. Bearing in mind that this corresponds to thousands of sailing points and not only a couple of them, their prediction capability proves good. The use of statistical models though in combination with first-principal models demonstrated a prediction accuracy of the steady-state digital twin, better than 5% of mean absolute percentage error.

What needs to be the modelling fidelity level of different components?

Ship energy systems consist of many components that show non-linear behaviour. Detailed first-principle modelling of all those components would result in increased computational cost. It is common practise when modelling the whole energy system of the vessel to use semi-empirical models to model gearboxes and shaft losses. The practise of using just a constant efficiency even in part-load operation was shown in Chapter 2 to be non-accurate. Propeller modelling using open water diagrams demonstrates sufficient accuracy for energy efficiency applications, though translation of open water scale-results into real scale wake performance can be challenging, as seen in Chapter 3. Differences can be observed in modelling main and auxiliary power suppliers, for example diesel engines with the modelling complexity increasing when prediction of transient behaviour is important. The results of this dissertation demonstrate the sufficiency of regression models and fuel consumption maps in predicting both instant fuel consumption, but especially the amount of fuel consumed over continuous operating periods of more than four hours.

How can we achieve the best trade-off between prediction accuracy and computational cost?

The answer to this research question summarises the answer provided to previous research questions on modelling approaches. A sufficient trade-off is characterised by the selected modelling type, first principle, statistical or hybrid, modelling formulation, time-dependency and modelling fidelity. This dissertation concludes that a steady-state hybrid model of main system components using propeller thrust and vessel speed can accurately predict energy performance indicators under the aggregate effect of operational and environmental uncertainty at computational time feasible to handle, even by computationally expensive algorithms like the genetic ones.

5.1.3 *Design by optimisation of ship energy systems*

What is a complete and holistic optimisation framework for topology selection and sizing of different systems?

Such a framework in the context of this work needs to address representative simulation scenarios, optimisation objectives examining decisions from different angles, design variables and problem formulation describing the examined problem, and a problem resolution allowing the selection of converging and computationally efficient solvers. In Chapter 4, such a framework is proposed for the hybrid propulsion system of an ocean patrol vessel, the details of which are provided as answers to the following research questions.

What are the needed objectives?

Many techno-economic analyses involve environmental, financial and technical objectives. Results obtained in this dissertation suggest that the optimal system design can vary with the prioritisation of different objectives. The environmental aspect in this work is described using carbon intensity evaluation over actual sailing profiles, the financial using capital and operational expenditure, and the technical evaluating the total weight of the system. Other emissions such as nitrogen or sulphur oxides (NOx and SOx), contribute mainly to air contamination, require much more detailed models and fall out of the scope of this work. On the financial part, capital and operational expenditure are used instead of life cycle cost, as the sensitivity of the result on fuel and acquisition prices can implement bias. Finally, technical objectives can also include minimisation of captured volume or arrangement of the system, though this is not the case in naval vessels where weight is prioritised, and this interferes with a different branch of research topics.

What are the sufficient simulation scenarios to capture actual operational and environmental conditions at sea?

The specific operational and environmental conditions encountered by a vessel influence drastically optimal design decisions. The clearest

indication of the importance of using actual profiles in the optimisation of ship energy systems' operation is the result of the different optimal solutions obtained for the different profiles of the three vessels.

What are the constraints?

In this work, constraints were organised into bound constraints for the decision variables, technical, redundancy, and efficiency constraints. Bounds were selected, based on the experience of similar systems. Technical constraints include the installation of sufficient electricity supply of the system, avoid the installation of unnecessary electrical supply. Redundancy calls for the hotel load being served by only one diesel engine.

What is the mathematical optimisation problem type and solving method?

Ship energy system architecture, sizing and energy management optimisation problems usually involve a mix of integer and real value decision variables. The nature of most used objective functions is non-linear, so are most of the constraints of the problem. Apart from being non-linear, those objectives are also non-convex, thus multi-starts methodologies need to be applied in order to find globally optimal solutions.

How can a computational efficient digital twin approach be used to extend design space exploration?

An extended design space exploration over rich simulation scenarios and with methods calculating objective function values some thousands of times would be almost impossible to handle in reasonable times, even with the increased computational capabilities of super-computers like Delftblue supercomputer. The steady-state hybrid modelling approach introduced in Chapter 3 coupled with simulation over actual sailing profiles through the use of the actual vessel speed and thrust distributions, allows the simulation of a candidate design of the system over more than a year of operations in the scale of multiple seconds. This improvement of computational speed allows the assessment of thousands of designs over hundreds of sailing points corresponding to conditions representative of the conditions at sea.

5.2 LIMITATIONS

This dissertation involves assumptions that were either unavoidable due to the availability of data or information, or important in making the problem solvable with respect to the available computational and time resources.

5.2.1 *Dataset restrictions*

The available dataset does not include logged parameters of propeller thrust, main diesel engine torque and propeller torque. These parameters were modelled using logged parameters for the components working points and available manufacturers' data. These models assume the components maintain performance under healthy condition. Therefore, the resulting extended dataset cannot be used to evaluate component energy efficiency degradation, but only energy efficiency under healthy and clean conditions.

5.2.2 *Modelling*

This piece of work focused on the prediction accuracy of carbon intensity over voyage intervals of at least five hours of continues sailing. An overall accuracy of 5% mean absolute percentage error justifies the capabilities of such a modelling approach. This doesn't mean that the point-wise accuracy of the developed model is the same. At the core of steady state modelling, we accept that the model might be inaccurate on transient or highly dynamic sailing points.

5.2.3 *Data quality*

The developed methodologies accept logged data as ground truth. It is not the scope of this work to consider the accuracy of sensor readings or the performance data provided by the component manufacturers and shipbuilder.

5.3 RECOMMENDATIONS

In addressing the research objectives, some topics have not been fully explored, and several new questions have arisen. Of note are the following recommendations for future research:

- A genetic algorithm is a computationally expensive evolutionary solving algorithm that in return provides quality results in mixed-integer non-linear optimisation programming problems. One research direction could exploit alternative problem formulations that allow the use of more computationally efficient gradient or search optimisation algorithms.

- Alternative optimisation problem formulations selecting from a number of actual diesel generators, thus solve a multi-objective combinatorial optimisation problem (MOCO).

- Installation of a thrust sensor would allow the examination of hull fouling and propeller performance degradation.

- Installation of a main engine torque sensor would allow the examination of main engine energy efficiency degradation.

- The recommended modelling approach could be used in optimisation problems also considering hybrid power supply, with the use of batteries and fuel cells, or with the design of different operational modes.

A

THE CASE STUDY VESSELS

Figure A.1: A dry-docked *Holland class* vessel.

The examined vessels in this dissertation are three *Holland class* Ocean Patrol Vessels (OPVs) of the Royal Netherlands Navy (RNLN), as the one seen in Figure A.1 [1]. This class of vessels is equipped with a hybrid propulsion system architecture. A schematic representation of their energy system can be found in Figure A.2. Two controllable pitch propellers are driven either mechanically by two main diesel engines or electrically by two electrical motors. Propeller shaft speed is reduced by two gearboxes which utilise one speed reduction stage in the case of mechanical propulsion or two stages in the case of electrical propulsion. Electrical power is provided by three diesel generators. All component specifications can be found in Table A.1. In order to

---

1 https://www.damennaval.com/
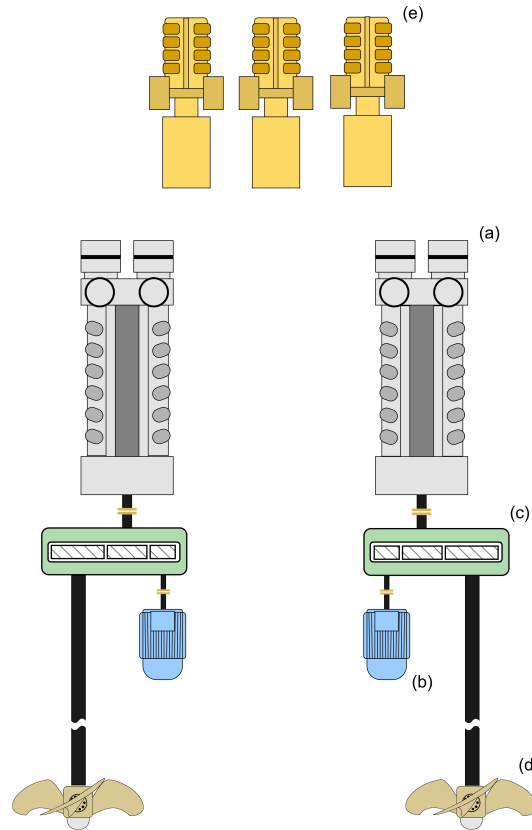
Figure A.2: The initial considered topology: (a) main diesel engine, (b) electrical motor, (c) gearbox, (d) controllable-pitch propeller, (e) diesel generator.

serve their multi-function mission, the examined OPVs use a number of operational modes. Table A.2 provides a description of the available operational modes.

The work conducted under this dissertation is based on operational data logged by the vessels' Integrated Platform Monitoring System (IPMS). A list of those parameters can be found in Table A.3. These parameters are all measured by the automation system, except for the thrust parameter, which is estimated based on the dataset enrichment methodology described in Chapter 2. Cleaning and pre-processing was done as in [115], but vessel speed was selected as the prime parameter and the top and bottom 0.1% percentile was used to discard outliers instead of standard deviation. The datasets are characterised by a sampling frequency of 3 seconds and cover a time window as seen in Table A.4.

Component manufacturers and the shipbuilder of the case study vessels provide information that is essential in building and validating the models introduced in this dissertation. This information includes resistance and propulsion tests of scale models in towing tank experiments, results of computer fluid dynamics (CFD) simulations,

Table A.1: Component specifications.

Diesel generators	Value	Unit
Nominal power	910	[ekW]
Nominal speed	1 800	[rpm]
Nominal fuel consumption (ISO)	235	[kg/h]
Main diesel engines		
Nominal power	5 400	[kW]
Nominal speed	1 000	[rpm]
Nominal fuel consumption (ISO)	1 077	[kg/h]
Electrical motors		
Nominal power	400	[kW]
Nominal speed	1 788	[rpm]
Gearboxes		
Reduction ratio (MDE)	4.355	[-]
Reduction ratio (M)	17.880	[-]
CPP Propellers		
Diameter	3.2	[m]
Nominal pitch to diameter	1.221	[-]
Zero-thrust pitch to diameter	0.144	[-]

Table A.2: Operational modes.

2 main diesel engines	transit
	manoeuvring
1 main diesel engine	trailing at full pitch
	shaft brake at 0-pitch
	blocked shaft at full pitch
2 electrical motors	

open water diagrams for the controllable-pitch propellers installed. Figure A.3 provides an estimation of Taylor's wake fraction w over vessels speed, and Figure A.4 provides the corresponding thrust deduction factor t. Moreover, Figure A.5 provides resistance curves in calm water and design conditions. Finally, Figures A.7 and A.8 provide the thrust and torque coefficients of the open water diagrams.

Table A.3: Logged IPMS parameters used.

Parameter	Unit
Main diesel engine speed	[rpm]
Main diesel engine fuel consumption	[kg/h]
Diesel generators speed	[rpm]
Diesel generators power	[kW]
Diesel generators fuel consumption	[kg/h]
Electrical motor speed	[rpm]
Electrical motor power	[kW]
Propeller shaft speed	[rpm]
Propeller shaft torque	[kNm]
Propeller pitch to dimaterer	[-]
Vessel speed through water	[knots]
Propulsion mode	-
Sailing mode	-
Ambient air temperature	[°C]
Relative wind speed	[knots]
Time	[sec]

Table A.4: Timespan and sailing days for the three examined vessels.

	Vessel 1	Vessel 2	Vessel 3
Timespan	440	573	958
Sailing time	87	103	131
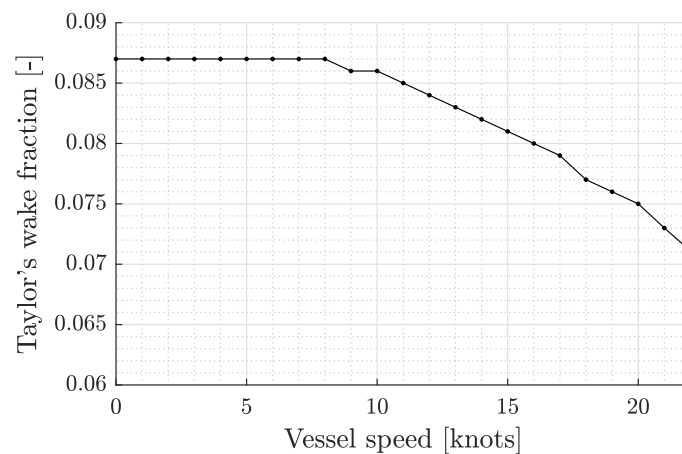
Figure A.3: Taylor's wake fraction based on towing tank tests.
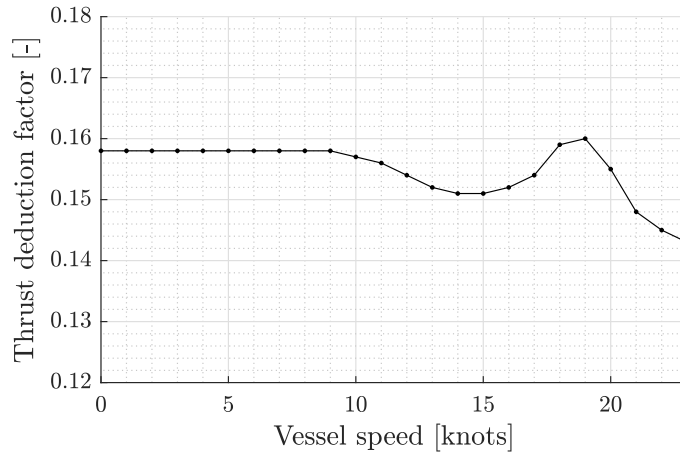
Figure A.4: Thrust deduction factor.
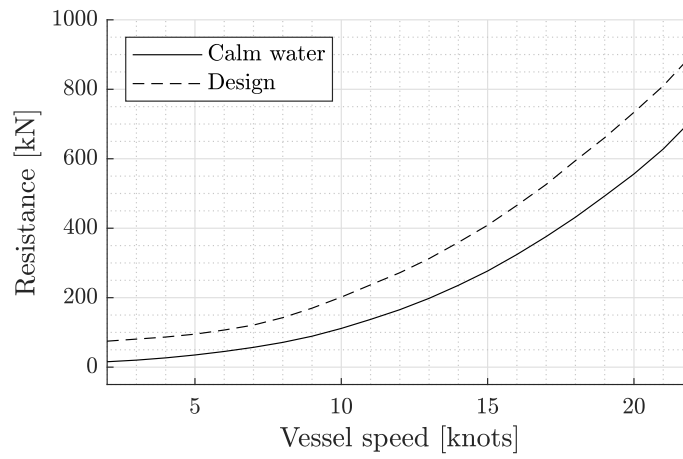
Figure A.5: Resistance curves from towing tank tests.
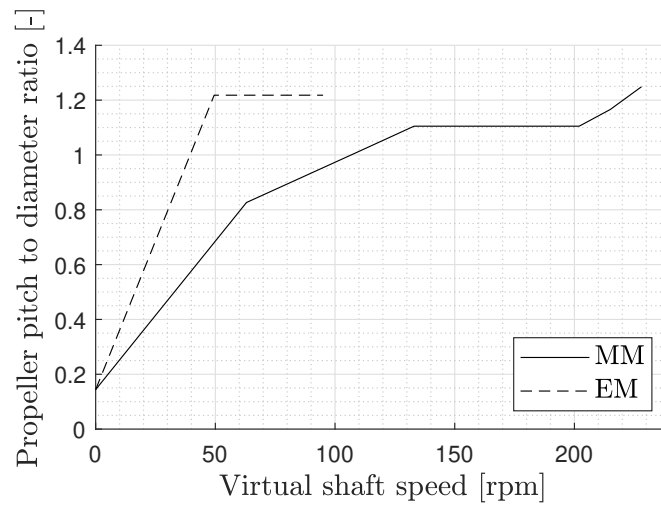
Figure A.6: Combinator curves: (MM) mechanical mode, (EM) electrical mode.
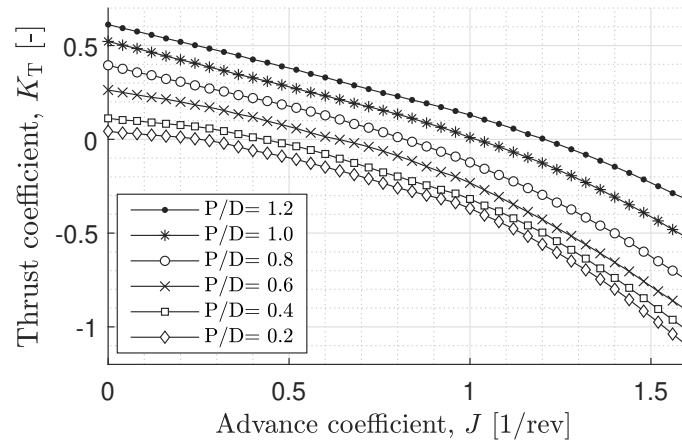
Figure A.7: Thrust coefficient open water diagram.
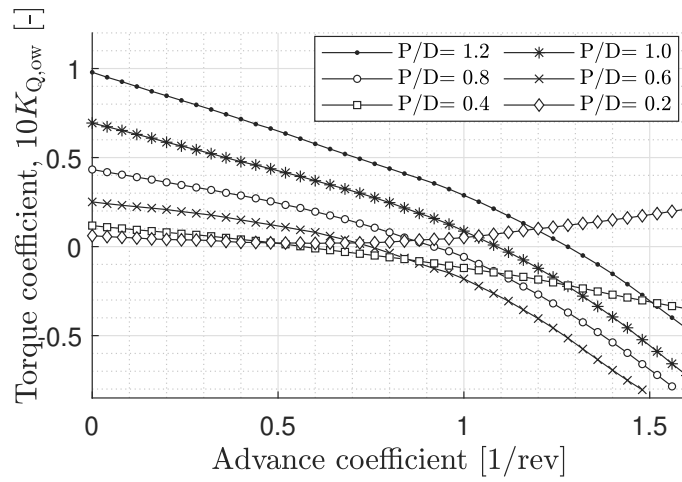
Figure A.8: Torque coefficient open water diagram.

BIBLIOGRAPHY

[1] IPCC, 'Climate change 2023: Synthesis report. contribution of working groups i, ii and iii to the sixth assessment reportof the intergovernmental panel on climate change', Intergovernmental Panel on Climate Change, Tech. Rep., 2023.

[2] M. Kalikatzarakis, R. Geertsma, E. Boonen, K. Visser and R. Negenborn, 'Ship energy management for hybrid propulsion and power supply with shore charging', *Control Engineering Practice*, vol. 76, pp. 133–154, 2018. DOI: 10.1016/j.conengprac.2018.04.009.

[3] J. Holtrop and G. G. J. Mennen, 'An approximate power prediction method', *International Shipbuilding Progress*, vol. 29, pp. 166–171, 1982.

[4] I. V. Pieter Tans Xin Lan and E. Dlugokencky, 'The power of greenhouse gases', National Oceanic and Atmosperic Administrtion, Global Monitoring Laboratory, Earth System Research Laboratories, Tech. Rep., 2023.

[5] G. M. L. E. S. R. Laboratories, 'The NOAA annual greenhouse gas index (AGGI)', National Oceanic and Atmosperic Administrtion, Tech. Rep., 2023.

[6] IPCC, 'Climate change 2014', Intergovernmental Panel for Climate Change, Tech. Rep., 2014.

[7] IPCC, *Summary for Policymakers. In: Climate Change 2021: The Physical Science Basis. Contribution of Working Group I to the Sixth Assessment Report of the Intergovernmental Panel on Climate Change.* Cambridge University Press, 2021.

[8] A. Bows-Larkin, 'All adrift: Aviation, shipping, and climate change policy', *Climate Policy*, vol. 15, no. 6, pp. 681–702, 2015. DOI: 10.1080/14693062.2014.965125.

[9] UNCTAD, *Review of maritime transport*. United Nations Conference on Trade and Development, 2022.

[10] IMO, 'Third IMO GHG study 2014', International Maritime Organization, Tech. Rep., 2014.

[11] MEPC, 'Resolution MEPC.203(62) ANNEX 19 Amendments to the annex of the protocol of 1997 to amend the international convention for the prevention of pollution from ships, 1973, as modified by the protocol of 1978 relating thereto (Inclusion of regulations on energy efficiency for ships in MARPOL Annex VI)', International Maritime Organization, Tech. Rep., 2011.

[12] IMO, 'Fourth IMO GHG study 2020', International Maritime Organization, Tech. Rep., 2020.

[13] MEPC, 'Resolution MEPC.304(72) ANNEX 11 Initial IMO strategy on reduction of GHG emissions from ships', International Maritime Organization, Tech. Rep., 2018.

[14] MEPC, 'Resolution MEPC.377(80) ANNEX 15 2023 IMO Strategy on reduction of GHG emissions from ships', International Maritime Organization, Tech. Rep., 2023.

[15] IMO, 'Study of Greenhouse Gas Emissions from Ships', International Maritime Organization, Tech. Rep., 2000.

[16] IMO, 'Second IMO GHG Study 2009', International Maritime Organization, Tech. Rep., 2009.

[17] MEPC, 'Resolution MEPC.245(66) ANNEX 5 Guidelines on the method of calculation of the attained energy efficiency design index (EEDI) for new ships', International Maritime Organization, Tech. Rep., 2014.

[18] MEPC, 'Resolution MEPC.333(76) ANNEX 7 2021 Guidelines on the method of calculation of the attained energy efficiency existing ship index (EEXI)', International Maritime Organization, Tech. Rep., 2021.

[19] MEPC, 'Resolution MEPC.336(76) ANNEX 10 2021 Guidelines on operational carbon intensity indicators and the calculation methods (CII guidelines, G1)', International Maritime Organization, Tech. Rep., 2021.

[20] J. Barreiro, S. Zaragoza and V. Diaz-Casas, 'Review of ship energy efficiency', *Ocean Engineering*, vol. 257, p. 111 594, 2022. DOI: 10.1016/j.oceaneng.2022.111594.

[21] N. I. Vasilikis, R. D. Geertsma and K. Visser, 'Operational data-driven energy performance assessment of ships: The case study of a naval vessel with hybrid propulsion', *Journal of Marine Engineering and Technology*, 2022. DOI: 10.1080/20464177.2022.2058690.

[22] H. N. Psaraftis and C. A. Kontovas, 'Speed models for energy-efficient maritime transportation: A taxonomy and survey', *Transportation Research Part C: Emerging Technologies*, vol. 26, pp. 331–351, 2013. DOI: 10.1016/j.trc.2012.09.012.

[23] C. Sui, P. de Vos, H. Hopman, K. Visser, D. Stapersma and Y. Ding, 'Effects of adverse sea conditions on propulsion and manoeuvring performance of low-powered ocean-going cargo ship', *Ocean Engineering*, vol. 254, p. 111 348, 2022. DOI: 10. 1016/j.oceaneng.2022.111348.

[24] E. Lindstad, H. Borgen, G. S. Eskeland, C. Paalson, H. Psaraftis and O. Turan, 'The need to amend IMO's EEDI to include a threshold for performance in waves (realistic sea conditions) to achieve the desired GHG reductions', *Sustainability*, vol. 11, no. 13, p. 3668, 2019. DOI: 10.3390/su11133668.

[25] J. Cichowicz, G. Theotokatos and D. Vassalos, 'Dynamic energy modelling for ship life-cycle performance assessment', *Ocean Engineering*, vol. 110, pp. 49–61, 2015. DOI: 10.1016/j.oceaneng.2015.05.041.

[26] N. L. Trivyza, A. Rentizelas and G. Theotokatos, 'A comparative analysis of EEDI versus lifetime CO_2 emissions', *Journal of Marine Science and Engineering*, vol. 8, no. 1, p. 61, 2020. DOI: 10.3390/jmse8010061.

[27] GRPE, 'ECE/TRANS/WP.29/2020/77 Proposal for a new UN Regulation on uniform provisions concerning the approval of light duty passenger and commercial vehicles with regards to criteria emissions, emissions of carbon dioxide and fuel consumption and/or the measurement of electric energy consumption and electric range (WLTC)', United Nations Economic Commision for Europe, Tech. Rep., 2020.

[28] Q. Cui and B. Chen, 'Aviation carbon transfer and compensation of international routes in africa from 2019 to 2021', *Scientific Data*, vol. 10, no. 1, p. 306, 2023. DOI: 10.1038/s41597-023-02219-7.

[29] MEPC, 'Guidelines for voluntary use of the ship energy efficiency operational indicators (EEOI)', International Maritime Organization, Tech. Rep., 2009.

[30] MEPC, 'MEPC(76) Consideration and adoption of amendments to mandatory instruments. Draft amendments to MARPOL Annex VI.', International Maritime Organization, Tech. Rep., 2021.

[31] EU, 'Regulation (EU) 2015/757 of the European Parliament and the Council of 29 April 2015', *Official Journal of the European Union*, 2015.

[32] EU, 'Regulation (EU) 2023/957 of the European Parliament and of the Council of 10 May 2023 amending Regulation (EU) 2015/757', *Official Journal of the European Union*, 2023.

[33]   EU, 'Proposal for a regulation of the European Parliament and of the Council on the use of renewable and low-carbon fuels in maritime transport and amending Directive 2009/16/EC', Tech. Rep., 2021.

[34]   EU, 'Annexes to the Proposal for a regulation of the European Parliament and of the Council on the use of renewable and low-carbon fuels in maritime transport and amending Directive 2009/16/EC', Tech. Rep., 2021.

[35]   H. N. Psaraftis, 'Market-based measures for greenhouse gas emissions from ships: A review', *WMU Journal of Maritime Affairs*, vol. 11, pp. 211–232, 2012. DOI: 10.1007/s13437-012-0030-5.

[36]   J. Vergara, C. McKesson and M. Walczak, 'Sustainable energy for the marine sector', *Energy Policy*, vol. 49, pp. 333–345, 2012. DOI: 10.1016/j.enpol.2012.06.026.

[37]   E. A. Bouman, E. Lindstad, A. I. Rialland and A. H. Strømman, 'State-of-the-art technologies, measures, and potential for reducing GHG emissions from shipping – A review', *Transportation Research Part D: Transport and Environment*, vol. 52, pp. 408–421, 2017. DOI: 10.1016/j.trd.2017.03.022.

[38]   L. van Biert, M. Godjevac, K. Visser and P. V. Aravind, 'A review of fuel cell systems for maritime applications', *Journal of Power Sources*, vol. 327, pp. 345–364, 2016. DOI: 10.1016/j.jpowsour.2016.07.007.

[39]   S. Horvath, M. Fasihi and C. Breyer, 'Techno-economic analysis of a decarbonized shipping sector: Technology suggestions for a fleet in 2030 and 2040', *Energy Conversion and Management*, vol. 164, pp. 230–241, 2018. DOI: 10.1016/j.enconman.2018.02.098.

[40]   R. D. Geertsma, R. R. Negenborn, K. Visser and J. J. Hopman, 'Design and control of hybrid power and propulsion systems for smart ships: A review of developments', *Applied Energy*, vol. 194, pp. 30–54, 2017. DOI: 10.1016/j.apenergy.2017.02.060.

[41]   A. Papanikolaou, 'Holistic ship design optimization', *Computer-Aided Design*, vol. 42, no. 11, pp. 1028–1044, 2010. DOI: 10.1016/j.cad.2009.07.002.

[42]   F. Baldi, 'Modelling, analysis and optimisation of ship energy systems', Ph.D. dissertation, Department of Shipping and Marine Technology, Chalmers University of Technology, Gothenburg, Sweden, 2016.

[43]   C. A. Frangopoulos, 'Recent developments and trends in optimization of energy systems', *Energy*, vol. 164, pp. 1011–1020, 2018. DOI: 10.1016/j.energy.2018.08.218.

[44] J. Moreno-Guti'errez, F. Calderay, N. Saborido, M. Boile, R. R. Valero and V. Dur'an-Grados, 'Methodologies for estimating shipping emissions and energy consumption a comparative analysis of current methods', *Energy*, vol. 86, pp. 603–616, 2015.

[45] N Bulten, 'With numerical simulations to more efficient ship designs', *Proceedings RINA Energy Efficient Ships conference, London, UK*, 2016.

[46] R. D. Geertsma, K. Visser and R. R. Negeborn, 'Adaptive pitch control for ships with diesel mechanical and hybrid propulsion', *Applied Energy*, vol. 228, pp. 2490–2509, 2018. DOI: `10.1016/j.apenergy.2018.07.080`.

[47] C. Sui, D. Stapersma, K. Visser, P. de Vos and Y. Ding, 'Energy effectiveness of ocean-going cargo ship under various operating conditions', *Ocean Engineering*, vol. 190, 2019. DOI: `10.1016/j.oceaneng.2019.106473`.

[48] C. Sui, P. de Vos, D. Stapersma, K. Visser and Y. Ding, 'Fuel consumption and emissions of ocean-going cargo ship with hybrid propulsion and different fuels over voyage', *Journal of Marine Science and Engineering*, vol. 8, no. 588, p. 588, 2020. DOI: `10.3390/jmse8080588`.

[49] R. D. Geertsma, R. R. Negeborn, K. Visser, M. A. Loonstijn and J. J. Hopman, 'Pitch control for ships with diesel mechanical and hybrid propulsion: Modelling, validation and performance quantification', *Applied Energy*, vol. 206, pp. 1609–1631, 2017. DOI: `10.1016/j.apenergy.2017.09.103`.

[50] D. Hountalas, 'Prediction of marine diesel engine performance under fault conditions', *Applied Thermal Engineering*, vol. 20, pp. 1753–1783, 2000.

[51] M. Kalikatzarakis, A. Coraddu, G. Theotokatos and L. Oneto, 'Development of a zero-dimensional model and application on a medium-speed marine four-stroke diesel engine', *Proceedings of MOSES2021 Conference*, 2021.

[52] A. Coraddu, M. Kalikatzarakis, G. Theotokatos, R. Geertsma and L. Oneto, 'Engine modeling and simulation. energy, environment, and sustainability.', A. K. Agarwal, D. Kumar, N. Sharma and U. Sonawane, Eds. Springer, Singapore, 2021, ch. Physical And Data-driven Models Hybridisation For Modelling The Dynamic State Of A Four-stroke Marine Diesel Engine, pp. 145–193. DOI: `10.1007/978-981-16-8618-4_6`.

[53] A. I. Parkes, A. J. Sobey and D. A. Hudson, 'Physics-based shaft power prediction for large merchant ships using neural networks', *Ocean Engineering*, vol. 166, pp. 92–104, 2018. DOI: `10.1016/j.oceaneng.2018.07.060`.

[54] I. Georgescu, M. Godjevac and K. Visser, 'Efficiency constraints of energy storage for on-board power systems', *Ocean Engineering*, vol. 162, pp. 239–247, 2018. DOI: 10.1016/j.oceaneng.2018.05.004.

[55] A. Vrijdag, 'Estimation of uncertainty in ship performance predictions', *Journal of Marine Engineering and Technology*, vol. 13, no. 3, pp. 45–55, 2014.

[56] F. Tillig, J. W. Ringsberg, W. Mao and B. Ramne, 'Analysis of uncertainties in the prediction of ships' fuel consumption – from early design to operation conditions', *Ships and Offshore Structures*, vol. 13, no. sup1, pp. 13–24, 2018. DOI: 10.1080/17445302.2018.1425519.

[57] A. Vrijdag, E.-J. Boonen and M. Lehne, 'Effect of uncertainty on techno-economic trade-off studies: Ship power and propulsion concepts', *Journal of Marine Engineering & Technology*, vol. 18, no. 3, pp. 122–133, 2018. DOI: 10.1080/20464177.2018.1507430.

[58] F. Baldi, U. Larsen and C. Gabrielii, 'Comparison of different procedures for the optimisation of a combined Diesel engine and organic Rankine cycle system based on ship operational profile', *Ocean Engineering*, vol. 110, pp. 85–93, 2015. DOI: 10.1016/j.oceaneng.2015.09.037.

[59] E. Esmailian, S. Steen and K. Koushan, 'Ship design for real sea states under uncertainty', *Ocean Engineering*, vol. 266, p. 113 127, 2022. DOI: https://doi.org/10.1016/j.oceaneng.2022.113127.

[60] L. Aldous, T. Smith, R. Bucknall and P. Thompson, 'Uncertainty analysis in ship performance monitoring', *Ocean Engineering*, vol. 110, pp. 29–38, 2015. DOI: 10.1016/j.oceaneng.2015.05.043.

[61] D. Trodden, A. Murphy, K. Pazouki and J. Sargeant, 'Fuel usage data analysis for efficient shipping operations', *Ocean Engineering*, vol. 110, pp. 75–84, 2015, Energy Efficient Ship Design and Operations. DOI: https://doi.org/10.1016/j.oceaneng.2015.09.028.

[62] L. Nikolopoulos and E. Boulougouris, 'A novel method for the holistic, simulation driven ship design optimization under uncertainty in the big data era', *Ocean Engineering*, vol. 218, p. 107 634, 2020. DOI: https://doi.org/10.1016/j.oceaneng.2020.107634.

[63] M. Diez, E. F. Campana and F. Stern, 'Stochastic optimization methods for ship resistance and operational efficiency via cfd', *Structural and Multidisciplinary Optimization*, vol. 57, no. 2, pp. 735–758, 2018. DOI: 10.1007/s00158-017-1775-4.

[64] I. Gypa, M. Jansson, R. Gustafsson, S. Werner and R. Bensow, 'Controllable-pitch propeller design process for a wind-powered car-carrier optimising for total energy consumption', *Ocean Engineering*, vol. 269, p. 113 426, 2023.

[65] N. L. Trivyza, A. Rentizelas and G. Theotokatos, 'A novel multi-objective decision support method for ship energy systems synthesis to enhance sustainability', *Energy Conversion and Management*, vol. 168, pp. 128–149, 2018. DOI: 10.1016/j.enconman.2018.04.020.

[66] J. Zhu, L. Chen, B. Wang and L. Xia, 'Optimal design of a hybrid electric propulsive system for an anchor handling tug supply vessel', *Applied Energy*, vol. 226, pp. 423–436, 2018. DOI: 10.1016/j.apenergy.2018.05.131.

[67] J. Zhu, L. Chen, L. Xia and B. Wang, 'Bi-objective optimal design of plug-in hybrid electric propulsion system for ships', *Energy*, vol. 177, pp. 247–261, 2019. DOI: 10.1016/j.energy.2019.04.079.

[68] D. Stapersma and H. Klein Woud, 'Matching propulsion engine with propulsor', *Journal of Marine Engineering & Technology*, vol. 4, no. 2, pp. 25–32, 2005. DOI: 10.1080/20464177.2005.11020189.

[69] A. Coraddu, L. Oneto, F. Baldi and D. Anguita, 'Vessels fuel consumption forecast and trim optimisation: A data analytics perspective', *Ocean Engineering*, vol. 130, pp. 351–370, 2017. DOI: 10.1016/j.oceaneng.2016.11.058.

[70] A. Coraddu, S. Lim, L. Oneto, K. Pazouki, R. Norman and A. J. Murphy, 'A novelty detection approach to diagnosing hull and propeller fouling', *Ocean Engineering*, vol. 176, pp. 65–73, 2019. DOI: 10.1016/j.oceaneng.2019.01.054.

[71] A. Coraddu, L. Oneto, F. Baldi, F. Cipollini, M. Atlar and S. Savio, 'Data-driven ship digital twin for estimating the speed loss caused by the marine fouling', *Ocean Engineering*, vol. 186, p. 106 063, 2019. DOI: 10.1016/j.oceaneng.2019.05.045.

[72] P. Mizythras, E. Boulougouris and G. Theotokatos, 'Numerical study of propulsion system performance during ship acceleration', *Ocean Engineering*, vol. 149, pp. 383–396, 2018. DOI: 10.1016/j.oceaneng.2017.12.010.

[73] A. Haseltalab and R. R. Negenborn, 'Model predictive maneuvering control and energy management for all electric autonomous ships', *Applied Energy*, vol. 251, 2019. DOI: 10.1016/j.apenergy.2019.113308.

[74]   A. Haseltalab and R. R. Negenborn, 'Adaptive control for autonomous ships with uncertain model and unknown propeller dynamics', *Control Engineering Practice*, vol. 91, p. 104 116, 2019. DOI: `10.1016/j.conengprac.2019.104116`.

[75]   S. V. A. A. Harvald, *Resistance and propulsion of ships*. Wiley-Interscience Publication, John Wiley & Sons, 1983.

[76]   A. F. Molland, S. R. Turnock and D. A. Hudson, *Ship resistance and propulsion: practical estimation of ship propulsive power*. Cambridge University Press, 2011.

[77]   ITTC, 'Recommended Procedures and Guidelines - Testing and Extrapolation Methods, Propulsion, Performance, Predicting Powering Margins 7.5-02-03-01.5', International Towing Tank Conference, Tech. Rep., 2008.

[78]   W. Shi, H. Grimmelius and D. Stapersma, 'Analysis of ship propulsion system behaviour and the impact on fuel consumption', *International Shipbuilding Progress*, vol. 57, no. 1-2, pp. 35–64, 2010. DOI: `10.3233/ISP-2010-0062`.

[79]   F. Baldi, H. Johnson, C. Gabrielii and K. Andersson, 'Energy and exergy analysis of ship energy systems - The case study of a chemical tanker', *International Journal of Thermodynamics*, vol. 18, no. 2, pp. 82–93, 2015. DOI: `10.5541/ijot.70299`.

[80]   G. Shu, P. Liu, H. Tian, X. Wang and D. Jing, 'Operational profile based thermal-economic analysis on an organic rankine cycle using for harvesting marine engine's exhaust waste heat', *Energy Conversion and Management*, vol. 146, pp. 107–123, 2017. DOI: `10.1016/j.enconman.2017.04.099`.

[81]   A. Yrjänäinen, T. Johnsen, J. S. Dæhlen, H. Kramer and R. Monden, 'A holistic approach to ship design', A. Papanikolaou, Ed. Springer, 2019, ch. 4: Market conditions, mission requirements and operational profiles, pp. 75–122.

[82]   S. Jafarzadeh and I. Schjølberg, 'Operational profiles of ships in Norwegian waters: An activity-based approach to assess the benefits of hybrid and electric propulsion', *Transportation Research Part D: Transport and Environment*, vol. 65, pp. 500–523, 2018. DOI: `10.1016/j.trd.2018.09.021`.

[83]   D. Vassalos, J. Cichowicz and G. Theotokatos, 'Performance-based ship energy efficiency - The way forward', *Influence of EEDI on Ship Design*, T. Royal Institution of Naval Architects, Ed., London, UK, 2014.

[84]   X. Sun, X. Yan, B. Wu and X. Song, 'Analysis of the operational energy efficiency for inland river ships', *Transportation Research Part D: Transport and Environment*, vol. 22, pp. 34–39, 2013. DOI: `10.1016/j.trd.2013.03.002`.

[85] M. Godjevac, J. Drijver, L. de Vries and D. Stapersma, 'Evaluation of losses in maritime gearboxes', *Proc IMechE, Part M: J Eng Marit Environ*, 1 – 16, 2015, Cited by: 3.

[86] H. Klein Woud and D. Stapersma, *Design of Propulsion and Electric Power Generation Systems*. IMarEST, The Institute of Marine Engineering, Science and Technology, 2002.

[87] C. F. Kutscher, 'Heat Exchange Effectiveness and Pressure Drop for Air Flow Through Perforated Plates With and Without Crosswind', *Journal of Heat Transfer*, vol. 116, pp. 391–399, 1994.

[88] G. P. Narayan, K. H. Mistry, M. H. Sharqawy, S. M. Zubair and V. John H. Lienhard, 'Energy effectiveness of simultaneous heat and mass exchange devices', *Frontiers in Heat and Mass Transfer*, vol. 1, 2010. DOI: 10.5098/hmt.v1.2.3001.

[89] T. J. Kotas, *The Exergy Method of Thermal Plant Analysis*. Butterworths, 1985.

[90] O. F. A. van Straten and M. J. de Boer, 'Optimum propulsion engine configuration from fuel economic point of view', *Proceedings of the 11th International Naval Engineering Conference and Exhibition (INEC)*, 2012. DOI: 10.24868/issn.2515-818X.2020.066.

[91] E. Sofras and J. Prousalidis, 'Developing a new methodology for evaluating diesel-electric propulsion', *Journal of Marine Engineering & Technology*, vol. 13, no. 3, pp. 63–92, 2014. DOI: 10.1080/20464177.2014.11658123.

[92] N. Vasilikis, R. Geertsma and A. Coraddu, 'A digital twin approach for maritime carbon intensity evaluation accounting for operational and environmental uncertainty', *Ocean Engineering*, vol. 288, p. 115 927, 2023. DOI: 10.1016/j.oceaneng.2023.115927.

[93] R Damerius, A. Schubert, C Rethfeldt, G Finger, S Fischer, G Milbradt, M Kurowski, M Gluch and T Jeinsch, 'Consumption-reduced manual and automatic manoeuvring with conventional vessels', *Journal of Marine Engineering & Technology*, pp. 1–12, 2022.

[94] M. Tadros, M. Ventura and C. G. Soares, 'Optimization procedures for a twin controllable pitch propeller of a ROPAX ship at minimum fuel consumption', *Journal of Marine Engineering & Technology*, vol. 22, no. 4, pp. 167–175, 2022. DOI: 10.1080/20464177.2022.2106623.

[95] K. Avgouleas and P. D. Sclavounos, 'Fuel-Efficient Ship Routing', *NAUSIVIOS CHORA Part C: Natural Sciences and Mathematics*, vol. 5, pp. 39–72, 2014.

[96]   C. Zhang, D. Zhang, M. Zhang and W. Mao, 'Data-driven ship energy efficiency analysis and optimization model for route planning in ice-covered Arctic waters', *Ocean Engineering*, vol. 186, p. 106 071, 2019. DOI: `10.1016/j.oceaneng.2019.05.053`.

[97]   T. P. V. Zis, H. N. Psaraftis and L. Ding, 'Ship weather routing: A taxonomy and survey', *Ocean Engineering*, vol. 213, p. 107 697, 2020. DOI: `10.1016/j.oceaneng.2020.107697`.

[98]   Y. B. A. Farag and A. I. Ölçer, 'The development of a ship performance model in varying operating conditions based on ANN and regression techniques', *Ocean Engineering*, vol. 198, p. 106 972, 2020. DOI: `10.1016/j.oceaneng.2020.106972`.

[99]   A. Coraddu, M. Figari and S. Savio, 'Numerical investigation on ship energy efficiency by Monte Carlo simulation', *Proceedings of the Institution of Mechanical Engineers, Part M: Journal of Engineering for the Maritime Environment*, vol. 228, no. 3, pp. 220–234, 2014. DOI: `10.1177/1475090214524184`.

[100] A. Fan, X. Yan, R. Bucknall, Q. Yin, S. Ji, Y. Liu, R. Song and X. Chen, 'A novel ship energy efficiency model considering random environmental parameters', *Journal of Marine Engineering & Technology*, vol. 19, no. 4, pp. 215–228, 2020. DOI: `10.1080/20464177.2018.1546644`. eprint: `https://doi.org/10.1080/20464177.2018.1546644`.

[101] G. N. Sakalis and C. A. Frangopoulos, 'Intertemporal optimization of synthesis, design and operation of integrated energy systems of ships: General method and application on a system with diesel main engines', *Applied Energy*, vol. 226, pp. 991–1008, 2018. DOI: `10.1016/j.apenergy.2018.06.061`.

[102] E. K. Dedes, D. A. Hudson and S. R. Turnock, 'Assessing the potential of hybrid energy technology to reduce exhaust emissions from global shipping', *Energy Policy*, vol. 40, pp. 204–218, 2012. DOI: `10.1016/j.enpol.2011.09.046`.

[103] E. K. Dedes, D. A. Hudson and S. R. Turnock, 'Investigation of diesel hybrid systems for fuel oil reduction in slow speed ocean going ships', *Energy*, vol. 114, pp. 444–456, 2016. DOI: `10.1016/j.energy.2016.07.121`.

[104] M. A. Ancona, F. Baldi, M. Bianchi, L. Branchini, F. Melino, A. Peretto and J. Rosati, 'Efficiency improvement on a cruise ship: Load allocation optimization', *Energy Conversion and Management*, vol. 164, pp. 42–58, 2018. DOI: `10.1016/j.enconman.2018.02.080`.

[105] S. Barsali, C. Miulli and A. Possenti, 'A control strategy to minimize fuel consumption of series hybrid electric vehicles', *IEEE Transactions on energy conversion*, vol. 19, 2004, pp. 187–195.

[106] B. Zuurendok, 'Advanced fuel consumption and emission modeling using Willans line scaling techniques for engines', Technische Universiteit Eindhoven, Department Mechanical Engineering, Dynamics and Control Technology Group, Tech. Rep., 2005.

[107] M. Zhou, H. Jin and W. Wang, 'A review of vehicle fuel consumption models to evaluate eco-driving and eco-routing', *Transportation Research Part D: Transport and Environment*, vol. 49, pp. 203–218, 2016. DOI: 10.1016/j.trd.2016.09.008.

[108] B. Zahedi, L. E. Norum and K. B. Ludvigsen, 'Optimized efficiency of all-electric ships by dc hybrid power systems', *Journal of Power Sources*, vol. 255, pp. 341–354, 2014. DOI: 10.1016/j.jpowsour.2014.01.031.

[109] A. Haseltalab, M. A. Botto and R. R. Negenborn, 'Model predictive DC voltage control for all-electric ships', *Control Engineering Practice*, vol. 90, pp. 133–147, 2019. DOI: 10.1016/j.conengprac.2019.06.018.

[110] M. D. Al-Falahi, K. S. Nimma, S. D. Jayasinghe, H. Enshaei and J. M. Guerrero, 'Power management optimization of hybrid power systems in electric ferries', *Energy Conversion and Management*, vol. 172, pp. 50–66, 2018. DOI: 10.1016/j.enconman.2018.07.012.

[111] R. Lu, O. Turan, E. Boulougouris, C. Banks and A. Incecik, 'A semi-empirical ship operational performance prediction model for voyage optimization towards energy efficient shipping', *Ocean Engineering*, vol. 110, pp. 18–28, 2015. DOI: 10.1016/j.oceaneng.2015.07.042.

[112] C. Gkerekos, I. Lazakis and G. Theotokatos, 'Machine learning models for predicting ship main engine fuel oil consumption: A comparative study', *Ocean Engineering*, vol. 188, p. 106 282, 2019. DOI: 10.1016/j.oceaneng.2019.106282.

[113] L. Huang, B. Pena, Y. Liu and E. Anderlini, 'Machine learning in sustainable ship design and operation: A review', *Ocean Engineering*, vol. 266, p. 112 907, 2022. DOI: https://doi.org/10.1016/j.oceaneng.2022.112907.

[114] A. Coraddu, M. Kalikatzarakis, L. Oneto, G. J. Meijn, M. Godjevac and R. D. Geertsma, 'Ship diesel engine performance modelling with combined physical and machine learning approach', *Proceedings of the International Ship Control Systems Symposium (iSCSS)*, 2018.

[115] P. Karagiannidis and N. Themelis, 'Data-driven modelling of ship propulsion and the effect of data pre-processing on the prediction of ship fuel consumption and speed loss', *Ocean

Engineering, p. 108 616, 2021. DOI: `10.1016/j.oceaneng.2021.108616`.

[116]   M. Grieves and J. Vickers, 'Digital twin: Mitigating unpredictable, undesirable emergent behavior in complex systems', *Transdisciplinary Perspectives on Complex Systems: New Findings and Approaches*, F.-J. Kahlen, S. Flumerfelt and A. Alves, Eds. Cham: Springer International Publishing, 2017, pp. 85–113. DOI: `10.1007/978-3-319-38756-7_4`.

[117]   F. Mauro and A. A. Kana, 'Digital twin for ship life-cycle: A critical systematic review', *Ocean Engineering*, vol. 269, p. 113 479, 2023. DOI: `https://doi.org/10.1016/j.oceaneng.2022.113479`.

[118]   D. W. Taylor, *The speed and power of ships: A manual of marine propulsion*. John Wiley & sons, inc., 1910.

[119]   L. Huijgens, A. Vrijdag and H. Hopman, 'Hardware in the loop experiments on the interaction between a diesel-mechanical propulsion system and a ventilating propeller', *Journal of Marine Engineering Technology*, pp. 1–13, 2022.

[120]   ITTC, 'Recommended Procedures and Guidelines - 1978 ITTC Performance Prediction Method 7.5-02-03-01.4', International Towing Tank Conference, Tech. Rep., 2014.

[121]   J. Holtrop, 'A Statistical RE-Analysis of Resistance and Propulsion Data', *International Shipbuilding Progress*, vol. 31, no. 363, pp. 272–276, 1984.

[122]   J. S. Carlton, *Marine Propellers and Propulsion*. Butterworth-Heinemann, An imprint of Elsevier, 2019.

[123]   MAN Energy solutions, *Basic principles of ship propulsion Optimisation of hull, propeller, and engine interactions for maximum efficiency*, 2018.

[124]   S. Shalev-Shwartz and S. Ben-David, *Understanding machine learning: From theory to algorithms*. Cambridge university press, 2014.

[125]   I. Goodfellow, Y. Bengio and A. Courville, *Deep learning*. MIT press, 2016.

[126]   M. Fernández-Delgado, E. Cernadas, S. Barro and D. Amorim, 'Do we need hundreds of classifiers to solve real world classification problems?', *The journal of machine learning research*, vol. 15, no. 1, pp. 3133–3181, 2014.

[127]   M. Wainberg, B. Alipanahi and B. J. Frey, 'Are random forests truly the best classifiers?', *The Journal of Machine Learning Research*, vol. 17, no. 1, pp. 3837–3841, 2016.

[128] D. H. Wolpert, 'The supervised learning no-free-lunch theorems', *Soft Computing and Industry: Recent Applications*, R. Roy, M. Köppen, S. Ovaska, T. Furuhashi and F. Hoffmann, Eds. London: Springer London, 2002, pp. 25–42. DOI: 10.1007/978-1-4471-0123-9_3.

[129] C. C. Aggarwal, *Data mining: the textbook*. Springer, 2015.

[130] L. Oneto, *Model selection and error estimation in a nutshell*. Springer, 2020. DOI: 10.1007/978-3-030-24359-3.

[131] H. Zou and T. Hastie, 'Regularization and variable selection via the elastic net', *Journal of the Royal Statistical Society Series B: Statistical Methodology*, vol. 67, no. 2, pp. 301–320, 2005.

[132] J. Shawe-Taylor and N. Cristianini, *Kernel methods for pattern analysis*. Cambridge Universtity Press, 2004.

[133] Z.-H. Zhou, *Ensemble methods: foundations and algorithms*. CRC press, 2012.

[134] F. Rosenblatt, 'The perceptron: A probabilistic model for information storage and organization in the brain.', *Psychological review*, vol. 65, no. 6, p. 386, 1958.

[135] D. E. Rumelhart, G. E. Hinton and R. J. Williams, 'Learning representations by back-propagating errors', *Nature*, vol. 323, no. 6088, pp. 533–536, 1986.

[136] G. Cybenko, 'Approximation by superpositions of a sigmoidal function', *Mathematics of Control, Signals, and Systems*, vol. 2, no. 4, pp. 303–314, 1989.

[137] C. M. Bishop, *Neural networks for pattern recognition*. Oxford university press, 1995.

[138] B. Scholkopf, 'The kernel trick for distances', *Advances in neural information processing systems*, 2001, pp. 301–307.

[139] S. S. Keerthi and C. J. Lin, 'Asymptotic behaviors of support vector machines with gaussian kernel', *Neural computation*, vol. 15, no. 7, pp. 1667–1689, 2003.

[140] M. Z. Naser and A. H. Alavi, 'Error metrics and performance fitness indicators for artificial intelligence and machine learning in engineering and sciences', *Architecture, Structures and Construction*, pp. 1–19, 2021. DOI: 10.1007/s44150-021-00015-8.

[141] K. L. Sainani, 'The value of scatter plots', *Physical Medicine & Rehabilitation*, pp. 1213–1217, 2016. DOI: 10.1016/j.pmrj.2016.10.018.

[142] N. Vasilikis, R. Geertsma, L. Oneto and A. Coraddu, 'A design by optimisation approach for hybrid propulsion systems sizing using actual sailing profiles', *Proceedings of the ASME 43rd International Conference on Ocean, Offshore & Arctic Engineering (OMAE)*, 2024.

[143] A. Papanikolaou, *Ship Design Methodologies of Preliminary Design*. Zografou - Athens, Attiki, Greece: Springer, 2014. DOI: `10.1007/978-94-017-8751-2`.

[144] M. Jaurola, A. Hedin, S. Tikkanen and K. Huhtala, 'Optimising design and power management in energy-efficient marine vessel power systems: A literature review', *Journal of Marine Engineering & Technology*, vol. 18, no. 2, pp. 92–101, 2019. DOI: `10.1080/20464177.2018.1505584`. eprint: `https://doi.org/10.1080/20464177.2018.1505584`.

[145] F. Mylonopoulos, H. Polinder and A. Coraddu, 'A comprehensive review of modeling and optimization methods for ship energy systems', *IEEE Access*, vol. 11, pp. 32697–32707, 2023. DOI: `10.1109/access.2023.3263719`.

[146] I. Gypa, M. Jansson, K. Wolff and R. Bensow, 'Propeller optimization by interactive genetic algorithms and machine learning', *Ship Technology Research*, vol. 70, no. 1, pp. 56–71, 2021. DOI: `10.1080/09377255.2021.1973264`.

[147] M. Tadros, M. Ventura and C. G. Soares, 'Optimization procedure to minimize fuel consumption of a four-stroke marine turbocharged diesel engine', *Energy*, vol. 168, pp. 897–908, 2019. DOI: `10.1016/j.energy.2018.11.146`.

[148] S. D. Chatzinikolaou and N. P. Ventikos, 'Holistic framework for studying ship air emissions in a life cycle perspective', *Ocean Engineering*, vol. 110, pp. 113–122, 2015. DOI: `10.1016/j.oceaneng.2015.05.042`.

[149] K. Kim, G. Roh, W. Kim and K. Chun, 'A preliminary study on an alternative ship propulsion system fueled by ammonia environmental and economic assessments', *Journal of Marine Science and Engineering*, vol. 8, p. 183, 2020. DOI: `10.3390/jmse8030183`.

[150] C. A. Frangopoulos, 'Developments, trends, and challenges in optimization of ship energy systems', *Applied Sciences*, vol. 10, no. 13, p. 4639, 2020. DOI: `10.3390/app10134639`.

[151] G. A. Livanos, G. Theotokatos and D.-N. Pagonis, 'Techno-economic investigation of alternative propulsion plants for Ferries and RoRo ships', *Energy Conversion and Management*, vol. 79, pp. 640–651, 2014. DOI: `10.1016/j.enconman.2013.12.050`.

[152] S. Solem, K. Fagerholt, S. O. Erikstad and Patricksson, 'Optimization of diesel electric machinery system configuration in conceptual ship design', *Journal of Marine Science and Technology*, vol. 20, no. 3, pp. 406–416, 2015. DOI: `10.1007/s00773-015-0307-4`.

[153] F. Balsamo, C. Capasso, D. Lauria and O. Veneri, 'Optimal design and energy management of hybrid storage systems for marine propulsion applications', *Applied Energy*, vol. 278, p. 115 629, 2020. DOI: 10.1016/j.apenergy.2020.115629.

[154] X. Wang, U. Shipurkar, A. Haseltalab, H. Polinder, F. Claeys and R. R. Negenborn, 'Sizing and control of a hybrid ship propulsion system using multi-objective double-layer optimization', *IEEE Access*, vol. 9, pp. 72 587–72 601, 2021. DOI: 10.1109/access.2021.3080195.

[155] M. Tadros, M. Ventura and C. G. Soares, 'A nonlinear optimization tool to simulate a marine propulsion system for ship conceptual design', vol. 210, p. 107 417, 2020. DOI: 10.1016/j.oceaneng.2020.107417.

[156] J.-P. Skeete, 'Examining the role of policy design and policy interaction in EU automotive emissions performance gaps', *Energy Policy*, vol. 104, pp. 373–381, 2017. DOI: 10.1016/j.enpol.2017.02.018.

[157] G. Fontaras, N.-G. Zacharof and B. Ciuffo, 'Fuel consumption and CO 2 emissions from passenger cars in europe – laboratory versus real-world emissions', *Progress in Energy and Combustion Science*, vol. 60, pp. 97–131, 2017. DOI: 10.1016/j.pecs.2016.12.004.

[158] J. L. Jiménez, J. Valido and N. Molden, 'The drivers behind differences between official and actual vehicle efficiency and CO2 emissions', *Transportation Research Part D: Transport and Environment*, vol. 67, pp. 628–641, 2019. DOI: 10.1016/j.trd.2019.01.016.

[159] M. Pfriem and F. Gauterin, 'Development of real-world Driving Cycles for Battery Electric Vehicles', *World Electric Vehicle Journal 8*, vol. 8, 2016.

[160] I. Pagoni and V. Psaraki-Kalouptsidi, 'Calculation of aircraft fuel consumption and co2 emissions based on path profile estimation by clustering and registration', *Transportation Research Part D: Transport and Environment*, vol. 54, no. Polythechniou, pp. 172–190, 2017. DOI: 10.1016/j.trd.2017.05.006.

[161] Q. Cui, Y. Lei and Y. Li, 'Protocol to calculate aircraft emissions for international air routes in South America', *STAR Protocols*, vol. 4, no. 1, p. 101 952, 2023. DOI: 10.1016/j.xpro.2022.101952.

[162] A. Godet, J. N. Nurup, J. T. Saber, G. Panagakos and M. B. Barfod, 'Operational cycles for maritime transportation: A benchmarking tool for ship energy efficiency', *Transportation Research Part D: Transport and Environment*, vol. 121, p. 103 840, 2023. DOI: 10.1016/j.trd.2023.103840.

[163] A. Godet, G. Panagakos, M. B. Barfod and E. Lindstad, 'Operational cycles for maritime transportation: Consolidated methodology and assessments', *Transportation Research Part D: Transport and Environment*, vol. 132, p. 104 238, 2024. DOI: 10.1016/j.trd.2024.104238.

[164] M. Duan, Y. Wang, A. Fan, J. Yang and X. Fan, 'Comprehensive analysis and evaluation of ship energy efficiency practices', *Ocean & Coastal Management*, vol. 231, p. 106 397, 2023. DOI: 10.1016/j.ocecoaman.2022.106397.

[165] 'Marine engine programme', MAN Energy solutions, Tech. Rep., 2023.

[166] 'Wärtsilä solutions for marine and oil & gas markets', Wärtsilä, Tech. Rep., 2023.

[167] J. Granacher, 'Overcoming decision paralysis—a digital twin for decision making in energy system design', vol. 306, 2022, p. 117 954. DOI: 10.1016/j.apenergy.2021.117954.

[168] M. T. M. Emmerich and A. H. Deutz, 'A tutorial on multiobjective optimization: Fundamentals and evolutionary methods', *Natural Computing*, vol. 17, no. 3, pp. 585–609, 2018. DOI: 10.1007/s11047-018-9685-y.

[169] N. V. Sahinidis, 'Mixed-integer nonlinear programming 2018', *Optimization and Engineering*, vol. 20, no. 2, pp. 301–306, 2019. DOI: 10.1007/s11081-019-09438-1.

[170] W. Stoecker, *Design of thermal systems*. McGraw-Hill Science/Engineering, 1989.

[171] A. Ravindran, K. M. Ragsdell and G. V. Reklaitis, *Engineering Optimization*. John Wiley & Sons, 2006.

[172] C. A. Frangopoulos, Ed., *Cogeneration: Technologies, Optimisation and Implementation* (Energy Engineering Series). The Institution of Engineering and Technology, 2017, vol. 87.

[173] M. Sakawa, *Genetic algorithms and fuzzy multiobjective optimization*. Springer science and business media, LLC, 2002. DOI: 10.1007/978-1-4615-1519-7.

[174] M. J. Kochenderfer, *Algorithms for optimization*, T. A. Wheeler, Ed. Cambridge: The MIT Press, 2019, 1 p.

[175] D. H. Wolpert and W. G. Macready, 'No free lunch theorems for optimization', *IEEE Transactions on Evolutionary Computation*, vol. 1, no. 1, pp. 67–82, 1997. DOI: 10.1109/4235.585893.

[176] A. R. Jordehi, 'A review on constraint handling strategies in particle swarm optimisation', *Neural Computing and Applications*, vol. 26, no. 6, pp. 1265–1275, 2015. DOI: 10.1007/s00521-014-1808-5.

[177] R. Martí, 'Multi-start methods', *Handbook of Metaheuristics*, F. Glover and G. A. Kochenberger, Eds. Boston, MA: Springer US, 2003, pp. 355–368. DOI: 10.1007/0-306-48056-5_12.

[178] N. I. Vasilikis, 'Operational data-driven energy efficiency and effectiveness assessment of a hybrid propulsion equipped naval vessel', *Proceedings of the 15th International Naval Engineering Conference and Exhibition (INEC)*, 2020.

PUBLICATIONS

Journal articles

(1). N. I. Vasilikis, R. D. Geertsma and K. Visser, 'Operational data-driven energy performance assessment of ships: The case study of a naval vessel with hybrid propulsion', *Journal of Marine Engineering and Technology*, 2022. DOI: 10.1080/20464177.2022.2058690

(2). N. Vasilikis, R. Geertsma and A. Coraddu, 'A digital twin approach for maritime carbon intensity evaluation accounting for operational and environmental uncertainty', *Ocean Engineering*, vol. 288, p. 115927, 2023. DOI: 10.1016/j.oceaneng.2023.115927

(3). N. Vasilikis, R. Geertsma and A. Coraddu, 'A robust multi-objective optimisation framework for the design of ship energy systems' (Submitted to a journal)

Conferences attended with papers

(1). N. I. Vasilikis, 'Operational data-driven energy efficiency and effectiveness assessment of a hybrid propulsion equipped naval vessel', *Proceedings of the 15th International Naval Engineering Conference and Exhibition (INEC)*, 2020

(2). N. Vasilikis, R. Geertsma, L. Oneto *et al.*, 'A design by optimisation approach for hybrid propulsion systems sizing using actual sailing profiles', *Proceedings of the ASME 43rd International Conference on Ocean, Offshore & Arctic Engineering (OMAE)*, 2024

ACKNOWLEDGMENTS

As I prepare to write this section, I find myself reflecting on my life before the start of my PhD. Would I make the same decisions if given the chance? Were all the sacrifices worth it? I vividly recall my ambition to continue on a steep learning curve and grow both personally and professionally by moving abroad. Yet, as with all carefully laid plans, reality often has a way of questioning our choices. Despite being numb after these demanding years, I am undoubtedly better prepared for whatever lies ahead and I feel lucky to have many people by my side.

First, I would like to thank Dr. Milinko Godjevac for offering me the opportunity to join TU Delft. A special thank you goes to my co-promotor, Dr. Ir. Rinze Geertsma. Rinze, over these years, we sailed in both stormy and calm seas. I deeply appreciate the mutual respect and commitment to reaching the end point of this journey. I would also like to thank my promotor, Dr. Andrea Coraddu. Andrea, I clearly remember that you joined TU Delft at a marginal moment for the continuation of my PhD, bringing crucial knowledge and experience in order for me to materialise my research plan. I also want to thank Ir. Klaas Visser for always being there when necessary, whether it was to write a letter to my landlord or to arrange an encrypted hard drive for my data. Finally, I extend my thanks to our project partners, especially at DAMEN Naval for sharing with me the datasets that became the foundation of my work.

In these past years, I have met many people who influenced me deeply, sharing life experiences that will remain unforgettable. I witnessed the MTT department going through different phases in which many people arrived and many left. During the challenging years of COVID, I was fortunate to be surrounded by people that made me feel accompanied. Then the post-COVID period. A boom of new people joining. This opened completely different opportunities; it marked though one of the most difficult periods of my life.

Rather than a long list of all the names of people to whom I am grateful, I would like to mention some of the moments we shared together. With some of you, we spent our Wednesday evenings having dinner and playing board games after work. We visited Christmas markets in Cologne. We learned that Beilstein is the best place on earth, we hiked over river bends, and we tried probably the most

tasteless wine on earth. We had late drinks online after participating in a hackathon. We went running early in the morning in a foggy German forest and climbed to the top of a watchtower in Texel. We saw castles behind river bends in central Europe, we drove for hours to the north-west edge of France, or all the way to Sweden. We cycled fast back home before the curfew and we spent countless hours playing Splendor during quarantines. With some of you, I fulfilled my ambition of becoming a tour guide, getting people acquainted with the rich history of Athens and the limits of human nature. We swam in blue waters in Greece and Turkey, we almost managed to have pizza in Napoli. We visited big museums, windmills at Kinderdijk, and the northernmost medieval cathedral in the world. To some of you, I offered lessons on the Greek language. We attended a summer school in Girona, tried Fideuà, and rode girocletas. We had lunch at Maria's introducing people to pastitsio and moussaka, and we rushed to queue in the city centre of Delft to get ice cream or the best appeltaart in town. We celebrated my birthday on the rooftop of a tall building in Rotterdam and we tried the best souvlaki in The Netherlands. We chased the northern lights out of an attic window in Norway like kids and we ended up strolling around in the streets and food markets of Singapore. We spent many Wednesday evenings and Saturday mornings bouldering, we cycled across Dutch fields, we played tennis, football, we went swimming, we played table tennis in parks, we tried playing golf for the first time. With some of you, we spent time working or not working at the library. I am sure that with many of you, we will continue building new experiences.

I would also like to thank my friends in Greece for proving that distance is not an obstacle when a friendship is built on strong foundations. Even after periods of sparse communication, catching up always felt natural, as if no time had passed.

To the person who encouraged me to move to the Netherlands during one of his visits back to Greece, I am grateful for providing me with all needed information, for hosting me, and for helping me connect with people at TU Delft.

I would like to thank the person that helped me shape my character and always keep my feet on the ground. I saw both paradise and hell on the face of the person that had been accompanying me for almost the whole of my adult life.

Special thanks to the person who helped me stay sane not once but twice during these years. Especially the first time was marginal. It is so much fun that this is the same person that couldn't find a cappuccino in Norway for months.

To the person that inspired me to push my physical limits. Thank you for the wonderful activities, and all the support you provided in the last two years. I didn't manage to cycle from Switzerland to the

Netherlands this year, I am confident though that we will make it next time.

To the person who inspired me to be curious, sensitive, and who taught me that true communists are life's greatest enjoyers, thank you. The countless kilometres we've walked and the hours we've spent discussing significantly shaped who I am today.

I would also like to thank the person that makes sense of my confusing descriptions, who once saved me from falling into the sewage system of a small island on the other side of the world, and who opened my mind to so many new ideas. I don't know if we will ever conclude over the debate of the largest cuisine variety, but we can definitely continue food-trying.

Finally, I extend my heartfelt gratitude to my family. My parents, my sister and brother-in-law, my grandma, my uncle and aunt, my cousins. Not until growing older, did I realise the importance of being raised in an environment in which I could feel safe, supported, and loved. Without them, I would not be the same person today.

Nikos Vasilikis
Delft, December 2024

CURRICULUM VITAE

Nikos Vasilikis was born in Athens on November 17, 1992. He attended the 11th High school and 12th Lyceum of Piraeus from 2004 until 2010. He obtained his Diploma in Naval Architecture and Marine Engineering at the National Technical University of Athens in 2016. His thesis title was "Hydrodynamic interaction and power absorption efficiency of wave energy converters in the frequency domain using the boundary element method". Following the fulfilment of the obligatory military service with the Hellenic Army, he worked from September 2018 to February 2024 as a PhD candidate with the Maritime, Transport and Technology department at Delft University of Technology towards the sustainable design and operation of ship energy systems. His research focuses on methodologies for the energy performance analysis, modelling, and optimisation of ship energy systems, utilising both data-driven and physics-based techniques. In 2024, he also started working part-time as a researcher with the same department, and also part-time as a data scientist with the Research, Development and Innovation department at DAMEN Naval.